Optimal Power Management System of EVs Charging from PV System in a Low Voltage Distribution Network

An integration between EVs, PV system and grid

Muhammad Shiddiq Sumitro

Technische Universiteit Delft

Optimal Power Management System of EVs Charging from PV System in a Low Voltage Distribution Network

An integration between EVs, PV system and grid

by

Muhammad Shiddiq Sumitro

in partial fulfillment of the requirements for the degree of

Master of Science
in Sustainable Energy Technology

at the Delft University of Technology,
to be defended publicly on Thursday, August 16th 2018 at 09:00 AM

Supervisor:	Prof. dr. ir. P. Bauer,	TU Delft
Advisor:	Dr. ir. G.R. Chandra Mouli,	TU Delft
	Dr. S. Izadkhast,	TU Delft
Thesis committee:	Prof. dr. ir. P. Bauer,	TU Delft
	Prof. dr. ir. A.H.M. Smets,	TU Delft
	Dr. ir. L.M. Ramirez Elizondo,	TU Delft

Delft University of Technology

Abstract

An increase in carbon emission which mostly caused by the transportation sector and electric power generation has been a hot topic nowadays in most countries in the world. To tackle this problem, the share of renewable energy use has been increased by up to 14% in the Netherlands. Moreover, the number of electric vehicles (EVs) on the road also reaches a total of 120,000 EVs in 2018. However, the high penetration of renewable energy sources (RESs) such as solar & wind power and the EVs charging in the distribution network could result in a severe problem. One of the solutions to avoid this problem is that switching the uncontrolled charging of EVs into a controlled charging or called as smart charging. Further, an integration between the EVs, RESs and the distribution grid could potentially lead to technical and economic benefits.

The focus of this thesis is to develop an optimal power management system (PMS) between the EVs, PV system, and the distribution network. The goal of the power management system is to obtain the minimum operational cost while also considering the technical grid constraints, which subsequently could avoid the grid violation. The proposed power management system will be modeled in a mixed integer non-linear programming (MINLP) optimization problem and executed in General Algebraic Modelling System (GAMS) software. To evaluate the performance of the proposed power management system, a comparison between the with-grid and the no-grid constraints case will be performed through several case studies. This study shows that by implementing the proposed power management system of EVs charging from PV system considering the grid constraints, it could decrease the total operational cost remarkably by 18.16% - 214.08% when compared to the uncontrolled charging scheme. Besides, the grid problem caused by the uncontrolled charging process such as exceeding the allowable voltage deviation and the transformer rated power could be prevented. However, in comparison to the smart charging without considering the grid constraints, the operational cost is increased by 1.43% - 113.20%.

Acknowledgements

Alhamdulillahi rabbil 'alamin

My journey finally comes to an end. Therefore, I would like to express my sincere gratitude to the people who have supported me to receive the *ingenieur (ir.)* degree.

First of all, I would like to acknowledge my supervisor, Prof. dr. Pavol Bauer who has given me an opportunity to work on his project about EVs smart charging under the DC Systems, Energy Conversion & Storage (DCE&S) research group. I also feel honored to work with him as a teaching assistant for an online course on edX: Integration of PV system in Microgrid. Besides, I would also say many thanks to my thesis committees, Prof. dr. Arno Smets and Dr. ir. Laura Ramirez Elizondo for the helpful feedback and comments.

Secondly, my most profound appreciation to Dr. ir. Gautham Ram Chandra Mouli who has been being my daily advisor during the last nine months. He shared and taught me lots of knowledge in the field of EVs smart charging and smart grid. His honest and valuable feedback helped me to push my limit. Also, thanks to Dr. Seyedmahdi Izadkhast as my second advisor for sparing the time to read my thesis and discuss the project.

Thirdly, I would not have completed my master degree without the support of my Indonesian friends in Delft. Also, to all my board members in PPI Delft (Indonesian Student Association in Delft), thanks for the pleasant memories that we have been through for the past one year. I learned a lot from all of you.

Last but not least, the miles-away priceless lovely support from my family in Indonesia always try to keep my heads up when I am down. *Matur nuwun, Pak, Buk & Mbakky*. Moreover, I would like to say many thanks to Indonesia Endowment Fund for Education (in Bahasa: *Lembaga Pengelola Dana Pendidikan*, LPDP) that has provided my financial support for the two-year study in the Netherlands.

" For indeed, with hardship [will be] ease. Indeed, with hardship [will be] ease." - Quran 94:5-6

Delft, August 2018
Muhammad Shiddiq Sumitro

Contents

List of Figures

List of Tables

1

INTRODUCTION

1.1. ELECTRIC VEHICLES IN THE NETHERLANDS

The cutback of global warming effects and *CO2* emission has become one of the most primary concerns of lots of countries in the world. Fossil fuels are the most dominant energy sources for the transportation sector and electrical power generation. This huge problem is a call to find the alternative energy sources. Evolving the internal combustion engine (ICE) vehicle to the electric vehicle (EV) is one of the solutions that is being employed to decrease the carbon footprint in the transport sector. To achieve the 2020 European Union (EU) goals, The Netherlands have to reach a 14% renewable energy use [17]. This target has shown that at the end of 2017, approximately 2.2% of all passenger cars in The Netherlands were EVs [1].

The Netherlands Enterprise Agency (in Dutch: *Rijksdienst voor Ondernemend Nederland, RVO*), in its last report on January 2018, stated that at the end of 2017, the total number of Battery Electric Vehicles (BEV) and Plugin Hybrid Electric Vehicles (PHEV) steeply increased by 316% in comparison to the end of 2013 and 7% in contrast to the end of 2016 as depicted in Fig. 1.1.

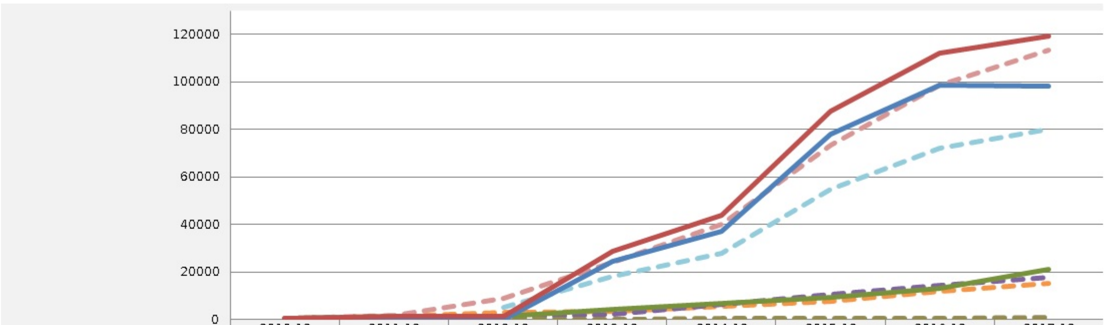

	2010-12	2011-12	2012-12	2013-12	2014-12	2015-12	2016-12	2017-12
Regular public	400	1250	2782	3521	5421	7395	11768	15288
Regular semi-public		576	829	2249	6439	10391	14320	17587
Fast charging		15	63	106	254	465	612	755
Private			5000	18000	28000	55000	72000	80000
Total charging points	400	1841	8674	23876	40114	73251	98700	113630
BEV Passenger car	266	1124	1252	4161	6825	9368	13105	21115
PHEV Passenger car	0	17	65	24512	36937	78163	98903	98217
BEV + PHEV	266	1141	1317	28673	43762	87531	112008	119332

Figure 1.1: The number of BEV and PHEV in The Netherlands from 2010 to 2017 [1]

Different manufacturers of EVs are taking parts in market share of The Netherlands. Fig. 1.2a and 1.2b illustrate that in 2017, Tesla Model S is leading the market share in the BEV sector, while Mitsubishi Outlander is surpassing the PHEV sector which equals to 44% and 38%, respectively. [1]. Additionally, every manufacturer has its specific battery capacity which is shown in Table 1.1.

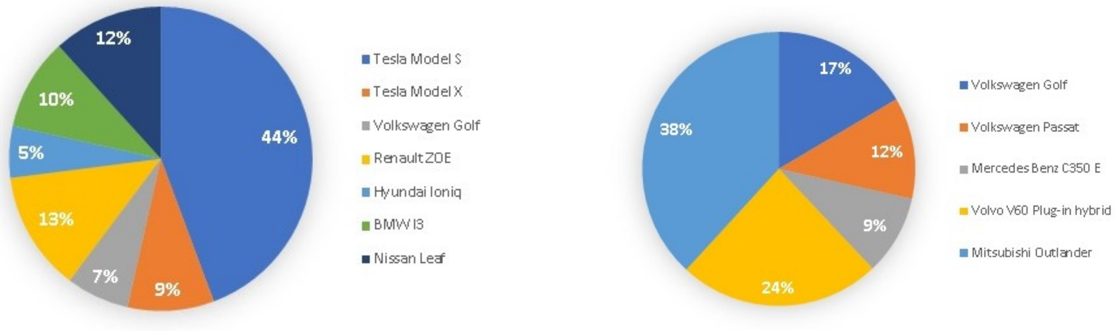

(a) BEV models (b) PHEV models

Figure 1.2: Top BEV and PHEV sold models in The Netherlands. Data is retrieved from [1]

Table 1.1: Battery capacity of top sold EVs in The Netherlands [15]

Types of EV	Battery capacity [kWh]
BMW i3	18.8
Nissan Leaf	24
Renault Zoe	22
Tesla Model X	90
Tesla Model S	60

In the Netherlands, based on the data from *Centraal Bureau van Statistiek* and depicted in Fig. 1.3, there are around 120,000 EVs in total. This vast number has shown a high possibility to reduce carbon emissions in the future. Furthermore, as can be seen in Fig. 1.4, the Netherlands has the highest number of PHEVs and FEVs sold in the EU.

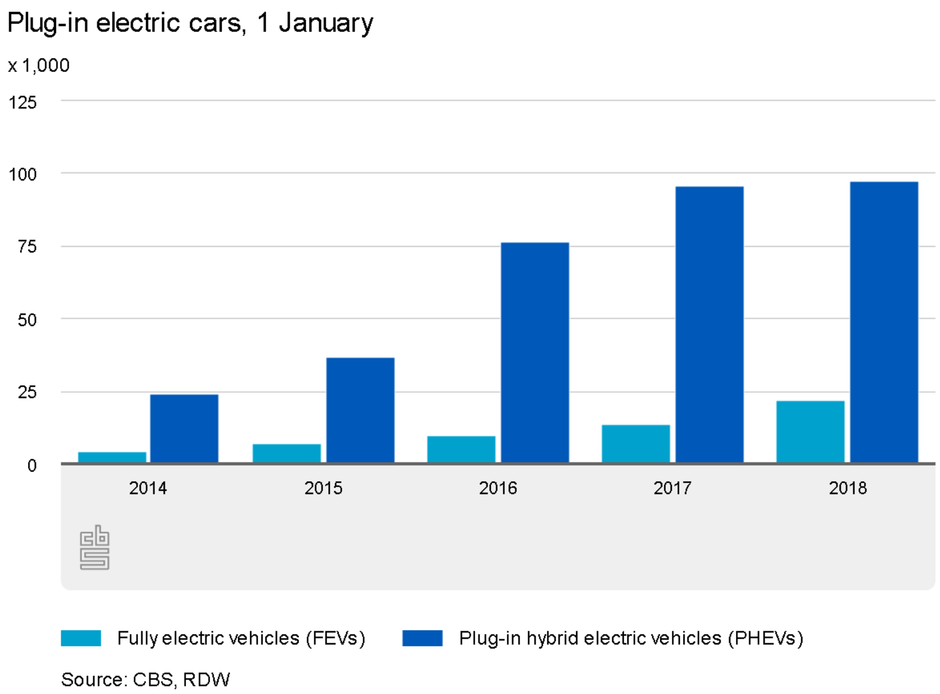

Figure 1.3: Total number of PHEVs and FEVs in the Netherlands per 1 January 2018 [2]

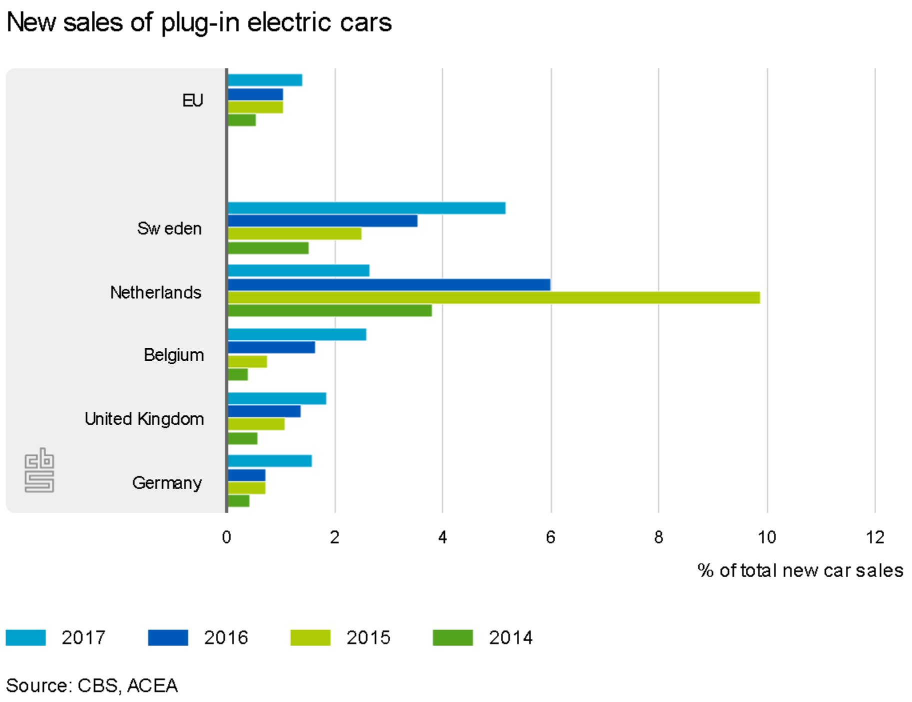

Figure 1.4: New sales of EVs in the EU [2]

1.2. PHOTOVOLTAIC POWER GENERATION

Carbon footprint has been being a hot issue during the last decade in most countries of the world. Moving towards into a greener energy by increasing the use of large-scale RES is one of the solutions to tackle this problem. As seen in Fig. 1.5, more than 104 GW of solar PV power has been installed in Europe in 2016 [3].

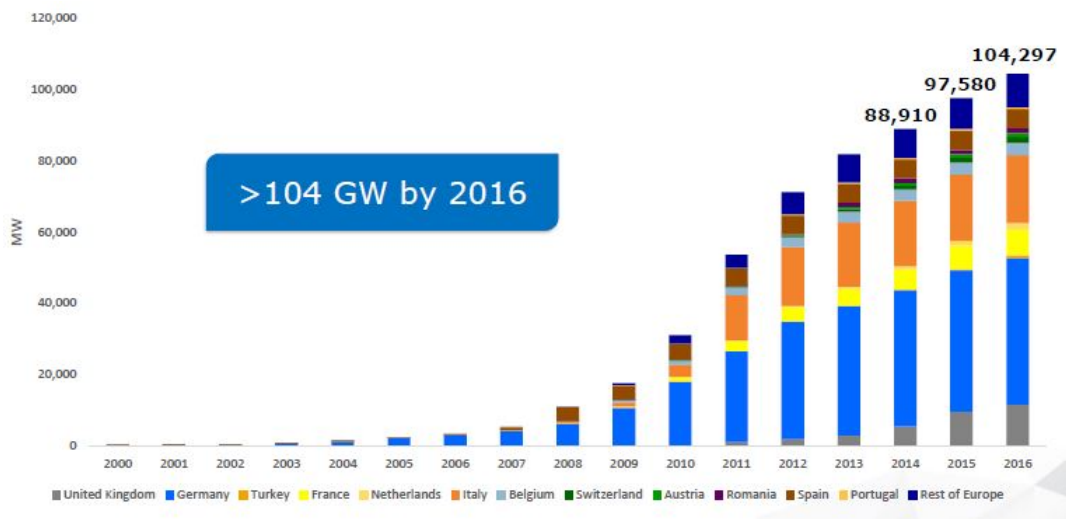

Figure 1.5: European total solar PV installed capacity 2000 - 2016 [3]

From Fig. 1.5, we may see that the penetration of PV in every country in the European Union (EU) is increasing slightly year by year. This increase shows that PV power generation has given a promising solution for the future. Solar PV panel has lots of benefits, for instance, ease of installation, long lifespan, low maintenance, etc. Thus, every citizen can also take part to help the governments to reach their target to boost up the shares of renewable energy use by putting PV on the rooftop. The citizen could receive money as they produce PV power to the grid, the so-called Feed-in Tariff subsidies. To keep promoting this, the governments of

EU countries have already set their target until 2020 as depicted in Fig. 1.6.

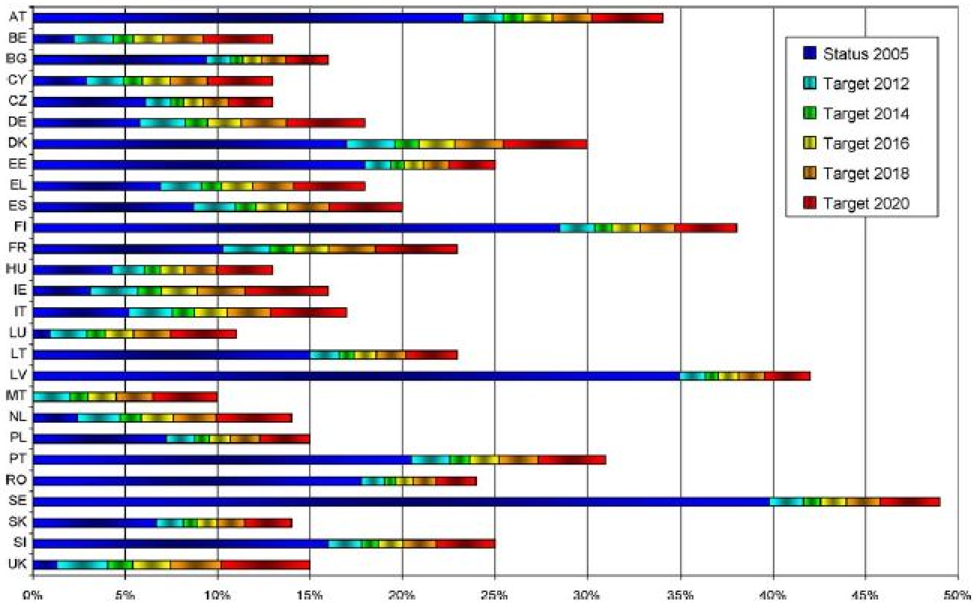

Figure 1.6: Target of the share of renewable energy use in the EU countries in 2020 [4]

In 2016, the Dutch Central Office for Statistics in its report states that renewable energy sources share around 5.9% of the total Dutch energy consumption. This amount of number was slightly the same in 2015 as illustrated in Fig. 1.7. From Fig. 1.6 and 1.7, we may conclude that the shares of RES in the Netherlands are still very low compared to other EU countries. In addition, based on National Energy Report (in Dutch: *Nationale Energieverkenning 2017 - NEV*) which was published by Dutch research institute *Energieonderzoek Centrum Nederland* (ECN) in cooperation with CBS, the Netherlands has installed approximately 2 GW of PV power and might be increasing to 20 GW by 2035 as shown in Fig. 1.7 [6].

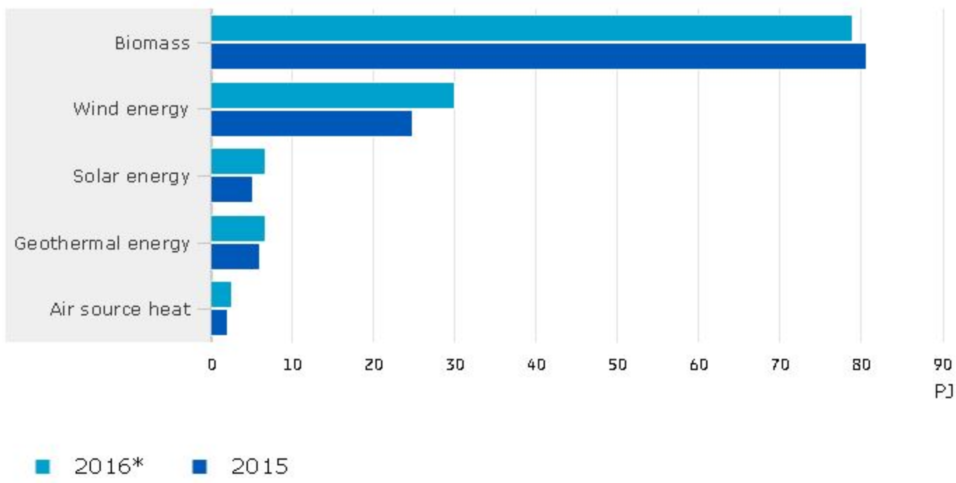

Figure 1.7: Renewable energy consumption by source in the Netherlands during 2015-2016 [5]

1.3. THE DUTCH POWER GRID

The Dutch electricity grid is well-known as immensely robust and reliable. The Dutch transmission system is strongly connected to the surrounding countries power grid such as Belgium, Germany, Norway (through HVDC connection) and Great Britain. The transmission system is operated by the government-owned limited

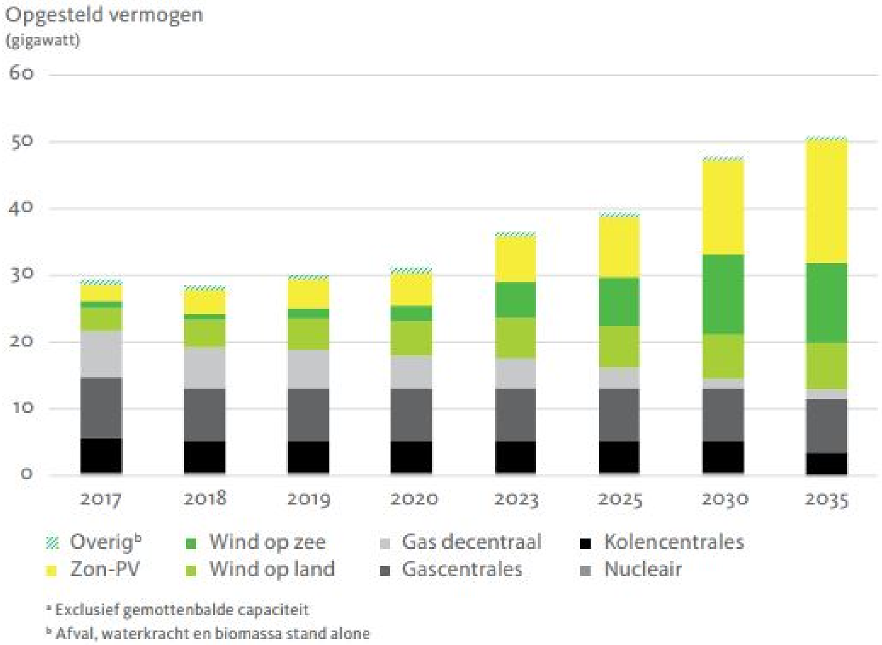

Figure 1.8: Development of installed capacity in the Netherlands in the period 2017-2035 [6]

liability company called TenneT B.V. The transmission system operator (TSO) manages and operates at the 110 kV voltage level and above. Also, the Dutch distribution grid is built over 325,000 kilometers long by almost all underground cables [18]. Currently, there are eight distribution system operators (DSOs) in the Netherlands with the three biggest DSOs are *Liander, Enexis*, and *Stedin.*

Based on the *Tarievencode Elektriciteit* 2009 by *Energiekamer*, the classification of transmission and distribution network is shown in Table 1.2. Besides, this thesis will mainly focus on the distribution network since the EV, and local residential loads are connected to a 0.4 kV of the voltage level.

Table 1.2: The definition of transmission and distribution network in the Netherlands [16]

	Voltage level name	**Voltage level range**	**Definition of network**
EHV	Extra High Voltage (*extra hoogspanning*)	380 / 220 kV	Transmission
HV	High Voltage (*hoogspanning*)	150 / 110 kV	
IMV	Intermediate Voltage (*tussenspanning*)	50 / 25 kV	Distribution
MV	Medium Voltage (*middenspanning*)	1 - 20 kV	
LV	Low Voltage (*laagspanning*)	0.4 kV	

1.4. PV AND EV INTEGRATION

The total installed capacity of PV power generation in the Netherlands, as previously stated in Section 1.2 has been increasing over year-by-year and hence will affect the penetration of renewable energy sources into the power system. The power generation from the PV system is intermittent which is depending on diurnal and seasonal time span. To store the excess of energy, its power is usually delivered to a stationary energy storage system. However, this solution has a high initial investment cost and therefore can increase the total investment cost. Therefore, to solve this issue, both PHEVs and BEVs can play a role as a dynamic energy storage system that will store the surplus energy from the PV system. The EVs can also deliver power to the grid during low power generation via vehicle to grid (V2G) concept. Assuming that an EV fleet parking area has its PV system, the integration of PV system and EVs can also help to reduce the total operational cost since the energy price of PV system is lower than the grid.

1.5. THESIS OBJECTIVES

Based on the explanations mentioned in the previous section, the following research objectives are listed below.

1. Developing an optimization model to find out an optimal power management system (PMS) of EVs charging from PV system in a low voltage distribution network considering the grid constraints
2. Investigating the economic analysis to find the reduction of the total operational cost in a one-day operation

1.6. RESEARCH QUESTIONS

To achieve the previously mentioned thesis objectives, several research (sub)questions are defined which will act as a guideline throughout the thesis project as explained below.

1. How to formulate the optimal power management system of EVs charging from PV system in a low voltage distribution network considering the grid constraints?
   (a) What are the EV constraints taken into considerations?
   (b) What are the PV system constraints taken into considerations?
   (c) What are the grid constraints taken into considerations?
   (d) What is the objective function of the proposed power management system?
2. What is the impact of considering the grid constraints on the proposed power management system for the identified case studies?
   (a) To what extent does the grid constraints affect the total operational cost for the identified case studies?
   (b) To what extent does the grid constraints avoid the grid violations for the identified case studies?
   (c) To what extent does the grid constraints increase the PV power allocated for EVs charging for the identified case studies?

1.7. THESIS OUTLINE

This thesis project comprises of six chapters as mentioned below.

- **Chapter 1: Introduction**
  A brief explanation of the research background and motivation is discussed in this chapter as well as the research objectives and questions.
- **Chapter 2: Literature Study**
  This chapter reviews the previously existing literature on optimization technique, EV smart charging, integration of renewable energy sources (RES) and Vehicle-to-Grid (V2G) concept. The contribution of this thesis project in the field of EV smart charging from renewable energy sources considering the distribution grid is discussed.
- **Chapter 3: Problem Formulation**
  In this chapter, the optimization model used in this study is defined. The mathematical formulation including the constraints for EV, PV system, and the grid is explained to solve the optimization problem.
- **Chapter 4: Data Characteristics and Case Studies**
  To evaluate the performance of the proposed power management system, several real-life input parameters need to be defined. Therefore, how these parameters data acquired is extensively described in this chapter. Additionally, several case studies are analyzed in this chapter to assess the technical and economic performances based on different parameters.
- **Chapter 5: Simulation Results and Analysis**
  Interfacing between GAMS and MATLAB software to simulate the model formulation in different case studies are done in this chapter. Also, the simulations are accomplished as a test and validation to prove the concept of the model formulation.

- **Chapter 6: Conclusions and Future Works**
  This is the last chapter of this thesis which compiles the main results of this study. The research questioned which are previously mentioned are answered as well. Several recommendations of future works for the improvement of the model are also presented.

2

Literature Study

This chapter aims at outlining the literature review of the thesis. A comprehensive literature study has been accomplished to provide the state of the art of this thesis project. Then, the structure of this chapter is explained as follows.

In section 2.1, the interaction between EV charging and distribution network is described. The challenges of integrating EV into power grid are also defined. Section 2.2 presents the cost-aware integration between renewable energy sources (RESs) and EVs charging. Section 2.3 conducts the technical aspect of integrating grid, RESs and EVs charging in a distribution system. These both sections are regarded as the main topic of this thesis. Lastly, section 2.4 points out several optimization techniques that will be selected to solve the problem of this thesis.

2.1. EV Charging and Distribution Grid Interaction

EVs can potentially become integral parts of a distribution network because they have capabilities to provide beneficial services to the grid other than just drawing power from the grid. EVs can also play an essential role as it could become dynamic energy storage to balance the intermittent RESs such as solar and wind power. On the distribution system level, the massive penetration of EVs charging turns into a new challenge to the Distribution System Operator (DSO) as it may affect the stability of the distribution grid [19]. Furthermore, the DSO always want to have the minimum power losses and acceptable power quality such as voltage profile, harmonics, etc [20]. One of the solutions to mitigate this problem is to shift the uncontrolled into controlled charging scheme or called as smart charging and will be discussed in the following sections.

2.1.1. EV Smart Charging

An uncoordinated charging happens when EVs start charging shortly after being connected to the charger until their battery is fully charged. Otherwise, controlled charging scheme provides the EVs fleet operator and the DSO to implement an EV charging profile scheduling and power control by programming an optimization technique to reach specific objectives, for instance minimizing charging cost and reducing power losses of the lines. The authors of [20] stated that the coordination of EV charging would be executed by smart metering and by transmitting signals to each EV in the parking area. Smart metering could make the EVs as controllable loads to perform the V2G concept and integrate with local RESs power generation.

In [21], the authors showed that to reduce the voltage drop due to large penetration of EVs, the voltage profile could be regulated by scheduling the reactive power or controlling the load demand. Additionally, a third-party entity known as the aggregator is responsible for coordinating and managing the EVs charging profile in the specific area. The function of this entity is to mediate between the EV owners, the electricity market, DSO and TSO [22, 23]. An aggregator has to offer the regulation in so-called desired scale. In reality, it prepares a contract with each EV owner. Then, the aggregator makes another contract with local DSO based on the amount of the EV owners. Furthermore, a power management system, put at the DSO operator, has to be worked optimally. So, in this case, the importance of the aggregator is obvious. The aggregator would optimize the coordinated charging by taking several EV users data such as historical data on arrival & departure time and the EVs SOC. Local RESs generation, the grid and energy prices from the market are also taken into considerations. The study conducted in [7] showed that the EVs smart charging could increase the

PV self-consumption as depicted in Fig. 2.1.

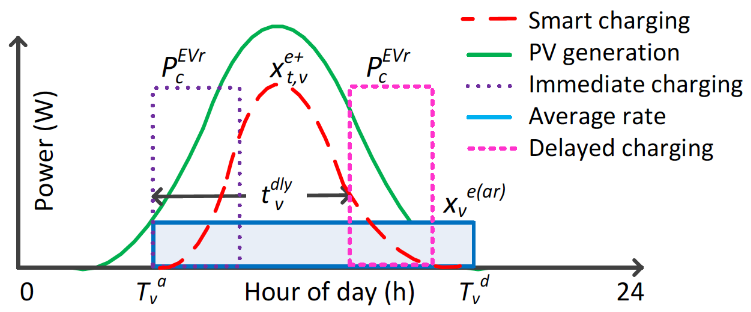

Figure 2.1: Power profile of EV smart charging [7]

2.1.2. EV WITH V2G TECHNOLOGY

EVs can act as loads or as distributed energy and power resources in a concept known as vehicle-to-grid (V2G) process [24]. V2G is capable to offer reactive power support, active power regulation, load balancing, and current harmonic filtering. The V2G concept can also enable several ancillary services to support the grid, for instance, frequency regulation, voltage control, and peak shaving which has been demonstrated in [25, 26]. Therefore, the concept of V2G has attracted attention from the grid operators (especially the DSO) and the EV owners as the end-users. Additionally, with V2G, an EV can take a role in most energy markets, from bulk energy to frequency control and spinning reserves [27]. In addition, several literature have discussed the concept of V2G in combination with renewable energy sources (RES), such as wind and solar energy [28–32]. This V2G system which is constructed via bidirectional Electric Vehicle Supply Equipment (EVSE) or EV charger is shown in Fig. 2.2.

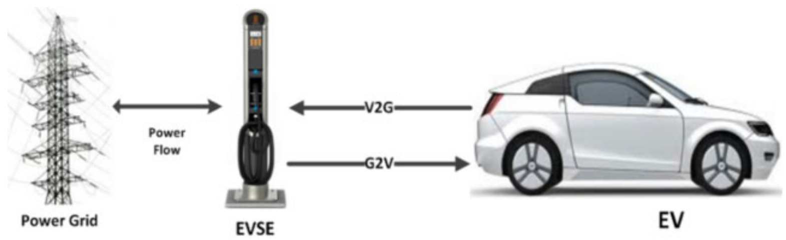

Figure 2.2: V2G technology concept [8]

The study was done in [33] observed that by managing the EV as a dynamic load and energy storage (via V2G technology), it could cut down the total operational cost by 26.5%. Moreover, the accomplishment of the V2G technology implementation depends on several aspects, for example, charging infrastructure, the technology of the battery, and smart charging technology [24]. One of the most significant challenges to the V2G concept is the technology of battery and the high initial investment costs if it is compared to internal combustion engine (ICE) vehicles. The detail explanation of how economically viable and technically feasible will be discussed later in the following sections.

2.2. ECONOMIC CONSIDERATION OF GRID, RESS AND EVS INTEGRATION

Providing EVs smart charging in a distribution system may result in financial profit both to the EV owners and the distribution system operator. In [34], the authors have proven in their results that by applying a coordinated charging scheme can minimize the total cost as well as decreasing the dependency on the distribution grid and improving PV self-consumption. The total cost was reduced by 118.44% and the profit was gained by 427.45%. The following sections will explain extensively how beneficial implementing EVs smart charging is for both the EV owners and the aggregator as an EV fleet operator.

2.2.1. MINIMIZING OPERATIONAL COST AND MAXIMIZING PROFIT

The aggregator is in charge of controlling the system operational cost of EVs fleet since they want to achieve maximum profits by coordinating the EVs charging. To give a better insight into the operational cost, Fig. 2.3 is illustrated. However, the scope of this thesis is only the integration between the distribution grid, PV system and the EVs fleet. Moreover, the research conducted in [35] performed that the scheduling from the

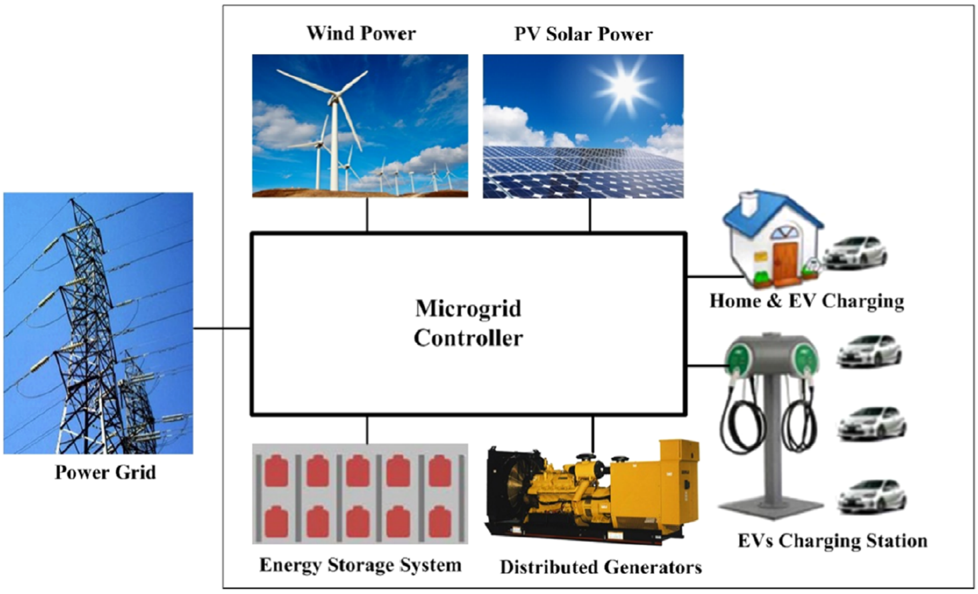

Figure 2.3: Integration between Grid, RESs and EVs [9]

aggregator could minimize the total operational cost. It was done by charging the EV batteries when the power generation from renewable energy sources (solar and wind power) is surplus, while discharging the EVs via V2G schemes in the low power generation condition.

The findings in [36] showed that by enabling a coordinated charging scheme with RESs in a smart grid way through a particle swarm optimization (PSO) could reduce the total cost by 0.9% as well as emission by 4.3% per day. In [37], the authors came up with energy management system for EVs charging in a smart grid infrastructure which intended to minimize operating costs and carbon emissions and result in decreasing the operational cost by 15% and carbon emissions by 8%. Additionally, the authors in [38] found that a coordinated EVs charging for a realistic case study with 50 EVs in one parking space can achieve a net cost reduction by 1% to 15%. These prior research added up the proof that by controlling the integration between grid, RESs and EVs may lead to economic benefits.

In addition, the operator of the aggregated EVs also has a target to achieve maximum profits for serving the EV owners to charge their cars. The interaction between EVs and RESs could help on reaching this target. Let say the PV system is installed to support the EVs charging, it can be done by increasing the PV self-consumption. As mentioned previously, the aggregator will not only accomplish in minimizing the operational cost but also maximizing the economic revenue.

2.2.2. MINIMIZING CHARGING COST

In this section, the economic aspect from the EV owners perspective will be discussed. The EV owners as the end-users always want to pay a low charging cost. To achieve this goal, researchers have employed several optimization techniques such as mixed-integer linear programming (MILP), quadratic programming (QP), stochastic programming, particle swarm optimization (PSO), etc. According to [39], the authors mentioned that the aggregator or the EV fleet operator controlled and managed the market participation to optimize the charging cost. The aggregator regulated the day-ahead market operation which would give beneficial impacts for the aggregated EVs in one specific area.

The study conducted in [40] also found that the EVs management could positively influence the charging cost. The aggregated EVs operator can join the electricity market share by regulating the dynamic loads of EVs via charging and discharging of the EVs batteries. Taking considerations of the previously mentioned explanation, this thesis would indicate reducing the charging cost seen from the perspective of the EV owners as the objective function of the optimization problem.

2.3. TECHNICAL CONSIDERATION OF GRID, RESSS AND EVS INTEGRATION

In the previous section, it has been discussed that applying smart charging may lead to obtaining minimum net operational costs and maximizing profits for the EV fleet operator. The integration of EVs in the distribution grid with RESs penetration can also help the DSO providing valuable services in terms of technical aspects. According to [41], with the modified IEEE 23 kV distribution system, the uncontrolled charging strategy in high (63%) or low (16%) penetration of the EVs produces serious voltage deviations up to 0.83 p.u. which is below allowable 0.9 p.u. based on European EN50160 standard, high power losses and high cost in the generation. On the contrary, with a controlled charging scheme, the voltage profile is increased up to 0.9 p.u. which is still in the range of acceptable voltage deviation. Furthermore, the increase of both BEVs and PHEVs penetration in the power grid contributes to a significant rise in power losses in the lines. This issue is substantial for the DSO point of view. It may produce lousy power quality for the other customers. In [20], the study on IEEE 34-node test proved that by implementing smart charging of PHEVs can reduce power losses up to 9%. This result was achieved with quadratic programming (QP) in minimizing the I^2R losses as the objective function. Moreover, the authors in [10] showed in their results that by applying a controlled charging for EVs, it leads to a more stable voltage profile as depicted in Fig. 2.4. This study was done in an IEEE 34-node residential test feeder.

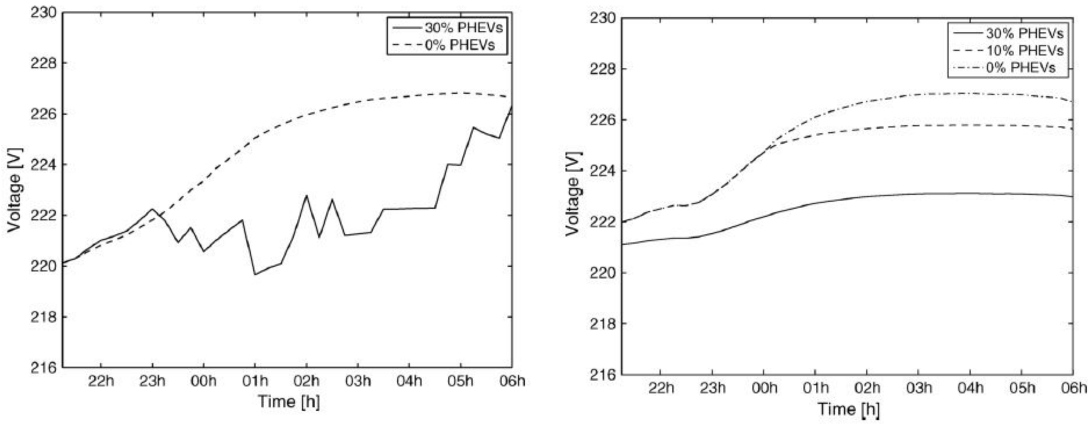

Figure 2.4: The EV penetration impact with controlled (left side) and uncontrolled (right side) charging on a distribution grid [10]

The authors in [42] showed in their findings that by implying such EV charging strategies using Monte Carlo technique could decrease the congestion problems due to the large penetration of EVs in the industrial grid. The charging strategy is done by cutting the peak power in an EVs parking space during the day. Moreover, the peak consumption was reduced by up to 55%. In [43], it is found that stimulating the integration between the RESs, EVs and the network may result in mitigating the grid violation. The study was done in a 33-bus distribution network with V2G operation by implementing a Mixed Integer Non-Linear Programming (MINLP) to obtain the minimum operational cost considering the distribution network constraints of the grid, such as voltage magnitude & angle and the transformer loading limit.

2.4. OPTIMIZATION TECHNIQUE

Optimization is a process of finding the best possible solution for a specific situation under a group of constraints which are required to be satisfied. In the application of power system, the optimization technique is generally used to obtain the most efficient operation between the three main parts: generation, transmission, and distribution [44]. There are several techniques of optimization to solve many different problems in the power system, but the most applicable ones are, i.e. Linear Programming (LP), Nonlinear Programming (NLP), Mixed Integer Linear Programming (MILP), and Mixed Integer Nonlinear Programming (MINLP) [44]. Table 2.1 shows the most used optimization model in the scope of the electrical power system. Additionally, each of the optimization problem mentioned below will be discussed further in the following sections.

Table 2.1: Types of optimization technique

Optimization Technique	Objective Function	Constraints	Decision Variables	
			Continuous	Discrete
LP	Linear	Linear	✓	-
NLP	Non-Linear	Non-Linear	✓	-
MILP	Linear	Linear	✓	✓
MINLP	Non-Linear	Non-Linear	✓	✓

2.4.1. LINEAR PROGRAMMING (LP)
Linear Programming (LP) can be described as an optimization problem to maximize or minimize the linear objective function which subject to linear equality or inequality constraints. The mathematical formulation is written in eqs. 2.1 as follows.

$$\begin{aligned} \text{minimize} \quad & f(x) \\ \text{subject to} \quad & A\mathbf{x} \leq \mathbf{b} \\ & lb \leq \mathbf{x} \leq ub \end{aligned} \tag{2.1}$$

where $f(x)$ is a linear function and x is a linear constraint. The lb and ub are the lower and upper bound of the variable x, respectively, in which give a limitation to the function. The linear constraints could be equalities or inequalities where the feasible region is found.

2.4.2. NON-LINEAR PROGRAMMING (NLP)
Non-linear programming is an mathematical process of obtaining the optimal non-linear function within a set of non-linear constraints. To define a satisfactory mathematical formulation, an MLP model usually follow several rules, such as setting a logical initial value & variable limit, and scaling variables and equations. Moreover, the NLP problem typically takes longer time to solve than the LP. The mathematical formulation is basically the same as the LP, but using the non-linear objective and constraints.

2.4.3. MIXED INTEGER LINEAR PROGRAMMING (MILP)
MILP is mathematically similar as the previously discussed LP optimization technique. However, when dealing with an MILP model, any decision variables should be constrained as integer values. Besides, the decision variables could be discrete where the binary variables are introduced in this optimization problem.

2.4.4. MIXED INTEGER NON-LINEAR PROGRAMMING (MINLP)
MINLP is a mathematical optimization programming with discrete and continuous variables and nonlinearities in the set of constraints and/or objective functions. MINLP is a combination between mixed integer programming and non-linear programming. To understand how MINLP solve the non-linear problem, the mathematical formulation in eqs. 2.2 is written as follows.

$$\begin{aligned} \text{minimize} \quad & f(x,y) \\ \text{subject to} \quad & g(x,y) \leq 0 \\ & x \in X, y \in Y \quad \text{integer} \end{aligned} \tag{2.2}$$

where $f(x,y)$ is a nonlinear objective function and $g(x,y)$ is a nonlinear constraint function. The x and y are the decision variables. The functions $f(x,y)$ and $g(x,y)$ are assumed to be convex and bounded over X and linear in y. The constraints may contain equality and inequality equations which bound the feasible solution. Therefore, the optimal solution of the optimization problem will be found in this boundary of the feasible region.

2.5. CONCLUSION
A large penetration of uncontrolled EVs charging in the distribution grid could lead to several serious problems, such as severe undervoltage, large power losses, etc. This situation can be prevented by scheduling the EVs charging, so that the EVs will not start charging shortly after being connected to the charger, or called as smart charging. Moreover, the EVs can also act not only as loads, but they can also become dynamic storage

in the distribution grid. This concept is known as a vehicle-to-grid (V2G) concept. V2G operation has several benefits, for instance active power regulation, load balancing, storing RESs excess energy, etc.

Changing the strategy of EVs charging from the uncontrolled way into a smart charging scheme would give both the technical and economic benefits for several parties. The authors in [34] showed in their findings that by applying a smart charging process, the charging cost was decreased by 118.44%. Besides, enabling a coordinated charging scheme could also avoid such a large voltage deviations in the distribution grid.

Furthermore, the previous related studies in [14] and [45] have shown that by implying the smart charging scheme, it could provide an economic and technical benefits, respectively. The study in [14] found that the total operating cost of EVs charging could be reduced by around 153.35%. Also, the author [45] proved in her study that by implying a smart charging strategy in a distribution network could mitigate the grid violations, such as the voltage deviations and the distribution transformer power limit. To provide a scientific contribution, this thesis project would combine two previous related studies which have been done in [14] and [45]. Therefore, both of the technical and economic aspect will be discussed further in this thesis. From the technical aspect, this thesis will include the grid constraints which is aimed to mitigate the grid violations. Also, an economic analysis regarding the calculation of the total operational cost will be also included in this thesis project.

By the end of this chapter, several optimization techniques have been discussed. One of the aforementioned optimization problem will be implemented in this thesis to achieve its objective. In addition, to select which optimization model is suitable to solve the problem, the mathematical formulations needs to be first defined. Therefore, the selection of the optimization model will later be chosen in the following chapter.

3

Problem Formulation

Nomenclature

Indexes and sets

n	Nodes, running from 1 to N
c	Electric vehicles, running from 1 to C
t	Time, running from 1 to T minutes

Parameters

EV parameters

$EC_{c,n}^{max}$	Maximum energy that can be stored in the cth EV at the nth node for all time periods t [kWh]
$P_{EV_{c,n}}^{+,max}$	Maximum charging power of the eth EV at the cth bus and the nth node [kW]
$P_{EV_{c,n}}^{-,max}$	Maximum discharging (V2G) power from the cth EV at the nth node to the grid [kW]
$EC_{arrival_{c,n}}$	Energy stored in the cth EV at the nth node at arrival time [kWh]
$EC_{departure_{c,n}}$	Energy stored in the cth EV at the nth node at departure time [kWh]
ΔP_{EV}	Maximum EV (dis)charging rate of change in power (ramp rate) per time step t [kW]
$t_{arrival_{c,n}}$	Arrival time of the cth EV at the nth node [minute]
$t_{departure_{c,n}}$	Departure time of the cth EV at the nth node [minute]
η_{EV}	EV (dis)charging efficiency [-]

PV SYSTEM PARAMETERS

$P^{max}_{PV_{n,t}}$ Maximum DC power generated by PV system at the nth node during time period t [kW]

η_{inv} Solar inverter efficiency [-]

DISTRIBUTION GRID PARAMETERS

$P^{+,max}_{grid_{c,n}}$ Maximum power drawn from the grid to each cth EV at the nth node [kW]

$P^{-,max}_{grid_{c,n}}$ Maximum power fed to the grid from each cth EV at the nth node [kW]

P^{nom}_{tr} Nominal power of the distribution grid transformer [kW]

$P_{load_{n,t}}$ Local residential load power at the nth node during time period t [kW]

V^{nom}_{n} Nominal voltage magnitude at each node [V]

Z_n Cable impedance of a line that connects two neighboring nodes [Ω]

$G_{n,m}$ Real part of the element in Y_{bus} at the n row and m column [℧]

$B_{n,m}$ Imaginary part of the element in Y_{bus} at the n row and m column [℧]

λ_{deg} EV's battery degradation costs [€/kWh]

λ_{PV_t} Marginal energy buying price from the PV system during time period t [€/kWh]

λ_{G2V_t} Marginal energy buying price from the grid during time period t [€/kWh]

λ_{FIT_t} Marginal energy selling price to the grid during time period t [€/kWh]

VARIABLES

ELECTRIC VEHICLE VARIABLES

$EC_{c,n,t}$ Energy stored in the cth EV at the nth node during time period t [kWh]

$P_{EV_{c,n,t}}$ Total power exchange of the cth EV at the nth node during time period t [kW]

$P^{+}_{EV_{c,n,t}}$ Charging power of the cth EV at the nth node during time period t [kW]

$P^{-}_{EV_{c,n,t}}$ Discharging power of the cth EV at the nth node to the grid during time period t [kW]

PV SYSTEM VARIABLES

$P_{PV-EV_{c,n,t}}$ Power delivered from the PV system to the cth EV at the nth node during time period t [kW]

$P_{PV-grid_{n,t}}$ Power delivered from the PV system at the nth node to the grid during time period t [kW]

Distribution grid variables

$P^{+}_{grid_{n,t}}$	Power drawn from the grid to the all aggregated EVs at the nth node during time period t [kW]
$P^{-}_{grid_{n,t}}$	Power fed to the grid from the all aggregated EVs at the nth node during time period t [kW]
$V_{n,t}$	Voltage magnitude at the nth node during time period t [V]
$\theta_{n,t}$	Voltage angle at the nth node during time period t [rad]
C_{ch}	Charging costs from the grid and PV system [€]
R_{dis}	Revenues from discharging by V2G application and PV-to-Grid power [€]
TC	Total operational costs $(C_{ch} - R_{dis})$ [€]

Binary variables

$u_{c,n,t}$	Binary variable which determines whether the cth EV at the nth node during time period t is available for **charging** (1) or not (0) [-]
$v_{c,n,t}$	Binary variable which determines whether the cth EV at the nth node during time period t is available for **discharging** (1) or not (0) [-]

3.1. INTRODUCTION

In this chapter, the mathematical formulation of the optimization problem will be defined. Section 3.2 presents the constraints of EV, PV system and the distribution grid which are set to solve the optimization problem. Then, the objective function of the optimization model will be formulated into mathematical equations. Lastly, the optimization technique will be selected based on the mathematical formulations of the objective function and constraints.

3.2. MATHEMATICAL FORMULATION

3.2.1. ELECTRIC VEHICLE CONSTRAINTS

All modeled EVs contain Lithium-ion batteries. It is assumed that the EVs do not need to be fully charged upon departure time. Moreover, the battery capacity during the departure time is also set from the beginning. A single EV cannot be charged and discharged at the same time period t. It is only possible to charge single EV at one specific charging station.

Eqs. 3.1 will make sure that the charging power $P^{+}_{EVc,n,t}$ and the discharging power for the V2G concept $P^{-}_{EVc,n,t}$ are still within their respective bounds. The EV power is separated into two variables because the discharging power for the V2G operation $P^{-}_{EVc,n,t}$ will affect the calculation of the operational cost which includes the battery degradation costs.

$$
\begin{aligned}
0 \leq P^{+}_{EVc,n,t} \leq u_{c,n,t} \cdot P^{+,max}_{EV_{c,n}} \quad \forall c,n,t \\
0 \leq P^{-}_{EVc,n,t} \leq v_{c,n,t} \cdot P^{-,max}_{EV_{c,n}} \quad \forall c,n,t
\end{aligned}
\tag{3.1}
$$

Eq. 3.2 is constrained to avoid simultaneous charging and discharging of single EV at a certain charging station.

$$
u_{c,n,t} + v_{c,n,t} \leq 1 \quad \forall c,t \tag{3.2}
$$

To ensure the safety of operation, there will not be any charging or discharging process before the arrival of the EV ($t_{arrival_{c,n}}$) or after the departure of the EV ($t_{departure_{c,n}}$), hence, Eqs. 3.3 will be imposed on the model. The connection of the EV is checked by analyzing if the present time is between the arrival and departure time, so that the EV is available to either charge or discharge as shown in Fig. 3.1.

$$
\begin{aligned}
u_{c,n,t} = 0 \quad \text{if} \quad t < t_{arrival_{c,n}} \quad \text{or} \quad t > t_{departure_{c,n}} \quad \forall c,n \\
v_{c,n,t} = 0 \quad \text{if} \quad t < t_{arrival_{c,n}} \quad \text{or} \quad t > t_{departure_{c,n}} \quad \forall c,n
\end{aligned}
\tag{3.3}
$$

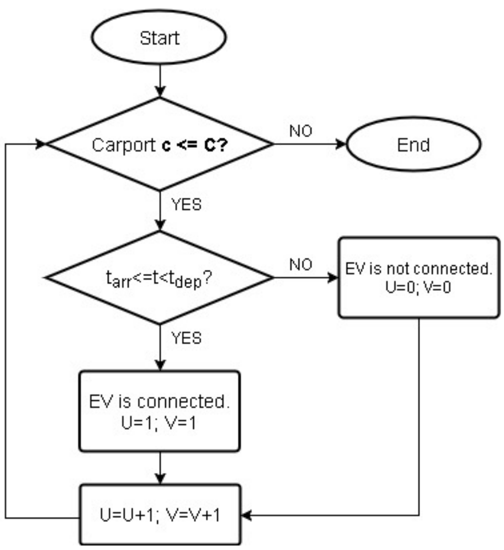

Figure 3.1: Checking the EV connection

POWER BALANCE

The total power exchange of the EV is constrained as follows.

$$P_{EV_{c,n,t}} = \eta_{EV} \cdot P^{+}_{EV_{c,n,t}} - \frac{1}{\eta_{EV}} \cdot P^{-}_{EV_{c,n,t}} \quad \forall c,n,t \tag{3.4}$$

$$\text{Subject to:}$$
$$P^{+}_{EV_{c,n,t}} \geq 0 \qquad \forall c,n,t$$
$$P^{-}_{EV_{c,n,t}} \geq 0 \qquad \forall c,n,t$$

where η_{EV} is the (dis)charging efficiency of the EV. The efficiency of charging and discharging are assumed constant in any different value of power. The authors in [46] showed that a semi-fast 22 kW charger (or called as Electic Vehicle Supply Equipment, EVSE) has an efficiency of 92% for charging and V2G application. Hence, this value is taken into consideration as the efficiency of (dis)charging of the EV.

To avoid a large variation in the EV charging rate (both charging and discharging) at each timestep which is unwanted, a rate of change is contrained as follows [47].

$$\begin{aligned}
&P^{+}_{EV_{c,n,t+1}} - P^{+}_{EV_{c,n,t}} \leq \Delta P_{EV} \quad \forall c,n,t \\
&P^{-}_{EV_{c,n,t+1}} - P^{-}_{EV_{c,n,t}} \leq \Delta P_{EV} \quad \forall c,n,t \\
&P^{+}_{EV_{c,n,t}} - P^{+}_{EV_{c,n,t-1}} \geq -\Delta P_{EV} \quad \forall c,n,t \\
&P^{-}_{EV_{c,n,t}} - P^{-}_{EV_{c,n,t-1}} \geq -\Delta P_{EV} \quad \forall c,n,t
\end{aligned} \tag{3.5}$$

where ΔP is a defined limit, in [kW], by which the charging rate can vary, compared to the charging rate at the previous timestep. The (dis)charging ramp rate is limited only by the EV charger maximum power which is 22 kW [48]. However, due to a security reason, the ramp rate limit is decreased by 10% which amounts to 20 kW.

ENERGY STORED IN THE EV BATTERY

To calculate the SOC of the EV's battery during time period t, the previous SOC at time period $t-1$ has to be added. Therefore, the energy content of the cth EV at the nth node during time period t is constrained as follows.

$$\begin{aligned}
&EC_{c,n,t} = EC_{c,n,t-1} + P_{EV\,c,n,t} \cdot \Delta t \quad \text{for} \quad t_{arrival_{c,n}} < t < t_{departure_{c,n}} \quad \forall c,n \\
&EC_{c,n,t} = EC_{departure_{e,c,n}} \quad \text{for} \quad t > t_{departure_{c,n}} \quad \forall c,n \\
&EC_{c,n,t} = 0 \quad \text{for} \quad t < t_{arrival_{c,n}} \quad \forall c,n
\end{aligned} \tag{3.6}$$

where Δt = timestep (1 minute). The EV's battery should not be charged over its maximum energy rating to protect the battery from overcharging nor discharged below 20% of its maximum energy rating [49]. Therefore, the energy content for each EV is constrained as follows.

$$0.2 \cdot E^{max}_{e,c,n} \leq E_{e,c,n,t} \leq E^{max}_{e,c,n} \quad \forall c,n,t \tag{3.7}$$

$$\begin{aligned}
&EC_{c,n,t} = EC_{arrival_{c,n}} \qquad \text{if } t = t_{arrival_{c,n}} \qquad \forall c,n \\
&EC_{c,n,t} = E_{departure_{c,n}} \qquad \text{if } t = t_{departure_{c,n}} \qquad \forall c,n
\end{aligned}$$

3.2.2. PV SYSTEM CONSTRAINTS

In the distribution network, a 32 kWp PV system is installed at every node. The PV power can both supply the EVs at the same node and feed its energy back to the distribution network. A solar inverter is equipped to the output of PV system. It is assumed that the PV system is using SMA Sunny Tripower 30000TL-US which has an efficiency of 98% [50]. Therefore, the PV power balance can be written as follows.

$$\frac{1}{\eta_{inv}} \cdot \left\{ \sum_{c=1}^{C} \left(P_{PV-EV_{c,n,t}}\right) + P_{PV-grid_{n,t}} \right\} \leq P_{PV_{n,t}}^{max} \quad \forall t \tag{3.8}$$

Subject to:

$$\begin{array}{lll} P_{PV-EV_{c,n,t}} \geq 0 & \text{if } t_{arrival_{c,n}} < t < t_{departure_{c,n}} & \forall c, n \\ P_{PV-EV_{c,n,t}} = 0 & \text{if } t < t_{arrival_{c,n}} \text{ or } t > t_{arrival_{c,n}} & \forall c, n \\ P_{PV-grid_{n,t}} \geq 0 & & \forall c, n, t \end{array}$$

where $P_{PV-EV_{c,n,t}}$ and $P_{PV-grid_{n,t}}$ are the PV power used to charge the cth EV and fed to the distribution grid at the nth node during time period t, respectively.

3.2.3. DISTRIBUTION GRID NETWORK CONSTRAINTS

The typical Dutch Low Voltage (LV) distribution grid with the voltage level of 230/400 V (50 Hz) will be implied for the optimization model of EVs charging in an EV-PV-Grid system. The model incorporates a 400 kVA, 10/0.4 kV step-down transformer. Separate power converters are implemented to integrate the EVs, PV system and the grid which are connected to a node. The PV system is connected to a solar inverter which convert DC to AC power which contains maximum power point tracking (MPPT). The EV is linked to a semi-fast AC charger for EVs. Furthermore, the model structure is based on CIGRE benchmark low voltage distribution network including all of its characteristics and specifications [11]. Moreover, the model implements a radial layout.

GRID MONITORING

The distribution network includes the PV system, local residential load and EVs. To ensure that the transformer will not be overloaded, the power which is fed to and drawn from the grid is constrained as follows.

$$\begin{gathered} 0 \leq \sum_{n=1}^{N} \left(P_{grid_{n,t}}^{+} + P_{load_{n,t}}\right) \leq P_{tr}^{nom} \quad \forall n, t \\ 0 \leq \sum_{n=1}^{N} \left(P_{grid_{n,t}}^{-} + P_{PV-grid_{n,t}}\right) \leq P_{tr}^{nom} \quad \forall n, t \end{gathered} \tag{3.9}$$

It is assumed that the local residential load at each node are supplied only by the grid as it is the DSO's responsibility to fulfill the base load consumption as it can be clearly seen in Eq. 3.9. Moreover, the PV system at each node only produces active power and no reactive power as well as the local load which only consume active power (p.f. = 1). As previously stated in Eq. 3.8, the PV system will feed its power to the distribution grid only when it has excess power for charging the aggregated EVs at one node. Furthermore, the nominal power of the grid transformer, P_{tr}^{nom}, is 400 kVA which is based on the CIGRE benchmark on low voltage microgrid network [11].

Based on mandatory European standard EN50160 [51], the voltage deviation which is allowed, is 10% above or under the nominal voltage and constrained as follows.

$$0.9 \cdot V_n^{nom} \leq V_{n,t} \leq 1.1 \cdot V_n^{nom} \quad \forall n, t \tag{3.10}$$

where the nominal voltage, V_n^{nom}, is set at 400 V for the low voltage distribution system.

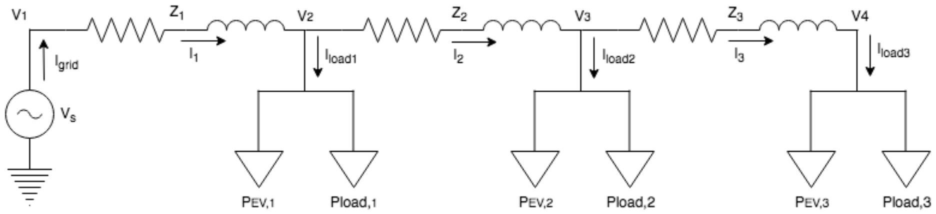

Figure 3.2: Schematic of implemented model

POWER FLOW BALANCE

For the grid used in the model shown in Fig. 3.2, the Kirchoff's current law (KCL) equations are:

$$\begin{aligned} I_{grid} &= \frac{V_1 - V_2}{Z_1} \\ \frac{V_1 - V_2}{Z_1} &= \frac{V_2 - V_3}{Z_2} + I_{load1} \\ \frac{V_2 - V_3}{Z_2} &= \frac{V_3 - V_4}{Z_3} + I_{load2} \\ \frac{V_3 - V_4}{Z_3} &= I_{load3} \end{aligned} \tag{3.11}$$

Eq. 3.11 can be rewritten in matrix notation as follows.

$$\begin{bmatrix} I_{grid} \\ I_{load1} \\ I_{load2} \\ I_{load3} \end{bmatrix} = \begin{bmatrix} \frac{1}{Z_1} & -\frac{1}{Z_1} & 0 & 0 \\ \frac{1}{Z_1} & -\frac{1}{Z_1} - \frac{1}{Z_2} & \frac{1}{Z_2} & 0 \\ 0 & \frac{1}{Z_2} & -\frac{1}{Z_2} - \frac{1}{Z_3} & \frac{1}{Z_3} \\ 0 & 0 & \frac{1}{Z_3} & -\frac{1}{Z_3} \end{bmatrix} \begin{bmatrix} V_1 \\ V_2 \\ V_3 \\ V_4 \end{bmatrix} \tag{3.12}$$

which equals to

$$\begin{bmatrix} I_{grid} \\ I_{load1} \\ I_{load2} \\ I_{load3} \end{bmatrix} = \begin{bmatrix} Y_{11} & Y_{12} & Y_{13} & Y_{14} \\ Y_{21} & Y_{22} & Y_{23} & Y_{24} \\ Y_{31} & Y_{32} & Y_{33} & Y_{34} \\ Y_{41} & Y_{42} & Y_{43} & Y_{44} \end{bmatrix} \begin{bmatrix} V_1 \\ V_2 \\ V_3 \\ V_4 \end{bmatrix} \tag{3.13}$$

where $Y_{11} = G_{11} + jB_{11}$ and it can be rewritten as follows.

$$Y_{n,m} = G_{n,m} + jB_{n,m} \tag{3.14}$$

where $G_{n,m}$ and $B_{n,m}$ are the real and imaginary part of the element in Y_{bus} at the n row and m column, respectively.

An AC model power flow in the distribution grid is implemented in optimization model. Then, the total active power at the node nth can be calculated below.

$$\sum P_{drawn_{n,t}} - \sum P_{fed_{n,t}} = \sum_{m=1}^{N} V_{n,t} \times V_{m,t} \left(G_{n,m} \cos\left(\theta_{n,t} - \theta_{m,t}\right) + B_{n,m} \sin\left(\theta_{n,t} - \theta_{m,t}\right)\right) \quad \forall t; m \neq n \tag{3.15}$$

where $\sum P_{drawn_{n,t}}$ and $\sum P_{fed_{n,t}}$ are the total active power which is drawn from and fed to the grid, respectively. Therefore, Eq. 3.15 is expanded and written as follows.

$$\begin{aligned} &\left(P^{+}_{grid_{n,t}} + P_{load_{n,t}}\right) - \left(P^{-}_{grid_{n,t}} + P_{PV-grid_{n,t}}\right) = \\ &\qquad \sum_{m=1}^{N} V_{n,t} \times V_{m,t} \left(G_{n,m} \cos\left(\theta_{n,t} - \theta_{m,t}\right) + B_{n,m} \sin\left(\theta_{n,t} - \theta_{m,t}\right)\right) \quad \forall t; m \neq n \end{aligned}$$

Subsequently, the power balance of the overall system can be derived by using equations mentioned previously.

$$\sum_{n=1}^{N}\sum_{c=1}^{C} \left(P_{PV-EV_{c,n,t}}\right) + \sum_{n=1}^{N} \left(P^{+}_{grid_{n,t}} - P^{-}_{grid_{n,t}}\right) = \sum_{n=1}^{N}\sum_{c=1}^{C} \left(P^{+}_{EVc,n,t} - P^{-}_{EVc,n,t}\right) \quad \forall t \tag{3.16}$$

3.2.4. OBJECTIVE FUNCTION

As all of the constraints have been discussed previously, finally the objective function of the optimization model is presented in this section. The goal of this thesis is to find the most possible minimum operational cost of the EVs charging from PV system in a low voltage distribution network. Furthermore, the obtained objective function may differ for each different identified case studies. Therefore, the mathematical formulation of the objective function is explained below.

MINIMIZE THE TOTAL OPERATIONAL COST

In this thesis, the energy price that is being implied to the optimization model is dynamic which is changing every one hour based on APX SPOT Power NL Day Ahead according to the related previous study [3]. The optimization will tend to charge the EVs from the grid when the buying price is low and apply the V2G concept when the selling price is high. However, the authors in [52] showed in their results that the utilization of V2G technology may result to a battery degradation. Therefore, a battery degradation cost will be introduced in the optimization model with a constant value of \$0.042/kWh or approximately €0.038/kWh [52]. The other way to charge the EVs can also be done by drawing the PV power which has a low constant price [53]. The detailed explanation on the energy price will be further discussed in 4.1.5. In addition, to add up more revenues in a one day operation, the PV power feed its energy back to the grid when the energy selling price is high. Then, the charging costs and revenues made by selling the PV power to grid or by utilizing V2G is written as follows in Eqs. 3.17 and 3.18.

CHARGING COSTS FROM GRID AND PV POWER

$$C_{ch} = \sum_{t=1}^{T}\sum_{n=1}^{N} \lambda_{G2V_t} \cdot P^{+}_{grid_{n,t}} \cdot \Delta t + \sum_{t=1}^{T}\sum_{n=1}^{N}\sum_{c=1}^{C} \lambda_{PV_t} \cdot P_{PV-EV_{c,n,t}} \cdot \Delta t \tag{3.17}$$

REVENUES FROM V2G AND SELLING PV POWER TO GRID

$$R_{dis} = \sum_{t=1}^{T}\sum_{n=1}^{N} \left(\lambda_{FIT_t} - \lambda_{deg}\right) \cdot P^{-}_{grid_{n,t}} \cdot \Delta t + \left(\lambda_{FIT_t} - \lambda_{PV_t}\right) \cdot P_{PV-grid_{n,t}} \cdot \Delta t \tag{3.18}$$

TOTAL OPERATIONAL COSTS

$$\min \quad TC = C_{ch} - R_{dis} \tag{3.19}$$

$$\begin{aligned} \min \quad TC = &\sum_{t=1}^{T}\sum_{n=1}^{N} \lambda_{G2V_t} \cdot P^{+}_{grid_{n,t}} \cdot \Delta t + \sum_{t=1}^{T}\sum_{n=1}^{N}\sum_{c=1}^{C} \lambda_{PV_t} \cdot P_{PV-EV_{c,n,t}} \cdot \Delta t \\ &- \sum_{t=1}^{T}\sum_{n=1}^{N} \left(\lambda_{FIT_t} - \lambda_{deg}\right) \cdot P^{-}_{grid_{n,t}} \cdot \Delta t - \sum_{t=1}^{T}\sum_{n=1}^{N} \left(\lambda_{FIT_t} - \lambda_{PV_t}\right) \cdot P_{PV-grid_{n,t}} \cdot \Delta t \end{aligned} \tag{3.20}$$

3.3. CONCLUSION

This chapter is considered as the main focus of this thesis work. The mathematical equations including the decision variables, the system constraints, and the objective function need to be defined as realistic as possible. This formulation represents the real-life condition based on its technical assumption. Moreover, after determining the aforementioned objective function of the proposed model, it is required to choose which optimization model is suitable to solve the problem. Therefore, an MINLP optimization technique, in which a combination between MILP and NLP, is selected in this thesis. The MINLP is mainly employed in scheduling and controlling the EVs charging under a set of technical constraints such as the bus voltage magnitude & angle boundaries and the grid transformer power limit. The distribution networks used in this thesis are constrained to determine the AC model power flow in the grid. The main reason of choosing the MINLP is due to the use of binary variables and the non-linear constraints as seen on Eqs. 3.2 and 3.15, respectively. Finally, to understand the process on how the proposed power management system is implemented to solve the optimization problem, Fig. 3.3 is depicted.

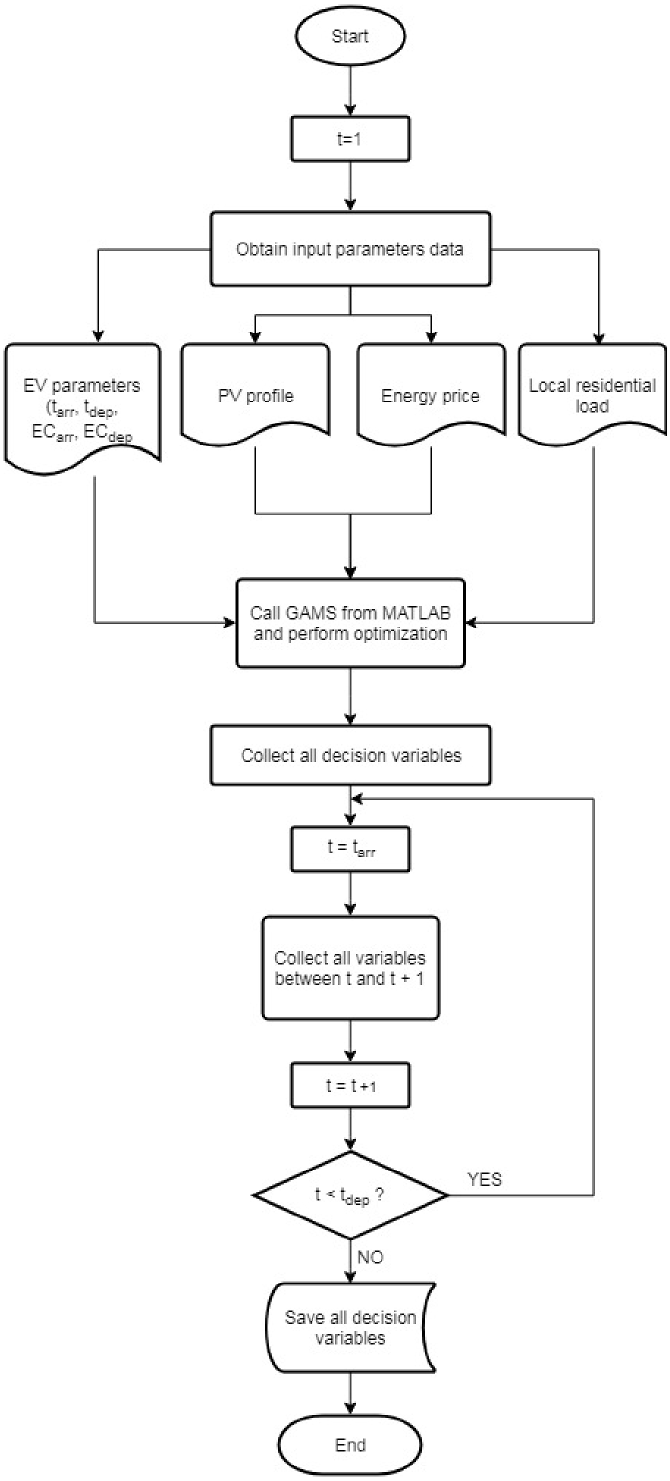

Figure 3.3: Flowchart of the proposed power management system

4

Data Characteristics and Case Studies

In this study, to check the performance of the proposed power management system, several parameters need to be taken into consideration based on various real-life case studies. Accordingly, the optimization model can be evaluated realistically. Section 4.1 discusses about how input parameters data are used in this thesis. Then, section 4.2 presents all identified case studies which will be used to evaluate the behavior of the proposed model. Moreover, this study will consider four different PV profiles and varied EV penetrations.

4.1. Parameters Data

Before performing the simulation of the optimization model, several input parameters data need to be obtained. The following sections will describe in detail how the input parameters get acquired.

4.1.1. Distribution Grid Characteristics

The distribution network that is applied to the optimization model is based on the CIGRE benchmark of low voltage distribution network [11]. The characteristics of the grid are modeled as real as possible. The grid configuration is a radial architecture. At each node, several semi-fast EV chargers with 22 kW maximum (dis)charging power can be connected. These chargers are generally known and installed on the road in The Netherlands [54–56]. Each node of the distribution network also consists of the distributed generation which is PV power generation and the residential load as base load. To make into a more real-life situation, cable impedance between neighboring nodes are taken into account as seen in Table 4.1. Moreover, the grid architecture is depicted in Fig. 4.1.

4.1.2. Residential Load Data

The local load data which is located at each node is based on the CIGRE low voltage microgrid network benchmark [11]. The authors in [12] observed that typically the transformer in a distribution network is half-loaded. Hence, the load scale is based on the average number of households connected to the typical Dutch distribution network which is 50-100 households [12]. A total number of 60 households is selected for this thesis which is divided into 20 houses per node. Furthermore, the average peak load of each typical Dutch house is 1.1 kVA. Hence, the daily residential load profile per node is illustrated in Fig. 4.2.

Table 4.1: Line characteristics based on CIGRE benchmark [11]

	Line type	Distance [km]	Impedance [Ω]
Slack Node - Node 1 (Z_{01})		0.8	0.2187
Node 1 - Node 2 (Z_{12})	Underground Line (3x15 mm^2 Al + 5 mm^2 Cu)	0.6	0.164
Node 2 - Node 3 (Z_{23})		0.7	0.1912

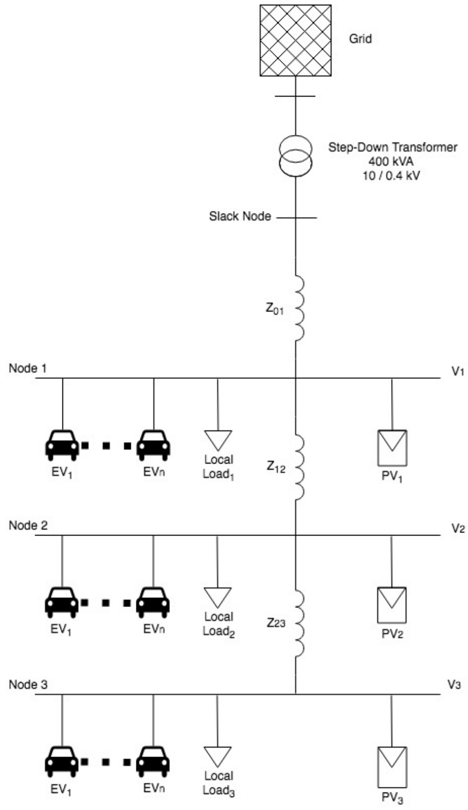

Figure 4.1: The implemented model of distribution network based on CIGRE benchmark [11]

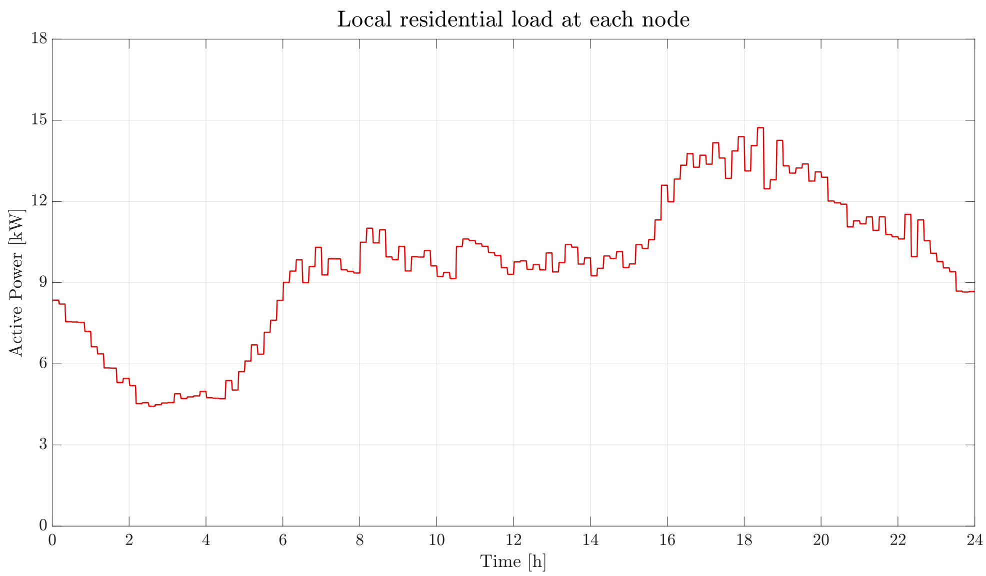

Figure 4.2: Dutch daily residential load profile per node (consisting of 20 houses) [12]

4.1.3. EV CHARACTERISTICS

The proposed power management system of EVs charging in this thesis require several EV input data such as arrival & departure time and the battery's SOC during arrival & departure time. Hence, several literature are taken into consideration to make these parameters as realistic as possible.

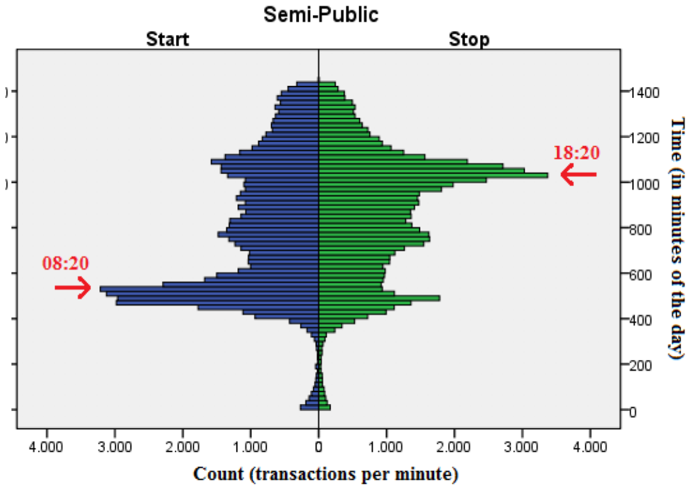

Figure 4.3: Charging behavior of the Dutch semi-public charging stations [13]

Table 4.2: Top Sold EVs' technical specification

	EV types		
	Tesla Model S	**Nissan Leaf**	**Renault ZOE**
Battery capacity [kWh]	90	30	22
Maximum charging power [kW]	120	5	43
Amount registered up to June 2018 [57]	9,661	3,351	2,993

CHARGING BEHAVIOR

The author in [13] found in his result that in 1198 semi-public charging points in the Netherlands, the EVs charging happen mostly in the morning at 08.20 AM and ends at 06.20 PM as seen in Fig. 4.3. Semi-public charging station is an EV charging point where is located in office area, but can also be used for public. Therefore, these parameters is considered to be used in this study.

BATTERY CAPACITY

There are so many different types of EVs in the Netherlands, but the top-three sold EVs are chosen as the input parameters for this study which is shown in Table 4.2. It is assumed in this study that every EV is not guaranteed to have a maximum battery capacity upon leaving the charging station as previously stated in section 3.2.1.

4.1.4. PV SYSTEM PROFILE

At every node of the distribution network, a PV system is installed to enhance the integration of EVs charging from the grid. The installation of the PV system can improve the revenue of the system which may lead to decreasing the total operational cost. Therefore, the PV system need to be sized adequately. To make the model as realistic as possible, the PV generation profile used in this thesis is based on [58] with the irradiance data taken from Royal Dutch Meteorological Institute (in Dutch: *Koninklijk Nederlands Meteorologisch Instituut*, KNMI) [59] with 1 minute time resolution. For the Summer, Winter, Spring and Autumn profile is taken in the first week of June, January, March and September, respectively. The study conducted in [58] simulated a 10 kW PV system and found a maximum annual energy yield which is 10,890 kWh over three years in 2011-2013.

To be implemented in this study, the PV system need to be scaled realistically. In the Netherlands, the four different season have variations in global irradiation. This variation may affect the local residential profile for the PV penetration [12]. Taking into account that there there are 20 households at every node as previously mentioned in section 4.1.2 and based on data from [12], it is found that every household with terraced house type has rated peak power 1.60 kWp. Then, assuming that every house has installed their own PV array, therefore the total amount of installed PV power generation at every node is $20 \times 1.6 \quad \text{kWp} \approx 32\text{kWp}$. Consequently, the PV system is scaled to 32 kWp of rated peak power per node of the distribution network. To sum up, Fig. 4.4 illustrates the different PV generation profile in the different season of 30 kWp installed at every node of

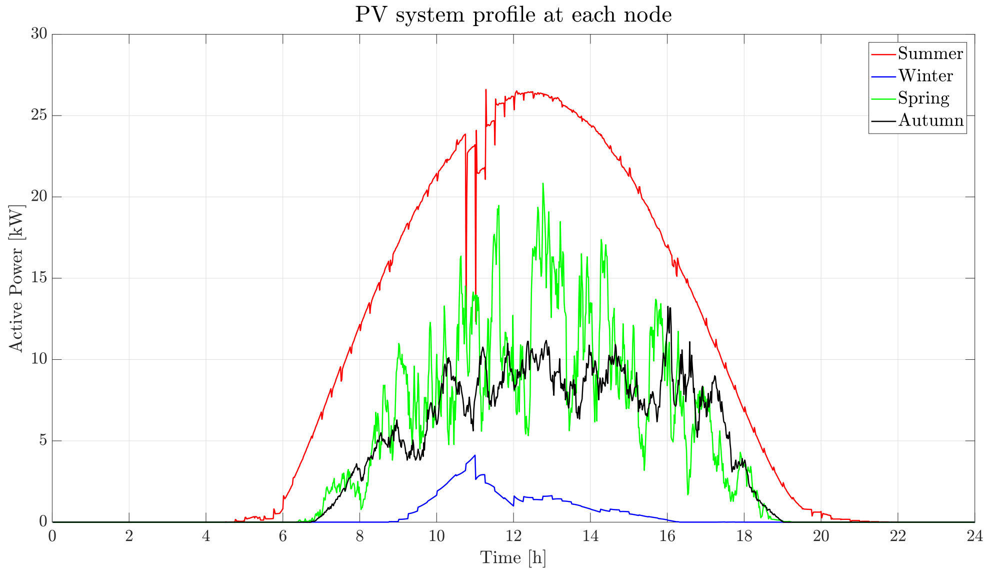

Figure 4.4: PV profiles at each node for different season

the distribution network.

4.1.5. ENERGY PRICE

Nowadays, many households in the Netherlands pay the same electricity cost during the entire day by per kWh of energy they consume. The Dutch electricity tariff amounts to approximately €0.16/kWh. Furthermore, the consumer of the electricity can also become a producer to receive money by selling back its energy from the RESs, for instance rooftop PV on households. However, the Netherlands does not make use of such a Feed-in Tariff, but rather s net-metering. Net-metering is a method that the electricity consumer can feed its generated renewable energy back to the grid where it can decrease the total consumption at the end of the month.

In addition, this thesis will imply a dynamic tariff to make a deeper understanding how the optimization model can work during fluctuating price during the whole day. Because this strategy is not yet carried out in the Netherlands, the data will be acquired from the scaled day-ahead hourly energy prices from APX Power NL. The author of [14] in a related previous study has already scaled the hourly energy price based on the data from APX Power as shown in Fig. 4.5. To apply such a financial stimulus, 90% of the dynamic energy price is selected to be applied for this study. Besides, the marginal costs of the PV generation needs to be considered as well. The authors of [53] showed in their findings that the marginal costs would be €0.097/kWh for rooftop PV system in the Netherlands. Therefore, this cost will be included in this study as depicted in Fig. 4.5.

4.2. CASE STUDIES

To assess the performance of the proposed power management system of EVs charging, several case studies based on previously mentioned data characteristics are simulated. First, four different season are examined to see the impact of the PV penetration to the grid. Then, the various number of EVs per node is considered in order to check when the optimization model results result in an infeasible solution. Then, a comparison between including and excluding the grid constraints is simulated which aims to study the impact on the total operational cost. For the no-grid constraints case, Eqs. 3.9 and 3.10 are removed from the optimization model. Besides, the EVs arrival & departure time and the initial & final SOC of each EV are first randomly chosen and then keep them at a fixed value to analyze the simulation results in a feature-for-feature comparison. Finally, the case studies simulated in this thesis is shown in Table 4.3.

4.3. CONCLUSION

The input parameters which are required to evaluate the performance of the proposed power management system were thoroughly discussed in this chapter. The parameters were acquired from the realistic data under

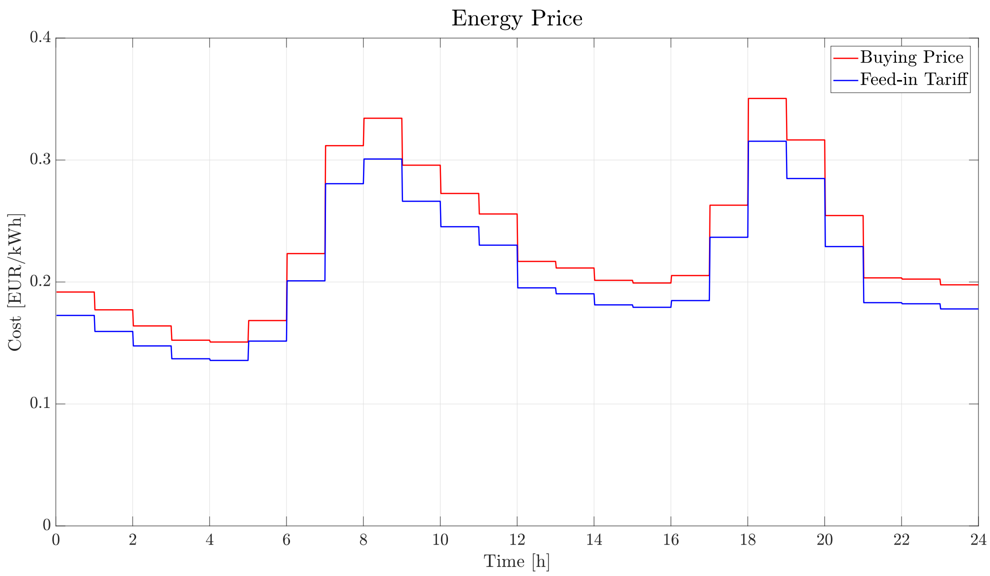

Figure 4.5: Energy price for one day based on APX Power NL data, reproduced from [14]

Table 4.3: Overview of case studies

Case Study	PV System Profile	Number of EVs per node	Grid Constraints
1A	*Summer*	2	✓
			-
1B		5	✓
			-
1C		7	✓
			-
1D		10	✓
			-
2A	*Winter*	2	✓
			-
2B		5	✓
			-
2C		7	✓
			-
2D		10	✓
			-
3A	*Spring*	2	✓
			-
3B		5	✓
			-
3C		7	✓
			-
3D		10	✓
			-
4A	*Autumn*	2	✓
			-
4B		5	✓
			-
4C		7	✓
			-
4D		10	✓
			-

several fundamental assumptions. The following explanations concludes the main remarks regarding the input parameters.

Firstly, the distribution network employed in this thesis is based on the CIGRE benchmark on the low voltage distribution grid. The distribution transformer is rated at 400 kVA with three buses connected to a single line. A line impedance between two neighboring nodes is also taken into consideration. Moreover, a 32 kW PV system, the residential loads and several EVs are connected to each node of the distribution line. Second, the residential load data is also taken from the CIGRE benchmark. Typically, 50-100 Dutch households with an average peak load of 1.1 kVA are supplied from the 400 kVA distribution grid. Then, 60 households which is divided proportionally at every node, is selected to be implied in the model. Thirdly, the charging behavior of the Dutch EV owners is taken from the study in [13]. It is found that the EVs mainly charge in the morning at around 08.20 AM and stop at 06.20 PM in the evening. In addition, the top sold EVs in the Netherlands, i.e. Tesla Model S, Nissan Lead, and Renault Zoe are selected to be used in this study. Fourthly, the PV system installed at each node needs to be sized and scaled sufficiently. The irradiance data of the whole year is taken from Royal Dutch Meteorological Institute. Lastly, a dynamic price is used in this thesis. The price is based on APX Power Hourly NL. It is assumed that every season uses the same price profile.

Furthermore, to combine all of the previously mentioned input parameters data. Several case studies are designed to test the performance of the proposed power management system of EVs charging from PV system in a low voltage distribution network. Hence, a total of 32 case studies are presented in Table 4.3.

5

Simulation Results and Analysis

In this chapter, the simulation results from all identified case studies are presented. All mathematical formulation discussed in section 3.2 are simulated by using General Algebraic Modelling System (GAMS) version 24.9.2 software and then plotted in MATLAB. Every case study discussed in this chapter consists of two different studied case which are the with-grid and no-grid constraints cases. Furthermore, a Discrete and Continuous Optimizer (DICOPT) solver is used to solve the MINLP model. The simulation results for case studies 1A-1D, 2A-2D, 3A-3D and 4A-4D which has been discussed previously are presented in section 5.1, 5.2, 5.3 and 5.4, respectively. The optimal solution which is obtained for all identified case studies are reached with a relative gap of 0.1%. Moreover, all plots of the results will not be shown here, but they can be found further in Appendix A.

5.1. Summer PV Profile

This section will evaluate the performance of the proposed power management system in a one-day operation during summer. The summer PV profile is considered as the best case study as it is more profitable to increase the operational revenues by selling the excess PV energy to the distribution grid. Besides, the total energy yield of PV production during summer case study is 654.45 kWh.

5.1.1. Results of Case Study 1A (Summer, 2 EVs per node)

This section presents the result of case study 1A which employs 2 EVs per node. Fig. 5.1 and 5.2 illustrates the one-day operation of EVs charging with-grid and no-grid constraints, respectively. It is clearly seen that in the morning between 08.30 AM and 09.00 AM, when the EVs arrive at the charging station, they started to discharge their battery as the energy selling price is very high. The same reason comes also to the PV power allocation where it tends to sell its energy back to the grid rather than feeding its energy to charge the EVs as depicted in Fig. A.2. On the other hand, at the end of the day starting from 02.00 PM, when the energy price is low, the PV power is preferable to feed its power to charge the EVs where λ_{PV_t} is always lower than λ_{G2V_t}. It can be said that the PMS decided to delay the charging of EVs when the energy price is low. During investigation, both graphs of Fig. 5.1 and 5.2 looks similar, the fact that it is supported by the simulation results shown in Table A.1. Besides, the PV power used for charging the EVs in the with-grid constraints case is the same as the no-grid constraints which amounts to 25.41%. As a result, the total operational cost of both scenarios are the same, in which €-64.82 that means the aggregator as the EVs fleet operator earn money for a one-day operation. This result has shown that an integration between EVs, PV system and grid is a promising potential to be employed in real life.

Fig. 5.3 displays the aggregated of all EVs power at all nodes and the aggregated EVs connected to each node. It is observed that the EVs charging behavior is closely similar at every node. This decision could happen due to the low penetration of EVs that still alleviate the distribution network constraints. As previously mentioned, the EVs are postponed to be charged during the peak price to reduce the charging costs. In the morning, it is more profitable to discharge via V2G technology when the energy price is significantly high.

As seen on Fig. 5.4, having a high penetration of PV generation may cause the voltage to rise. The end of the feeder seems to have the most severe impact. However, installing more PV system in the distribution network can bring benefits in which more number of EVs can be connected without arising the grid violations.

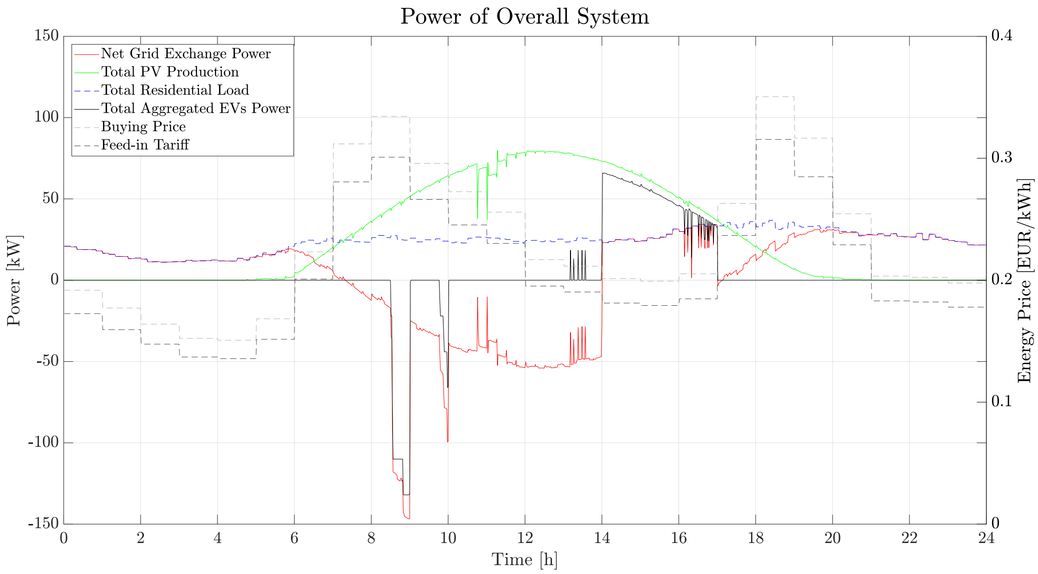

Figure 5.1: Power of overall system for case study 1A (With-Grid Constraints)

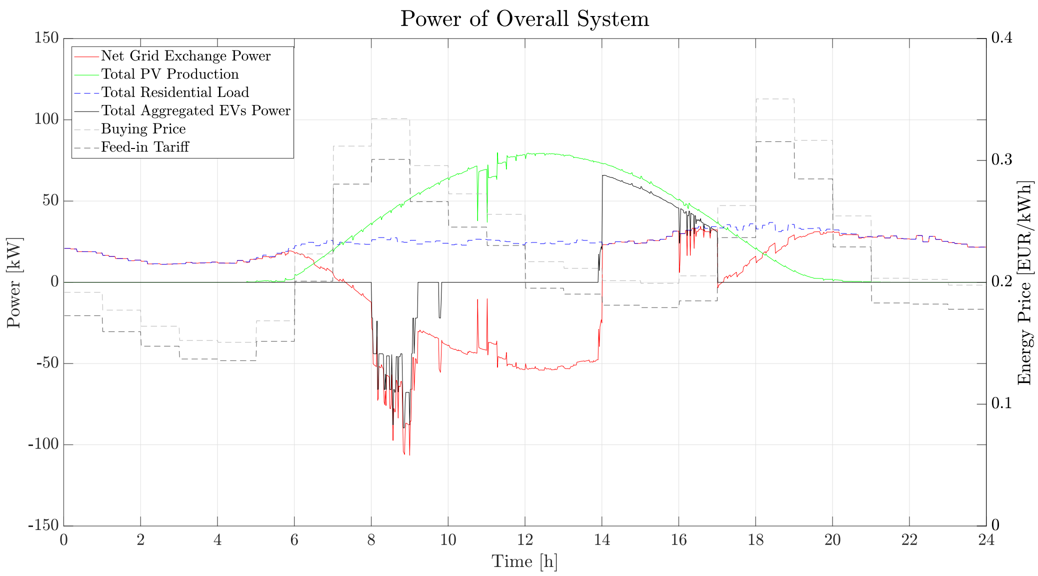

Figure 5.2: Power of overall system for case study 1A (No-Grid Constraints)

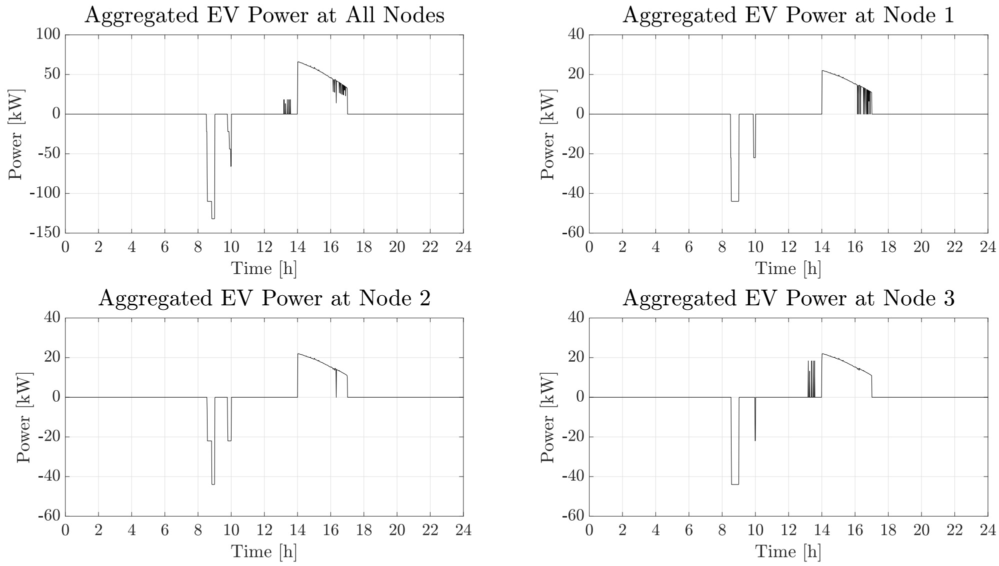

Figure 5.3: Aggregated EV power at all nodes for case study 1A (With-Grid Constraints)

This positive effect is proven in case study 1D that even connecting 10 EVs per node, in total of 30 EVs, the MINLP model can still come to a feasible and optimal solution. Moreover, as illustrated in Fig. 5.4, when the EVs are being charged starting at 02.00 PM, the voltage of each node starts to drop. As a result, node 3 has the worst impact due to the existence of line impedance between the neighboring nodes.

5.1.2. RESULTS OF CASE STUDY 1B (SUMMER, 5 EVS PER NODE)

This section presents the result of case study 1B which employs 5 EVs per node. Fig. 5.5 and 5.6 shows the operation in one-day of EVs charging with-grid and no-grid constraints, respectively. To drastically reduce the total operational costs, the power management system determines to discharge all of the EVs in the morning when the marginal cost of grid energy is high. Then, the EVs are postponed to charge starting from 12.00 PM when the energy price is inexpensive. During this range of time, all of the PV production are used to charge the EVs. The power from the grid is also drawn in combination with the PV power to charge the EVs represented by the red line in Fig. 5.5. Also, the PV power allocated for the EVs is similar for both with-grid constraints and no-grid constraints studied case that equals 48.72%. To have a more extending understanding on the PV power allocation, Fig. A.6 is depicted. In addition, considering the distribution network constraints may add up the total operational cost by 1.43% compared to no distribution network constraints. This result is supported on Table A.1.

Fig. 5.7 shows the aggregated of all EVs power at all nodes and the aggregated EVs connected to each node. Every node of the distribution grid seems to have a typical charging power behavior where the power of each node is around 22 kW, in total up to 66 kW. As previously mentioned, it can also be seen that the PMS procrastinates the EVs charging until the energy price is lower than in the morning. Typically, the model with no-grid constraints studied case has the same charging power manner as seen in Fig. A.5.

Fig. 5.8 shows the voltage profile at each node. During observing the graph, it is seen that at 12.00 PM, the voltage at node 3 which is at the end of the feeder has the worst voltage drop. However, it still lay within the limit of the allowable voltage deviation. The power drawn from the grid to charge the EVs at each node has a different time range. At node 1, 2 and 3, the PMS starts to draw more grid power at 03.00 PM, 02.00 PM and 12.00 PM, respectively. Therefore, it can be said that the PMS decides to take the grid power at different nodes alternately due to avoiding the grid violations. In addition, the voltage at node 3 is always staying at the border of the lower limit because of the longer distribution line to reach node 3. On the contrary, while without considering the distribution network constraints, the PMS allows the EVs to draws the same amount of power from the grid at each node as depicted in figureA.5, but it will lead to unwanted behavior.

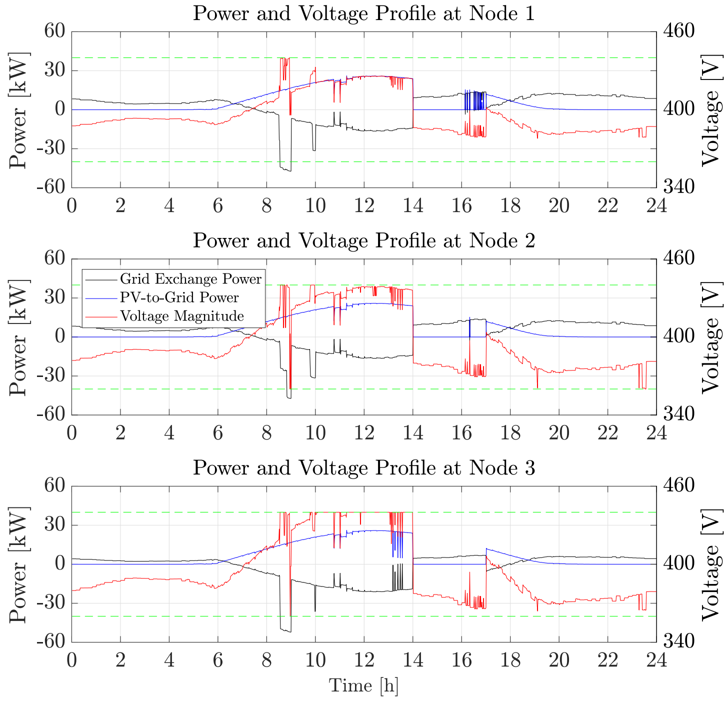

Figure 5.4: Voltage magnitude at all nodes for case study 1A (With-Grid Constraints)

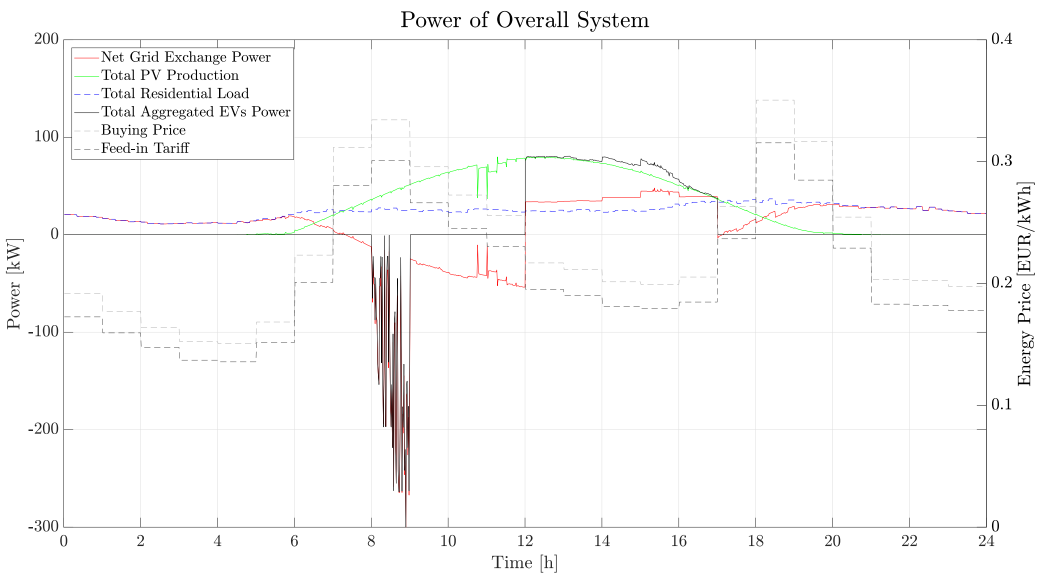

Figure 5.5: Power of overall system for case study 1B (With-Grid Constraints)

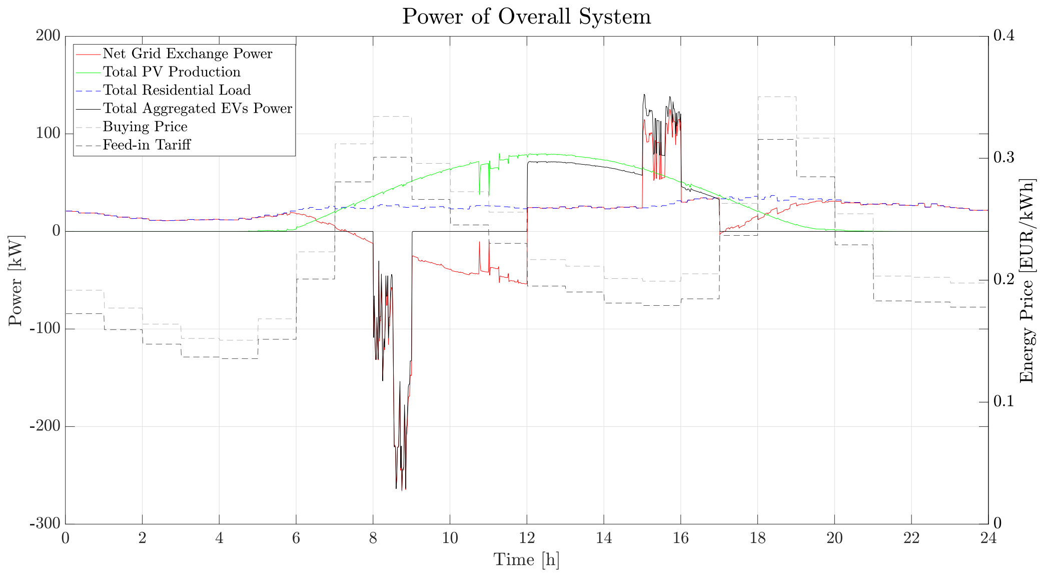

Figure 5.6: Power of overall system for case study 1B (No-Grid Constraints)

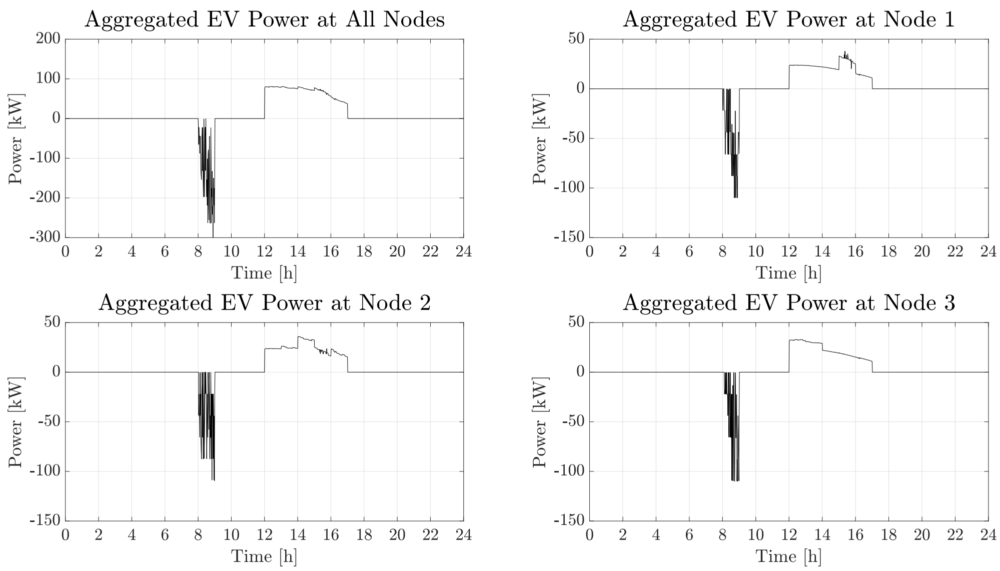

Figure 5.7: Aggregated EV power at all nodes for case study 1B (With-Grid Constraints)

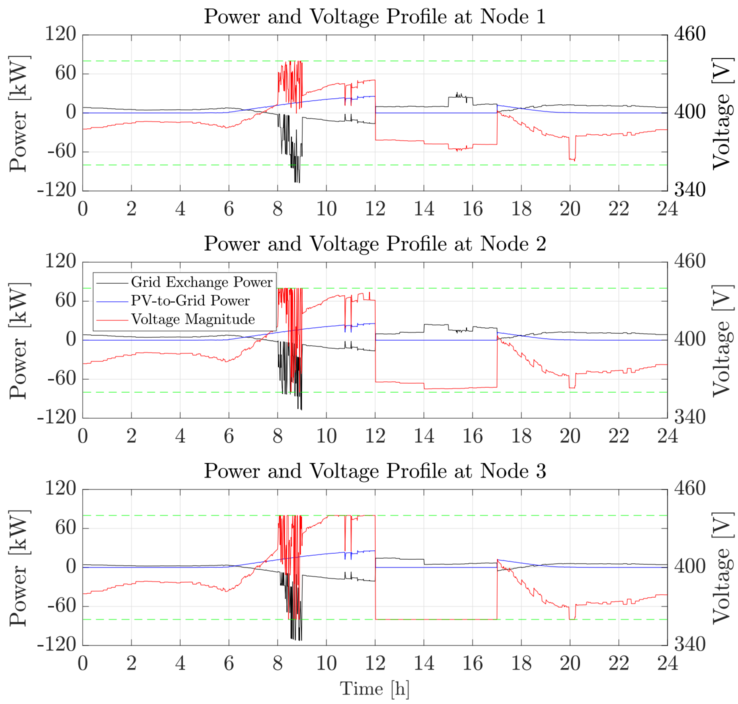

Figure 5.8: Voltage magnitude at all nodes for case study 1B (With-Grid Constraints)

5.1.3. Results of Case Study 1C (Summer, 7 EVs per node)

The current section outlines the result of case study 1C which employs 7 EVs per node, in a total of 21 EVs. Fig. 5.9 and 5.10 shows the entire day operation of EVs charging considering the grid and no-grid constraints, respectively. For the same reason as previous case study 1C, the PMS allows the EVs to discharge its battery during the morning and charge during the afternoon when the price is low. It is found that considering the grid constraints may result in increasing the operational cost by 22.12% when compared to no-grid constraints as shown on table A.1. Moreover, the PV power apportioned to the EVs equals 49.94% which is slightly higher than without considering grid constraints by 2.50%. Fig. A.10 and A.11 are depicted to have a deeper observation of the PV power allocation.

The aggregated all EVs power at all and each node are illustrated in Fig. 5.11. It is observed that at node 3, the end of the feeder, the PMS reduces the amount of charging power of the aggregated EVs. In addition, postponing the EVs charging until the low energy price is decided to have minimum charging costs. As seen in Fig. 5.11, at node 2 and 3, there is no discharging behavior. This phenomenon happens because if the EVs at node 2 and 3 are discharged via V2G, then the EVs need to draw lots of grid power during the valley period, so that it may lead to a severe undervoltage especially at the end of the feeder. Having the same argument as the previous case study 1B, the EVs charging power at each node for the no-grid constraints case is similar because it does not consider the voltage drop due to line impedance as shown in Fig. A.9.

Fig. 5.12 shows the voltage profile at each node over one-day operation. At node 1, the PMS allows the EVs to charge from the grid with higher power than at node 2 and 3 because the voltage drop will not be very much. Differently, at the end of the feeder, the EVs have to stop drawing power from the grid; hence it is preferable to charge by using the PV generation in order to prevent the stress on the distribution line as depicted further in Fig. A.10.

5.1.4. Results of Case Study 1D (Summer, 10 EVs per node)

This section presents the result of case study 1D which employs 10 EVs per node, in a total of 30 EVs. Fig. 5.13 and 5.14 show the one-day operation of EVs charging considering the grid and no-grid constraints, respectively. Upon observing the graph, there is no V2G appeared in a condition where the system is considering the distribution network constraints. Furthermore, the total operational cost is increased by 113.20% compared to no-grid constraints studied case. The PV self-consumption in the with-grid constraints case which

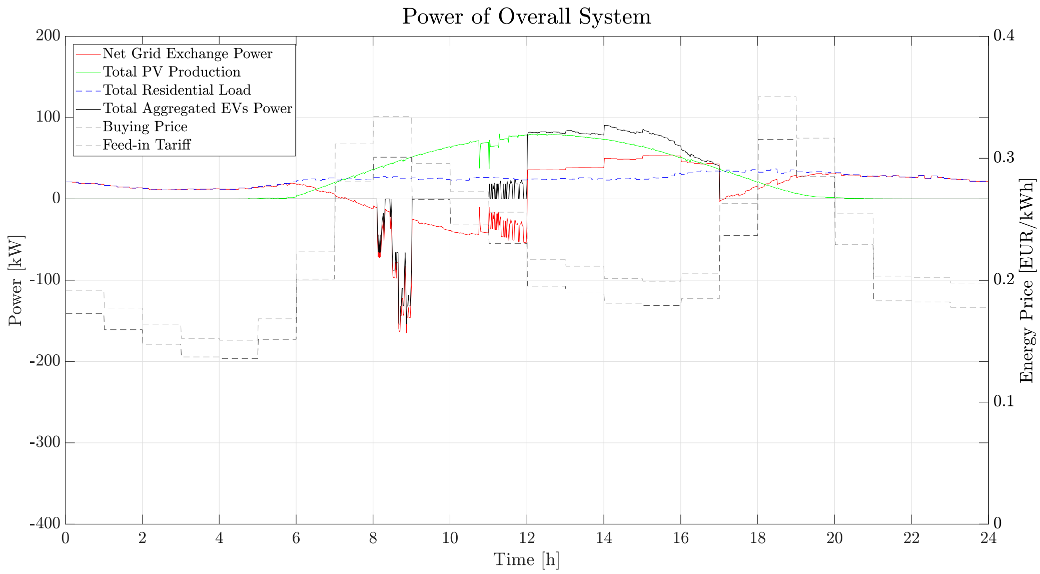

Figure 5.9: Power of overall system for case study 1C (With-Grid Constraints)

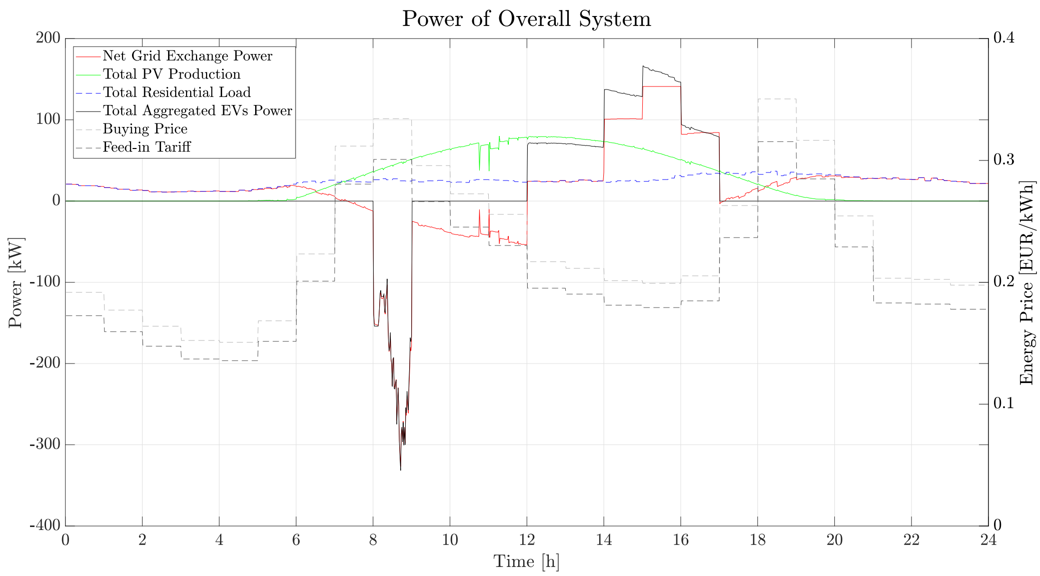

Figure 5.10: Power of overall system for case study 1C (No-Grid Constraints)

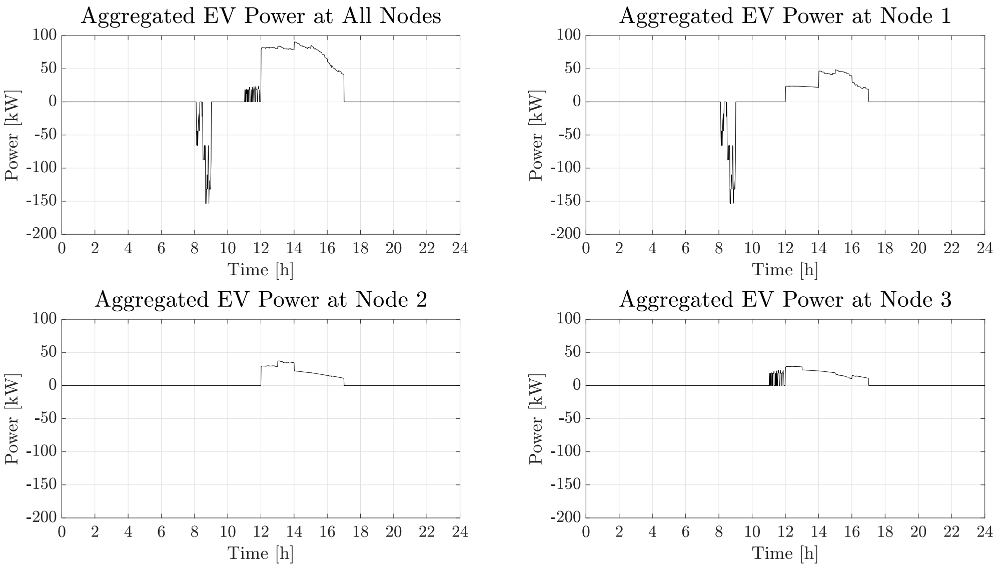

Figure 5.11: Aggregated EV power at all nodes for case study 1C (With-Grid Constraints)

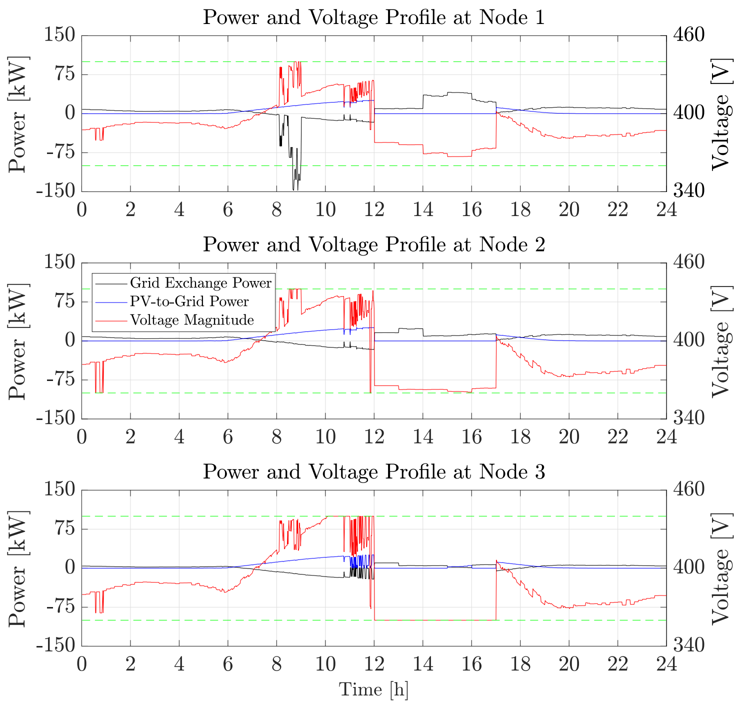

Figure 5.12: Voltage magnitude at all nodes for case study 1C (With-Grid Constraints)

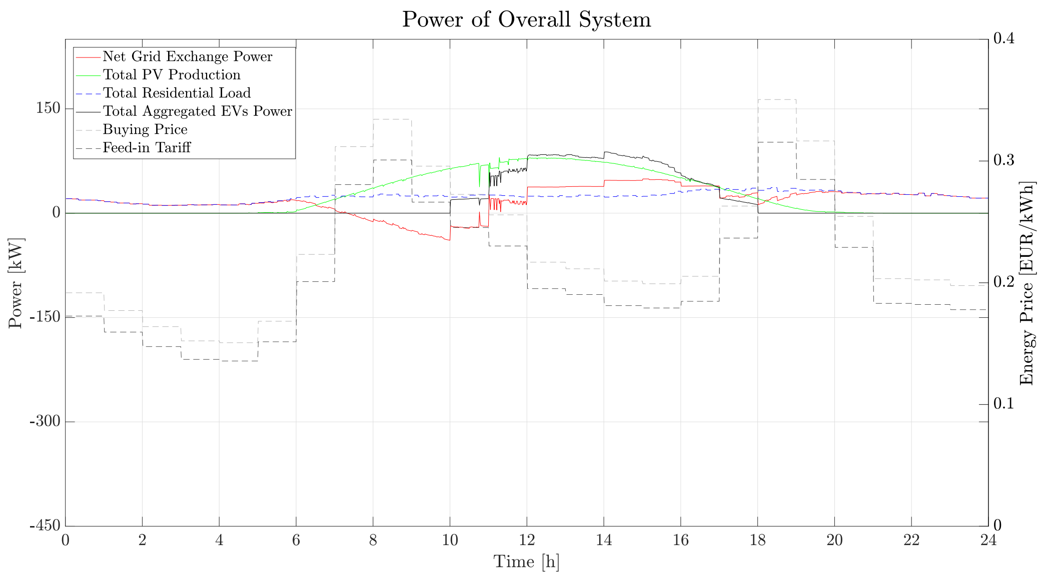

Figure 5.13: Power of overall system for case study 1D (With-Grid Constraints)

amounts to 62.22% is higher than the no-grid constraints case. Otherwise, in the no-grid constraints case for a different case study, the PMS always allows to discharge the EVs in the morning and re-charge its battery in the afternoon. It can be concluded that by having the same PV generation profile, the higher EV penetration is, the less viability to utilize the V2G operation.

The charging manner of all EVs at each node is depicted in Fig. 5.15. The charging power of all aggregated EVs is gradually increasing by the time. The peak power which amounts approximately 85 kW reaches during the noon when the energy price is low. To alleviate stress on the grid, the PMS decide to draw more power firstly at the first node, then the third node and last the first node.

The voltage profile at each node is illustrated in Fig. 5.16. As shown in the graph, in the morning around 10.00 AM, the EVs at the third node starts charging by using PV power. This strategy could bring a positive effect on the grid where the overvoltage affected by the PV penetration can be reduced since some of its power is being used to charge the EVs. Another important observation is found at 12.00 PM where the second node starts drawing more power than the other nodes. In addition, the voltage at node 3 is laying over the allowable lower boundary for the whole day which amounts to 90% of the nominal voltage.

5.2. WINTER PV PROFILE

The current section will assess how the proposed power management system behave in a one-day operation during winter. The winter PV profile is regarded as the worst case study as it comes to an infeasible solution even before implying a high EV penetration to the distribution grid. In addition, during winter with a low level of irradiation, the total energy yield of PV production over the entire day amounts to 28.40 kWh.

5.2.1. RESULTS OF CASE STUDY 2A (WINTER, 2 EVS PER NODE)

This section will discuss the results of case study 2A, in which employing 2 EVs at each node on the distribution network. Fig. 5.17 and 5.18 depicts a one-day operation of EVs charging considering the grid and no-grid constraints, respectively. Likewise as during summer profile, the power management system delays to draw power from the distribution network until the afternoon when the energy price is getting low. There is no V2G operation happen in the with-grid constraints case, while V2G always takes place in the no-grid constraints case when the price of grid energy is in the peak value as obviously illustrated in Fig. 5.18. Moreover, the PV self-consumption is significantly high which equals 71.96%. Finally, the total operational cost of the with-grid constraints studied case increases by 20.38% when compared to the no-grid constraints case as presented on table A.1.

Fig. 5.19 illustrates the aggregated EVs charging power at each node. During the day, all aggregated EVs draw power from the grid around 15 kW. The peak power happens at 03.00 PM which amounts to approxi-

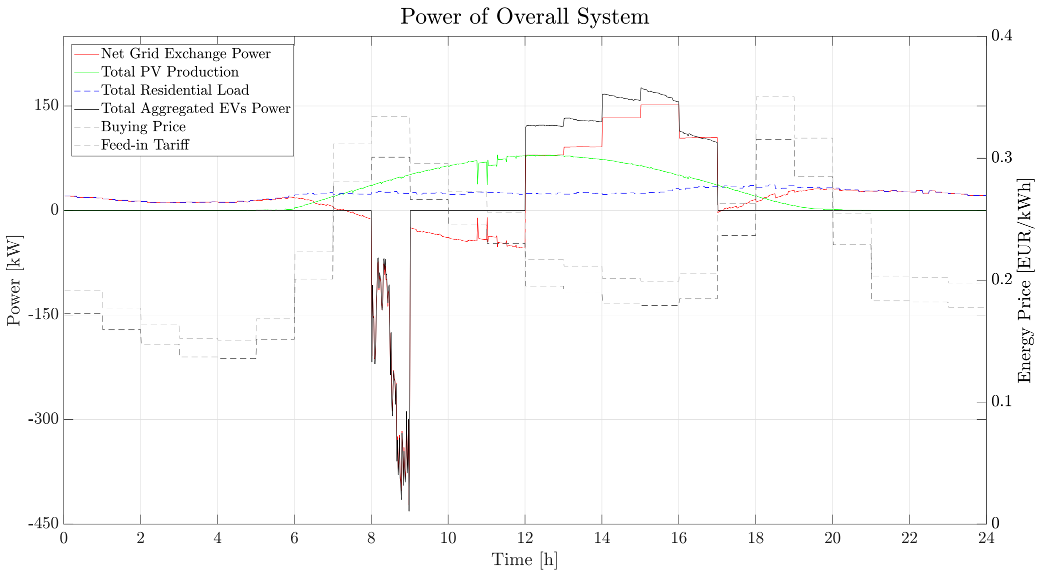

Figure 5.14: Power of overall system for case study 1D (No-Grid Constraints)

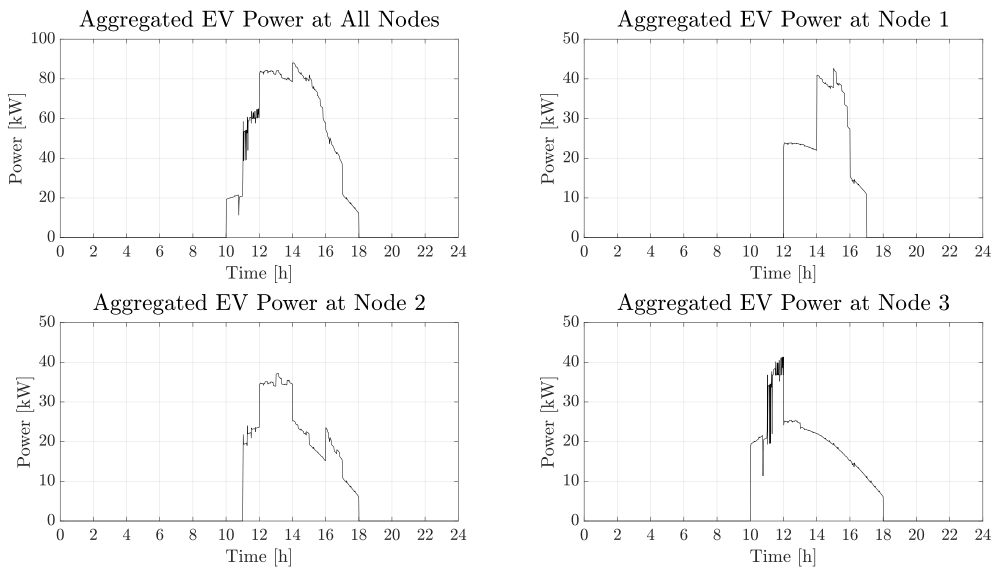

Figure 5.15: Aggregated EV power at all nodes for case study 1D (With-Grid Constraints)

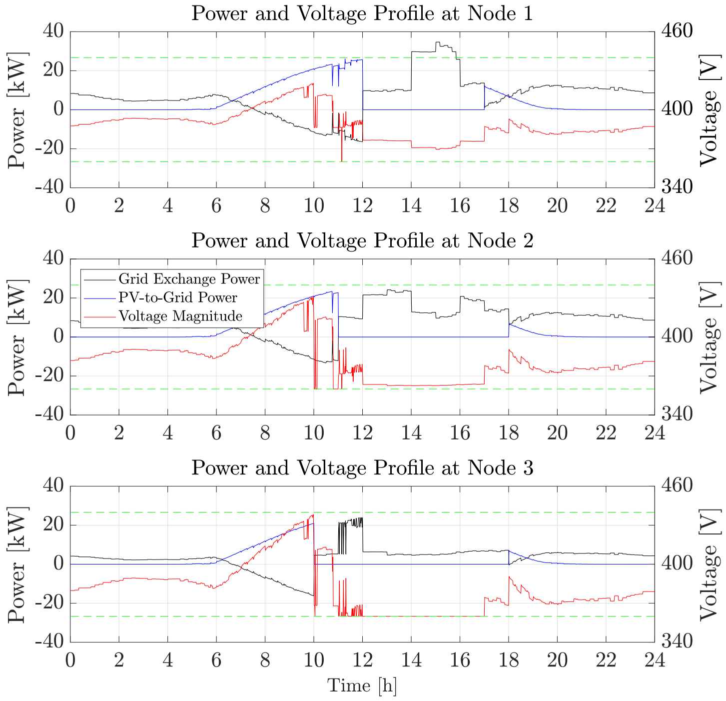

Figure 5.16: Voltage magnitude at all nodes for case study 1D (With-Grid Constraints)

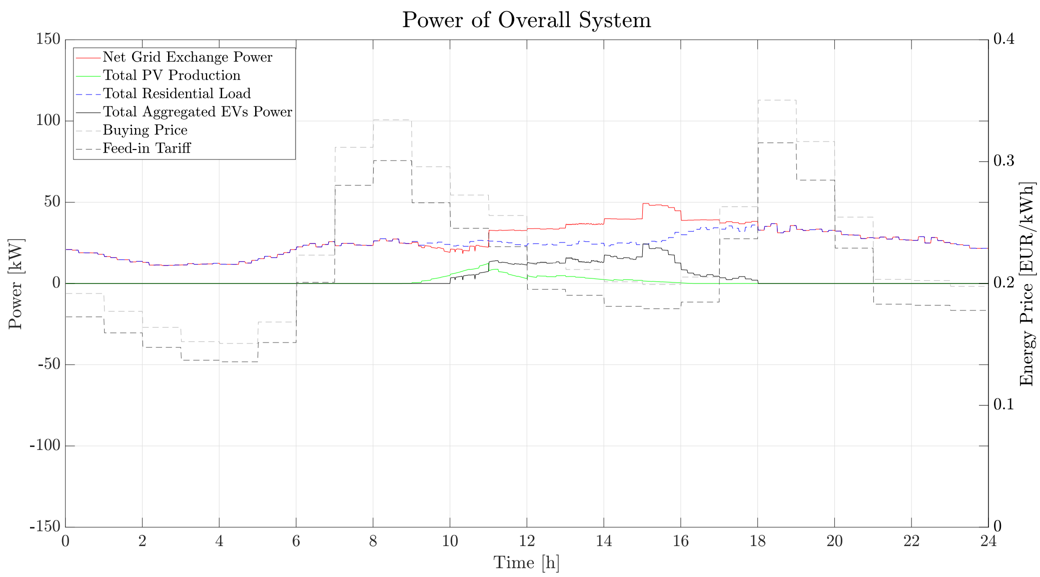

Figure 5.17: Power of overall system for case study 2A (With-Grid Constraints)

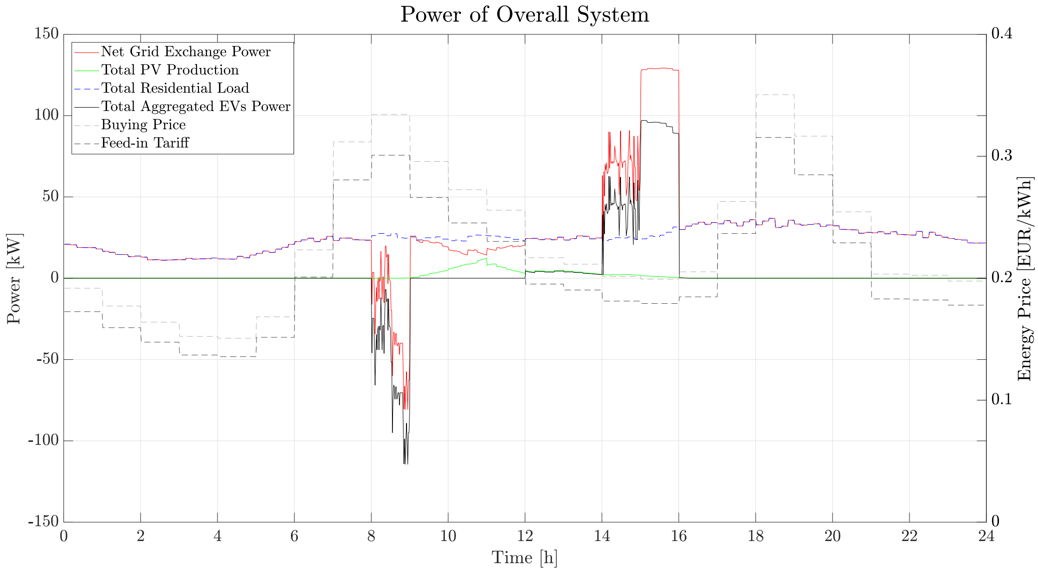

Figure 5.18: Power of overall system for case study 2A (No-Grid Constraints)

mately 25 kW. Then, as seen on the behavior of EVs charging, the PMS decide to draws more power the grid for each node in sequence, firstly at node 3, then node 2, and lastly node 1.

The voltage profile at each node is presented in Fig. 5.20. During winter, a serious overvoltage condition due to the PV penetration would never happen because the PV system only produces small amounts of energy. As seen in Fig. 5.20, the PMS decides to draw power from the grid at each node consecutively. Firstly, the third node draws more power, followed by the second and first node. In short, the worst voltage deviation still happens at the third node which is the end of the feeder as it has the longest line distance from the distribution transformer.

5.2.2. RESULTS OF CASE STUDY 2B (WINTER, 5 EVS PER NODE)

This section describes the results of case study 2B, which connects 5 EVs at each node on the distribution grid. The results are presented in Fig. 5.21, A.21 and A.22. In this case study, the MINLP problem leads to an infeasible solution. Therefore, only the no-grid constraints case simulation results are shown. However, the author tried to find a way how to solve the MINLP model so that it may come to an optimal solution. Once the author changes the lower limit of the allowable voltage deviation to 87%, the model could result in an optimal solution. Also, this result is not included in this thesis results as it already changed the previously defined parameters and system constraints. Then, to identify at what number of EVs per node could result in an infeasible solution, the author did a trial & error method. Furthermore, the author tested the simulation with 3 EVs per node, and the MINLP model leads to an optimal solution, in which the total operational cost is €30.00 as depicted in Fig. 5.47. This additional test is intended to find more data on the total operational cost which finally defines the operational cost comparison between the with-grid and no-grid constraints studied cases. Besides, it is found that by connecting 4 EVs per node, it has already come to an infeasible solution. In short, the following case study 2C and 2D which employs 7 EVs and 10 EVs per node, respectively for the with-grid constraints case will not reach an optimal solution, while for the no-grid constraints studied case, it always comes to an optimal solution.

As shown in Fig. 5.21, the behavior is completely similar to during summer, the PMS allows the EVs to operate V2G in the morning when the energy price at its highest value. Then, it postpones charging the EVs until in the afternoon when the price is the lowest during the day. Furthermore, the PV self-consumption equals 38.42% where it is more profitable to sell more PV energy back to the grid.

5.2.3. RESULTS OF CASE STUDY 2C (WINTER, 7 EVS PER NODE)

As previously discussed in the case study 2B, the MINLP model comes to an infeasible solution; hence only the no-grid constraints case is analyzed here. Fig. 5.22, A.24, and A.25 are presented. The overall system behavior is the same as the previous case study 2B. In addition, the PV power used for EVs charging is also

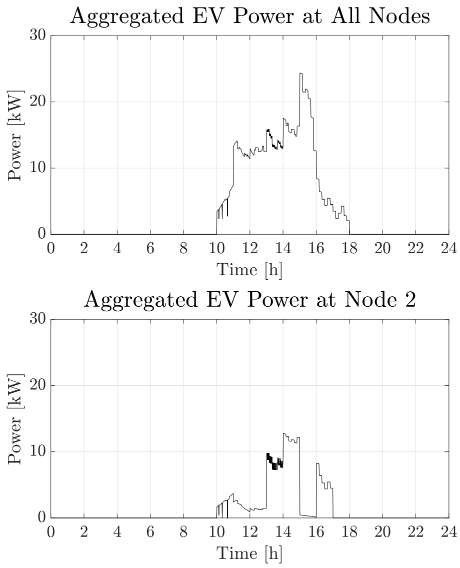

Figure 5.19: Aggregated EV power at all nodes for case study 2A (With-Grid Constraints)

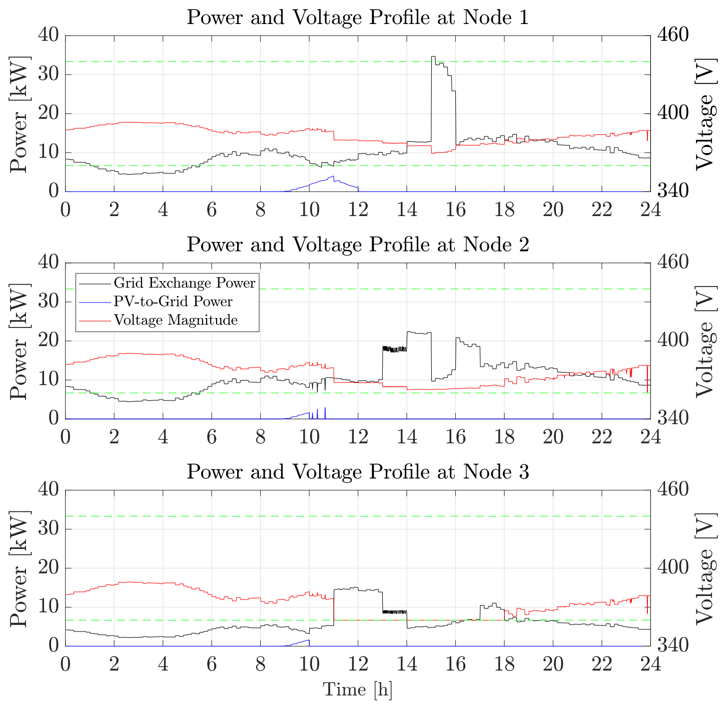

Figure 5.20: Voltage magnitude at all nodes for case study 2A (With-Grid Constraints)

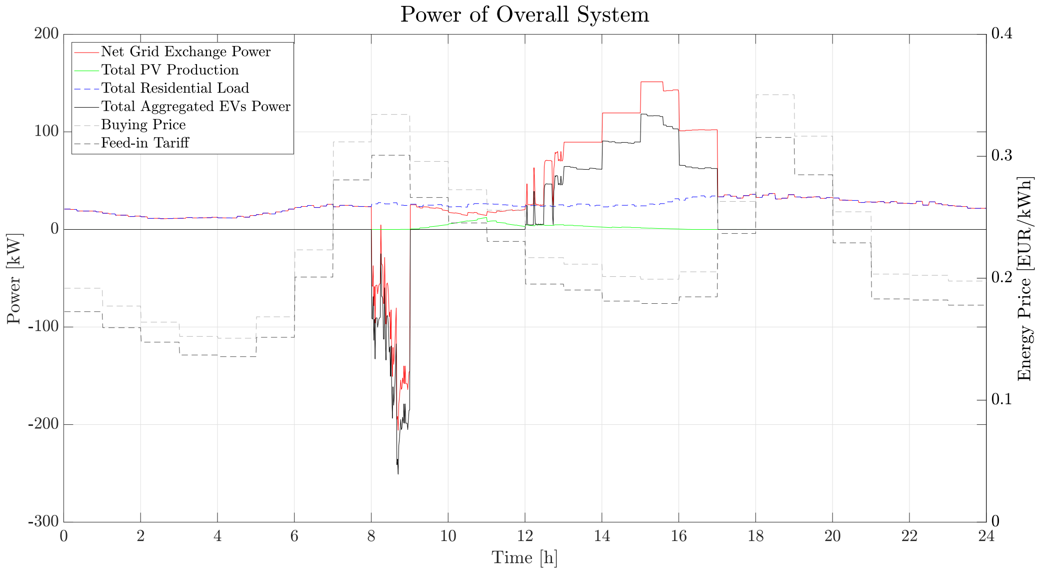

Figure 5.21: Power of overall system for case study 2B (No-Grid Constraints)

similar to the case study 2B, in which 38.42%.

5.2.4. RESULTS OF CASE STUDY 2D (WINTER, 10 EVS PER NODE)

Similarly, as the previous case study 2C, the MINLP problem cannot find the optimal solution; therefore only the no-grid constraints studied case result is presented in this section. The result is illustrated in Fig. 5.23, A.27, and A.28. It is shown that the higher a number of EVs connected per node is, the higher power fed to the grid for the V2G operation in the morning when the EVs arrive at the charging points. The graphs in Fig. 5.23 also shows that it has the same manner as the previously discussed case study. Also, the PV self-consumption has the same amount with the previous case study which is 38.42%.

5.3. SPRING PV PROFILE

This section is aimed to evaluate the accomplishment of the proposed power management system in a one-day operation during spring. Further, the total energy yield of PV production during spring case study equals 282.24 kWh.

5.3.1. RESULTS OF CASE STUDY 3A (SPRING, 2 EVS PER NODE)

This section presents the result of case study 3A which employs 2 EVs at each node. Fig. 5.24 and 5.25 shows the one-day operation of EVs charging for the with-grid and the no-grid constraints studied case, respectively. It is observed that the EVs charging closely follow the PV generation so that less power drawn from the distribution grid. In the morning, the V2G operation takes place when the energy cost is high. As a result, the PMS decide to delay recharging the EVs during the afternoon where it draws power from the grid in combination with the PV generation. Additionally, at the beginning of the day, feeding PV power to the grid is more economically beneficial in which the PV self-consumption amounts to 53.66% as referred to Fig. A.31. Comparing the total operational cost for both with-grid and no-grid constraints case, they are the same as similarly found in case study 1A. The total operational cost is €-16.93, so that means the EVs charging operator receives money for the one-day operation.

Fig. 5.26 illustrates the EVs charging manner during the whole day. During observing the result, the author found that every node of the distribution network has a typical charging behavior which occurs in the afternoon. The peak power of each node is equal to nearly 18 kW, results in the total of 54 kW. The other interesting point is that the aggregated EVs at each node utilizes a V2G process in the morning when the cost of grid energy is undoubtedly high.

The results presented in Fig. 5.27 is the voltage profile at each node for one-day operation. In the morning, when the operation of V2G takes place, the voltage at every node starts to rise until close to the upper limit.

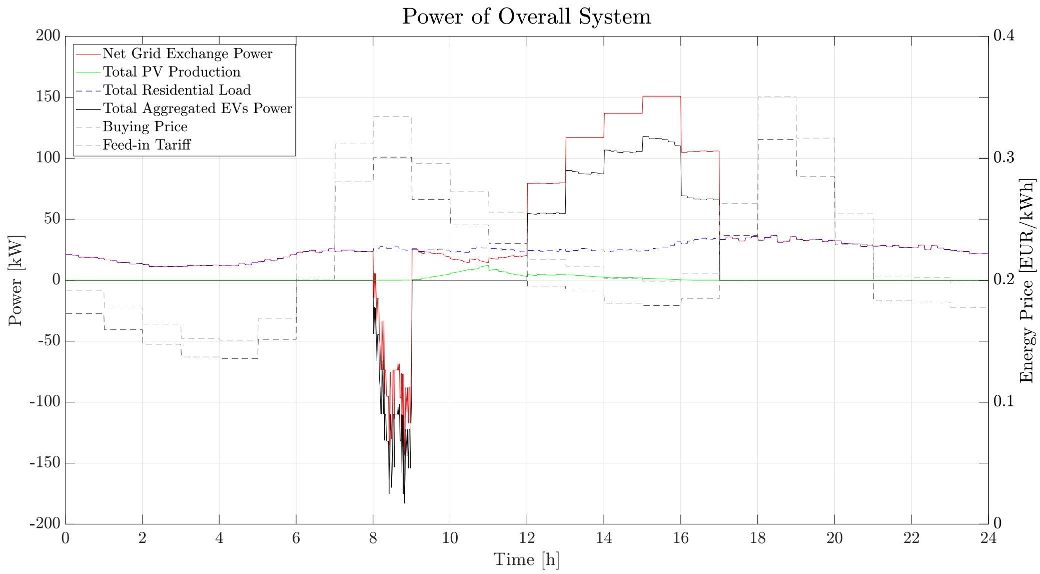

Figure 5.22: Power of overall system for case study 2C (No-Grid Constraints)

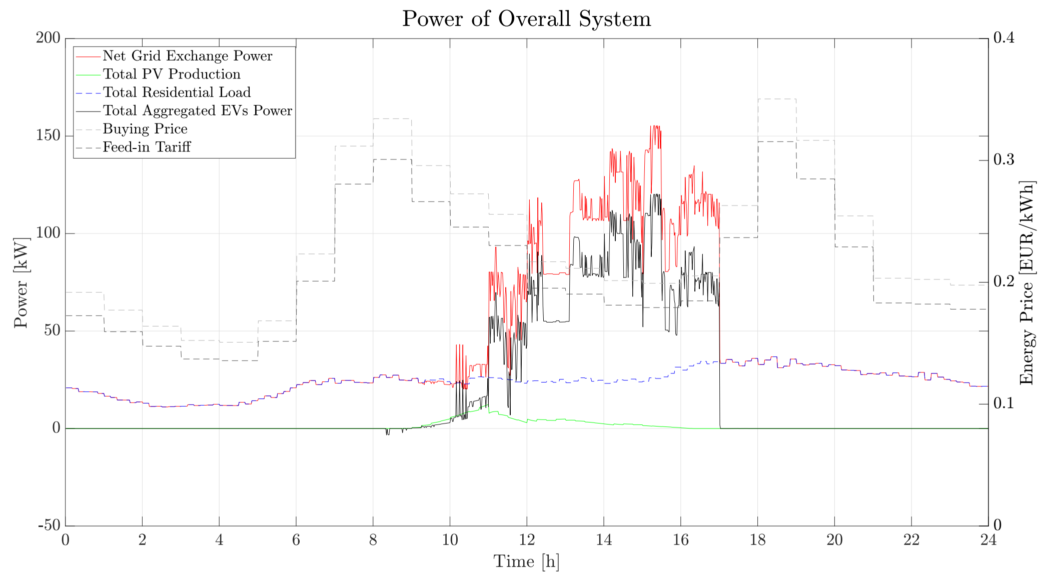

Figure 5.23: Power of overall system for case study 2D (No-Grid Constraints)

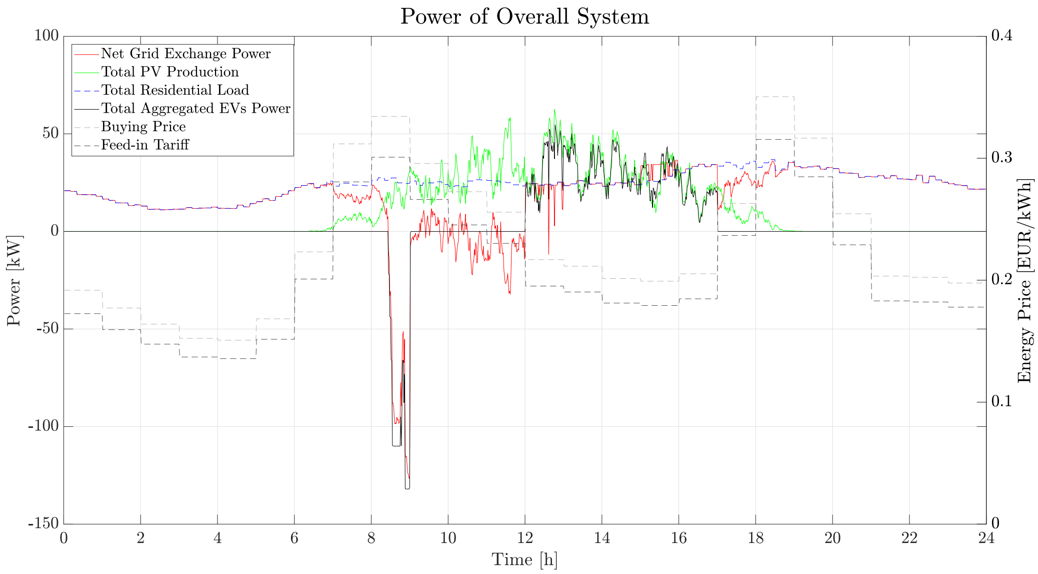

Figure 5.24: Power of overall system for case study 3A (With-Grid Constraints)

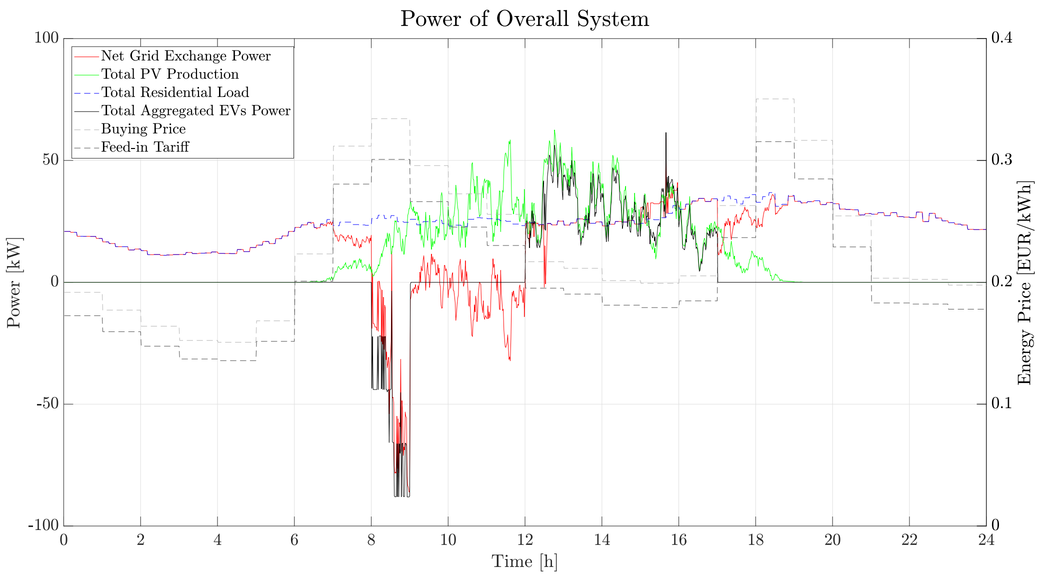

Figure 5.25: Power of overall system for case study 3A (No-Grid Constraints)

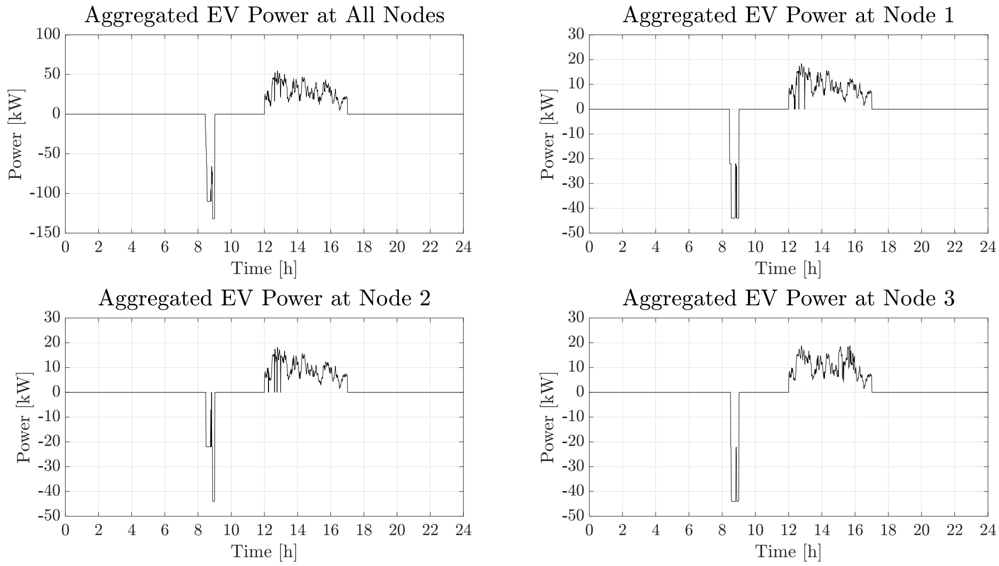

Figure 5.26: Aggregated EV power at all nodes for case study 3A (With-Grid Constraints)

Also, feeding the PV power back to the grid, starting from 09.00 AM to 12.00 PM, cause an overvoltage slightly above the nominal voltage.

5.3.2. RESULTS OF CASE STUDY 3B (SPRING, 5 EVS PER NODE)

This section presents the result of case study 3B which employs 5 EVs at each node. Fig. 5.28 and 5.29 shows the one-day operation of EVs charging with-grid and no-grid constraints, respectively. From Fig. 5.28, some interesting points can be observed. The PMS allows the V2G operation to take place in the morning once the EVs arrive. Similarly, as the previous case study 3A, the EVs charging follows the PV generation during the day in combination with the grid power when the grid price is in its valley period. Moreover, the operational cost is increased by 60.48% when compared to the no-grid constraints case. Also, the PV self-consumption is added up by 21.25%. To have a deeper understanding of the PV power allocation, Fig. A.35 is depicted.

Fig. 5.30 is illustrated to show the EVs charging manner at each node of the distribution grid. It is observed that the PMS selects postponing the EVs charging until the low grid price in order to have minimum charging costs. As seen in Fig. 5.30, at the second and third node, the V2G operation does not occur. This occurrence happens because if the EVs at node 2 and 3 are discharged via V2G technology, then the EVs need to draw much grid power to recharge the EVs battery during the valley stage, so that it may cause a harsh voltage drop especially at the end of the feeder.

Fig. A.35 shows the voltage profile at each node over a one-day operation. In the early morning, the PV power is penetrated to the grid so that it leads the voltage to rise around 6% above its nominal value. Another interesting detail is that the PMS manages to draw more grid power at each node sequentially. This strategy appoints to prevent the grid violations especially at the third node, the end of the feeder. During the day, even though the voltage at the third node is always at the border of the lower allowable voltage value, it never goes beyond its limit over a one-day operation.

5.3.3. RESULTS OF CASE STUDY 3C (SPRING, 7 EVS PER NODE)

This section outlines the result of case study 3C which employs 7 EVs per node. The results are presented in Fig. 5.32, 5.33, 5.34 and 5.35. One interesting point is that there is no V2G process occurred for the entire day. On the contrary, for the no-grid constraints case, as previously discussed, the PMS always allows the EVs to utilize a V2G operation when the energy cost is at its peak value and recharge the EVs battery in the early evening when the price is low. Moreover, the PMS starts drawing power from the grid, which is represented by the red line, in combination with PV generation even though in the morning when the energy price is not that low. Compared to the previous case study 3B, the PMS draws the grid power earlier in the morning since, within the same time span, it needs more power to charge more EVs penetration. Moreover, for the with-grid constraints case, the PV self-consumption amounts to 75.19% which is increased by 38.40 when compared to

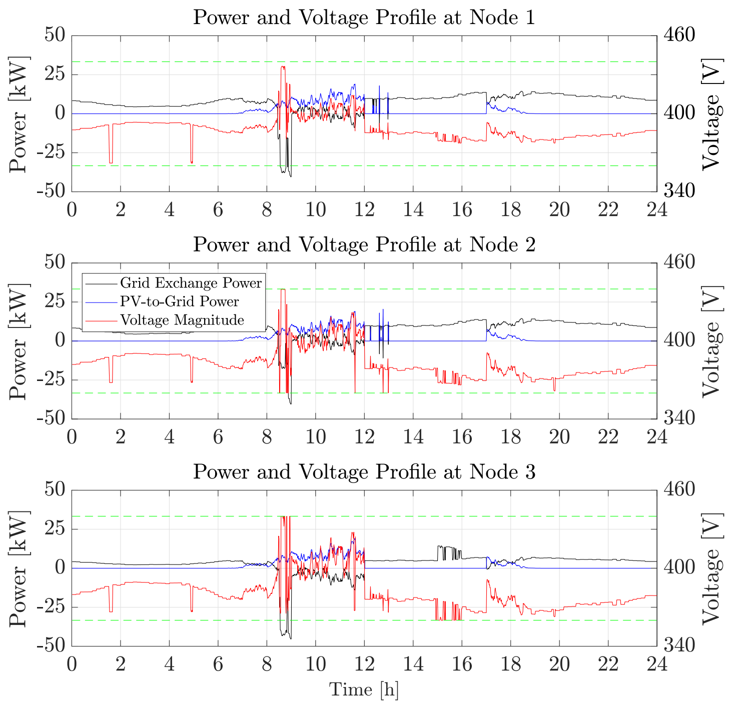

Figure 5.27: Voltage magnitude at all nodes for case study 3A (With-Grid Constraints)

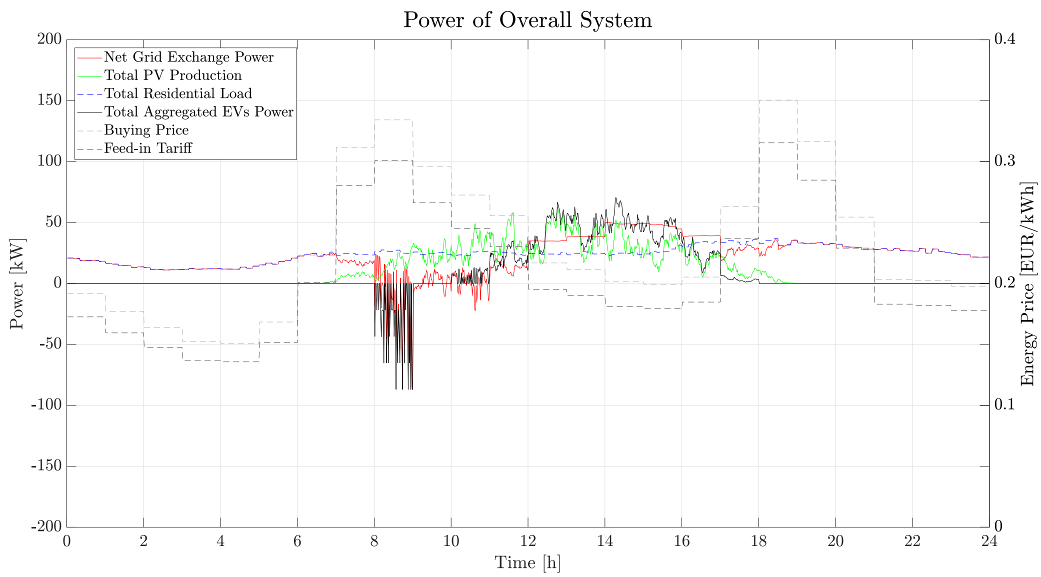

Figure 5.28: Power of overall system for case study 3B (With-Grid Constraints)

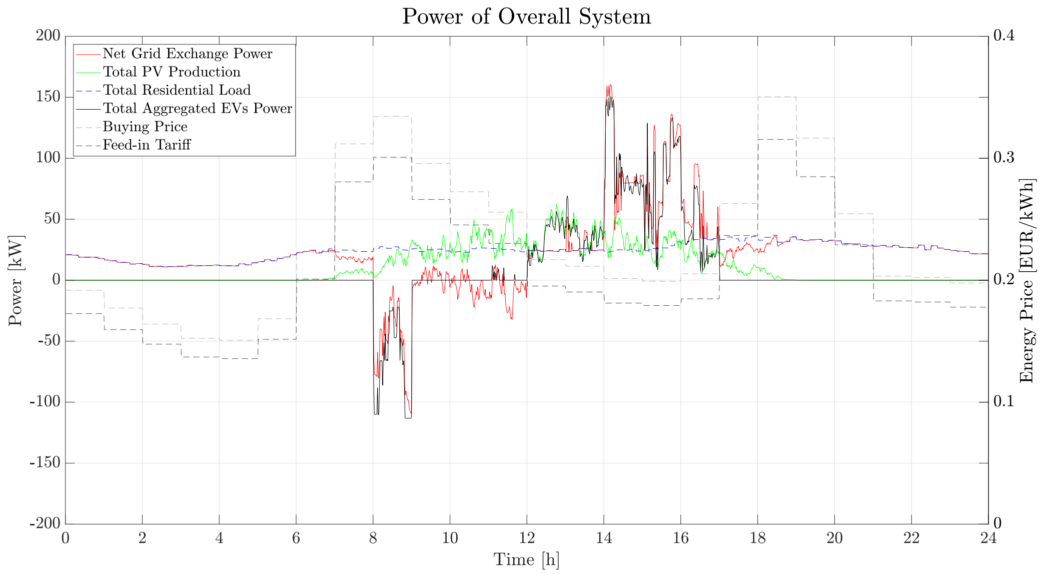

Figure 5.29: Power of overall system for case study 3B (No-Grid Constraints)

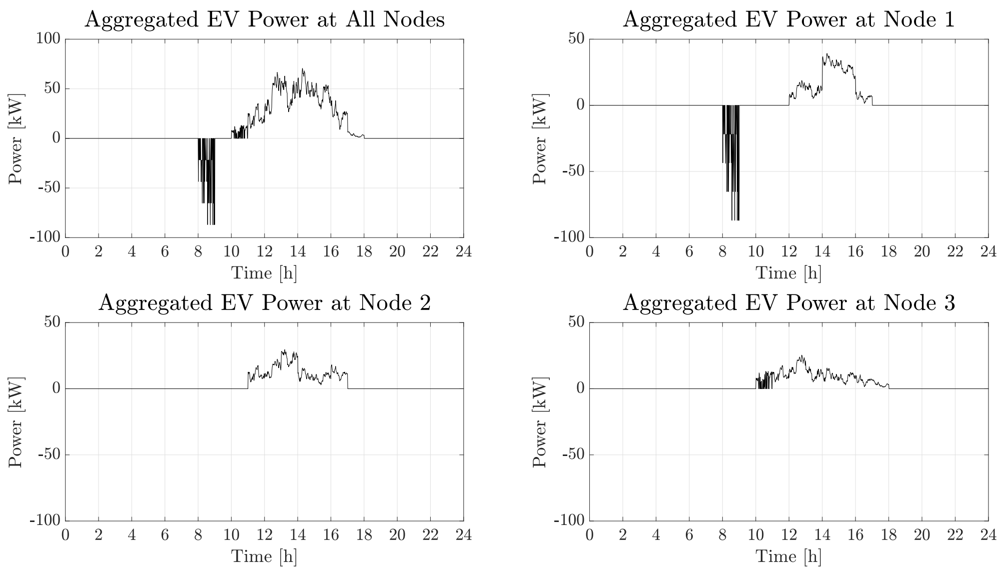

Figure 5.30: Aggregated EV power at all nodes for case study 3B (With-Grid Constraints)

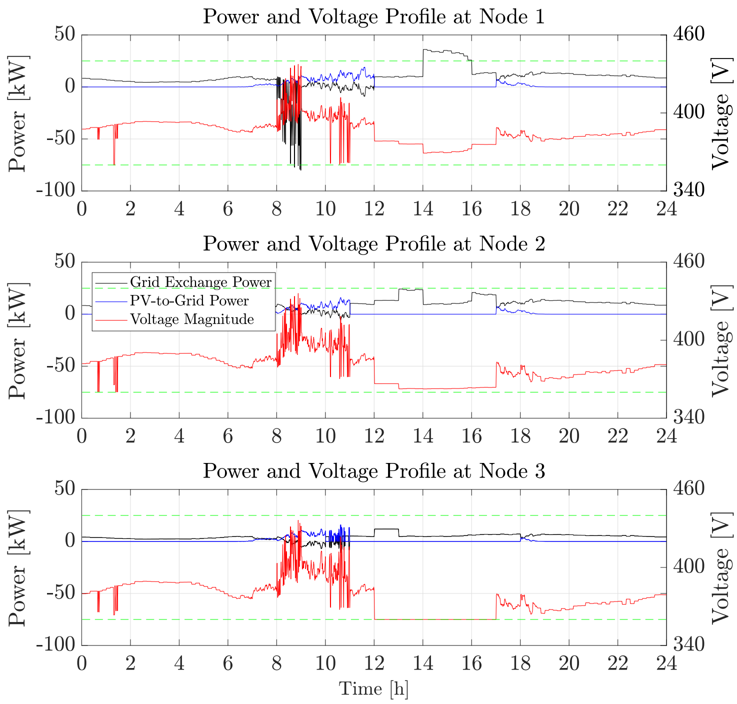

Figure 5.31: Voltage magnitude at all nodes for case study 3B (With-Grid Constraints)

the no-grid constraints case. The reason for the increment is when considering the grid constraints, it is more preferable to charge the EVs from the PV system in order to mitigate the stress on the grid especially at the end of the feeder. As a result, it is shown on table A.1 that the total operational cost is increased by 39.31%.

Fig. 5.34 depicts the charging power of aggregated EVs at each node of the distribution grid. The charging power of all aggregated EVs is slowly increasing from morning to afternoon. The peak power which equals approximately 70 kW reaches during the noon when the cost of grid energy is at its lowest value. To mitigate stress on the distribution network, the PMS allows to draw more power firstly at the third node, then the second node and last the first node.

Fig. 5.35 shows the voltage profile per node for the entire day. In the morning, the PMS allows drawing power from the grid amounts to around 20 kW in combination with the PV generation as clearly seen in Fig. A.39. At the third node, almost all of the PV production is used to charge EVs due to preventing the voltage goes down beyond 90% of its nominal value. Then, the second node starts to draw more grid power followed by the first node. It is obvious that during the day when the EVs charging starts processing, the third node which is the end of the feeder is having the most unfavorable condition of undervoltage.

5.3.4. Results of Case Study 3D (Spring, 10 EVs per node)

This section describes the results of case study 3D, which connects 10 EVs per node. The author found that the MINLP model cannot solve the optimization problem and leads to an infeasible solution. However, for the no-grid constraints studied case, it comes to a global optimum solution by running a MILP model; hence the results are presented in Fig. 5.36. A.42 and A.43. By using the same trial & error method as discussed previously in case study 2B, it is found that by connecting 8 EVs per node, the MINLP can still obtain an optimal solution as shown in Fig. 5.47. Once employing 9 EVs per node, the optimization model starts resulting in an infeasible solution, therefore connecting more than 9 EVs per node will always lead to an infeasible result.

5.4. Autumn PV Profile

The current section is intended to assess the performance of the proposed power management system for an entire day during autumn. Additionally, the total energy yield of PV production during autumn profile equals 238.39 kWh.

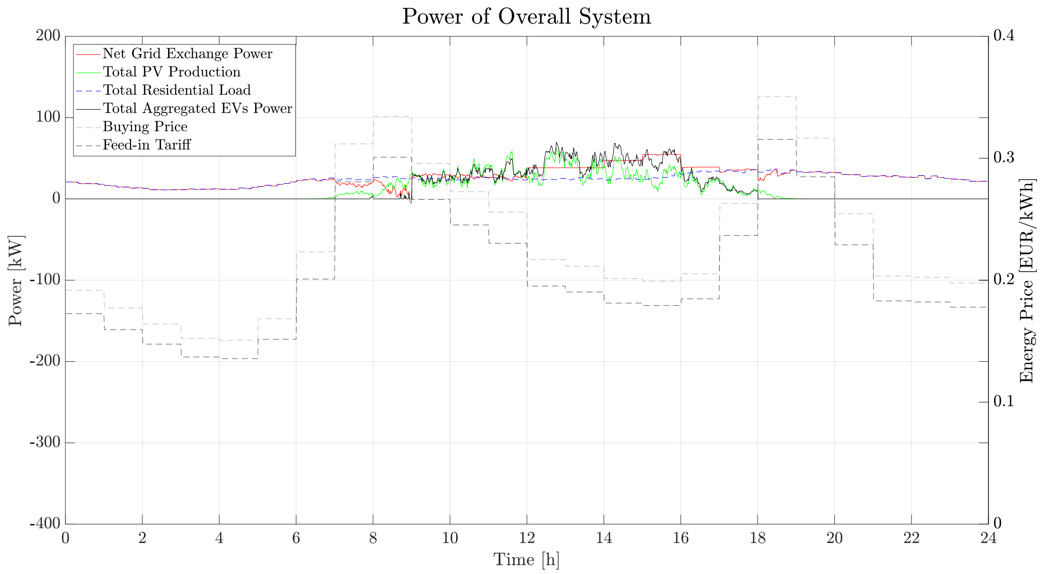

Figure 5.32: Power of overall system for case study 3C (With-Grid Constraints)

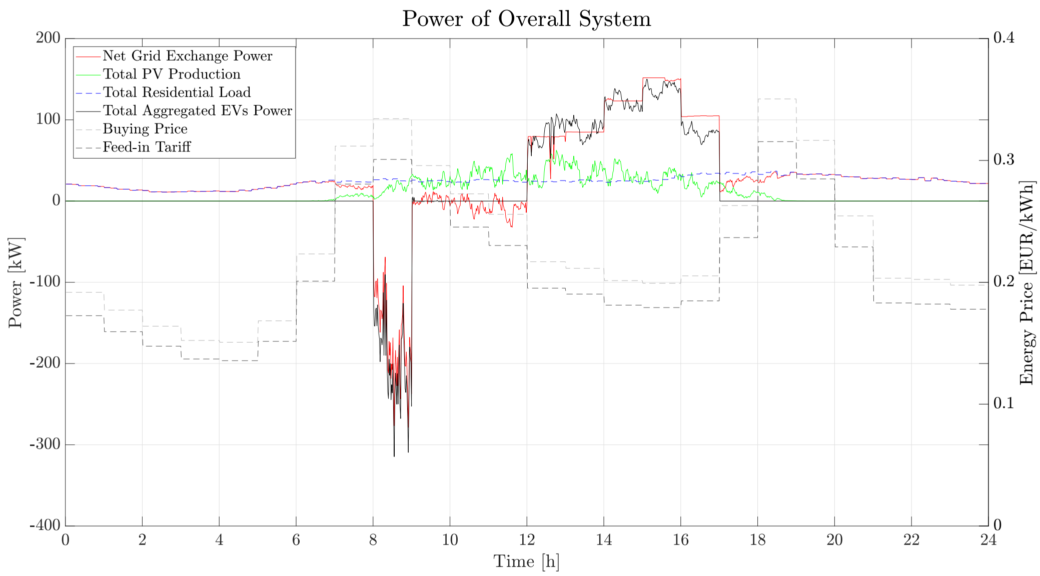

Figure 5.33: Power of overall system for case study 3C (No-Grid Constraints)

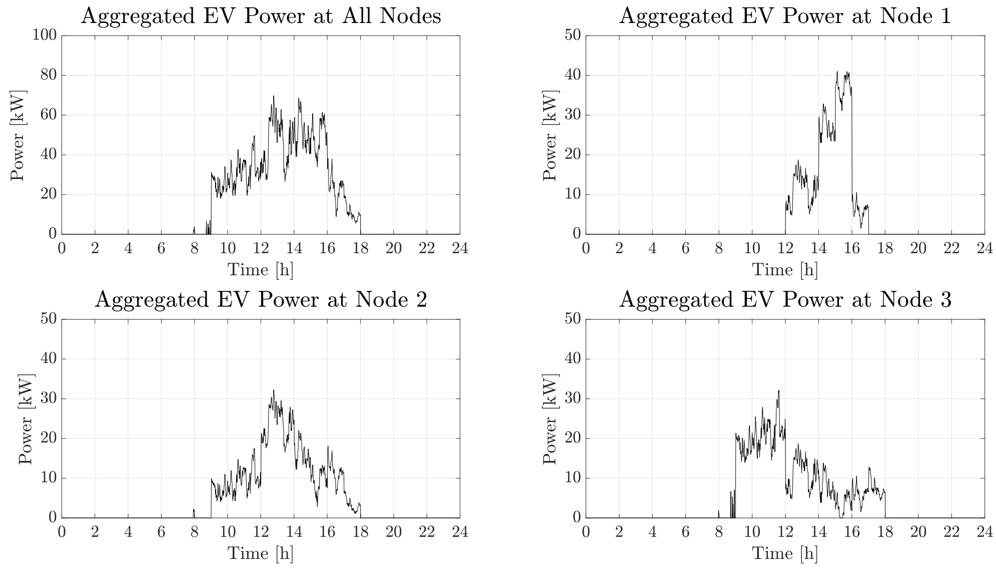

Figure 5.34: Aggregated EV power at all nodes for case study 3C (With-Grid Constraints)

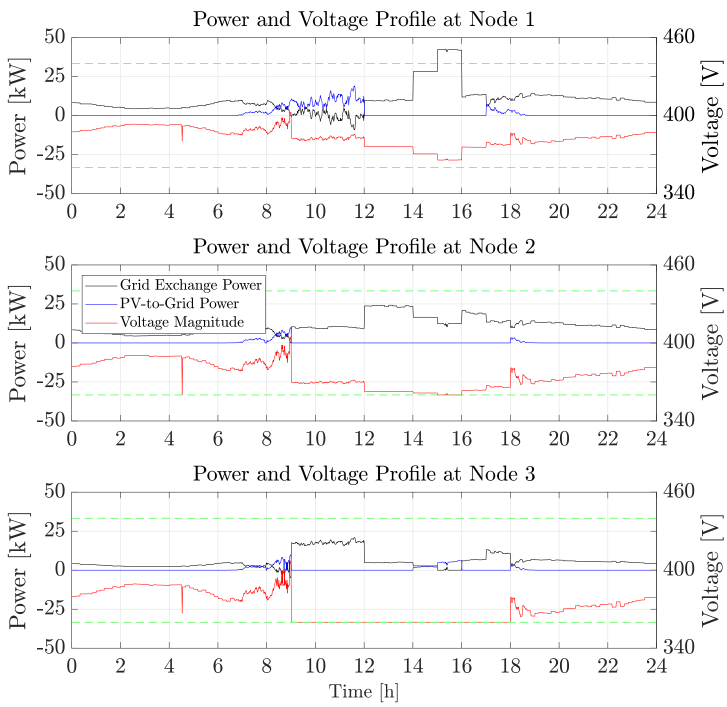

Figure 5.35: Voltage magnitude at all nodes for case study 3C (With-Grid Constraints)

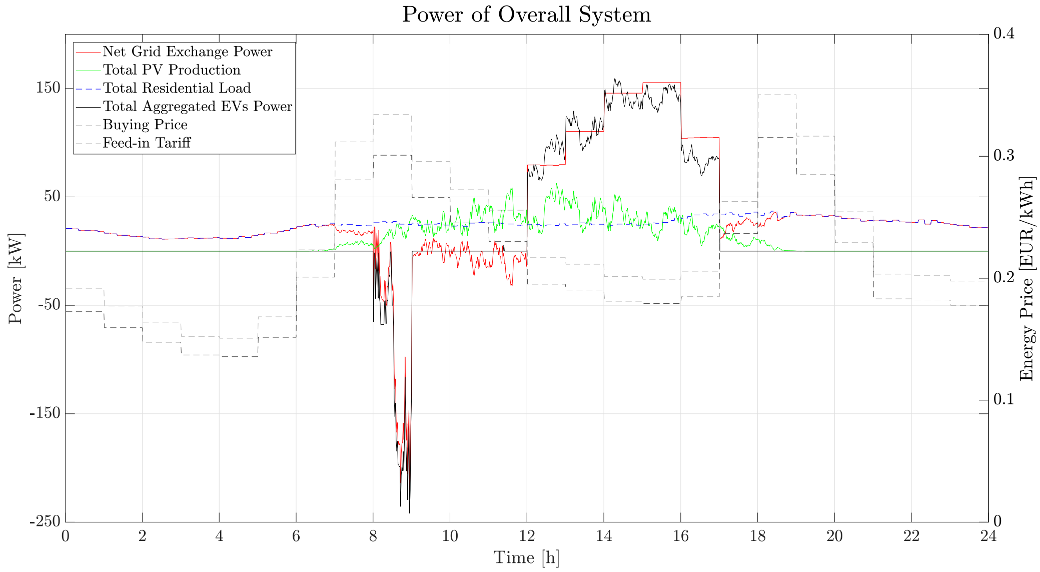

Figure 5.36: Power of overall system for case study 3D (No-Grid Constraints)

5.4.1. RESULTS OF CASE STUDY 4A (AUTUMN, 2 EVS PER NODE)

This section presents the result of case study 4A which employs 2 EVs at each node during autumn. Fig. 5.37 and 5.38 shows the one-day operation of EVs charging with-grid and no-grid constraints, respectively. In the morning, the EVs start discharging their battery when the energy price is high. Then, at 12.00 PM when the grid energy cost is decreasing, the PMS initiates re-charging the EVs from PV system since PV generation cost is always lower than the grid energy price ($\lambda_{PV_t} < \lambda_{G2V_t}$), hence it is more profitable. After the energy price is reaching its lowest value (from 03.00 PM - 04.00 PM), the PMS begins to draw as much power as possible. Observing the results of with-grid and no-grid constraints case from Fig. 5.37 and 5.38, the EVs charging behavior seems typically the same for the entire day. Additionally, the total operational cost of the with-grid constraints case is 0.43% higher than no-grid constraints case. Furthermore, the PV power fed to charge the EVs is the same which amounts to 54.34%.

The EVs charging behavior for the whole day is depicted in Fig. 5.39. Typically, every node has the same the charging manner where in the morning the aggregated EVs at each node exploit V2G operation and begin re-charging exactly at noon. The total peak power over the day equals around 45 kW. Also, the EVs charging power still follows the PV generation and simultaneously draws power from the grid to supplement the PV power.

The voltage profile for every node is presented in Fig. 5.40. In the morning, the V2G operation of the aggregated EVs results in a severe overvoltage at all nodes. Also, the PV penetration into the distribution network is making the overvoltage worse. However, the voltage still lay within the allowable voltage deviation which is between 90% and 110% of its nominal voltage. At around 12.00 PM until 02.00 PM, the reason of voltage deviation is the existence the residential load because, during this time span, the PMS charge all of aggregated EVs by using PV power as supported in Fig. A.46. Also, at each node, the PMS draws more power from the grid to support the PV generation in a sequence way, i.e., firstly the third node followed by the first and second node.

5.4.2. RESULTS OF CASE STUDY 4B (AUTUMN, 5 EVS PER NODE)

This section presents the result of case study 4B which employs 5 EVs per node, in a total of 15 EVs. The results are shown in Fig. 5.41, 5.42, 5.43 and 5.44. It is obviously seen in Fig. 5.41 that V2G process does not take place for the whole day. Otherwise, for the no-grid constraints case, the PMS always allows the EVs to perform a V2G utilization when the grid price is at its peak value and recharge the EVs battery in the early evening when the price is low. When compared to the result of the case study 4A, the PMS begins drawing the grid power earlier even though when the energy price is not at the valley period. This evidence is noticeable because, within the same time period, it is required to draw more power to charge more EVs. Moreover, the total cost of the with-grid constraints case is drastically increased by 42.12% when compared to the no-grid

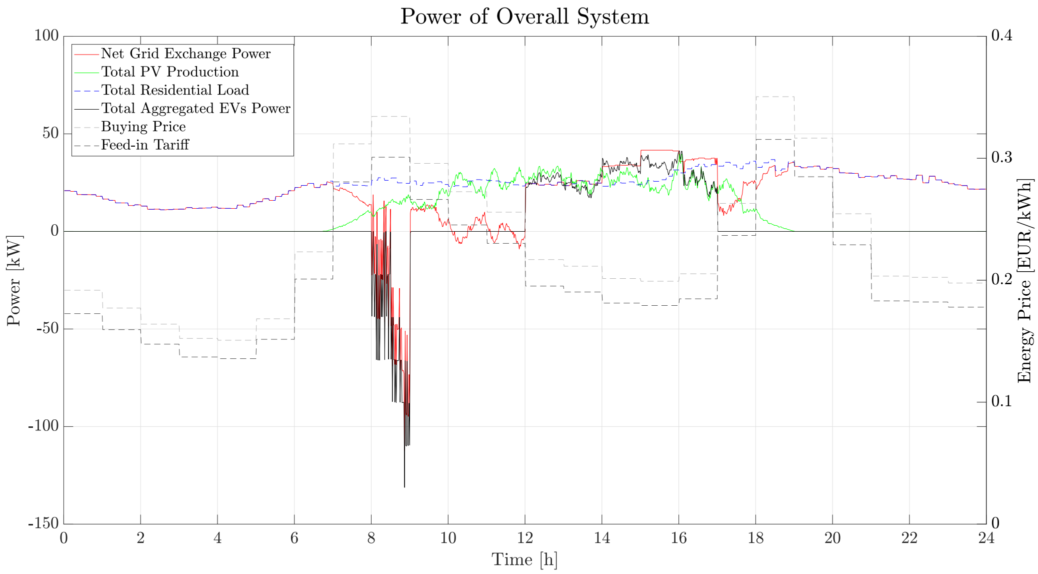

Figure 5.37: Power of overall system for case study 4A (With-Grid Constraints)

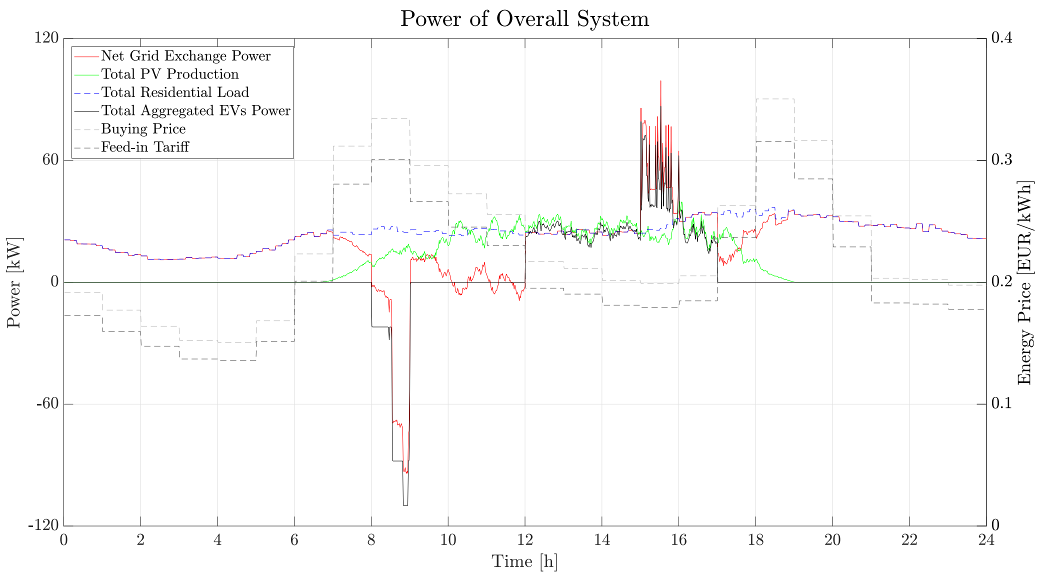

Figure 5.38: Power of overall system for case study 4A (No-Grid Constraints)

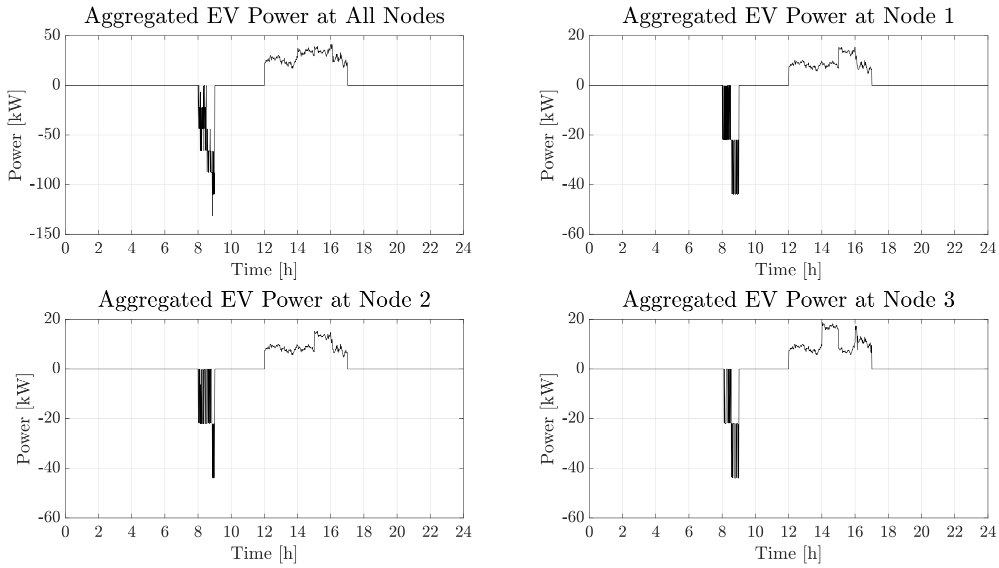

Figure 5.39: Aggregated EV power at all nodes for case study 4A (With-Grid Constraints)

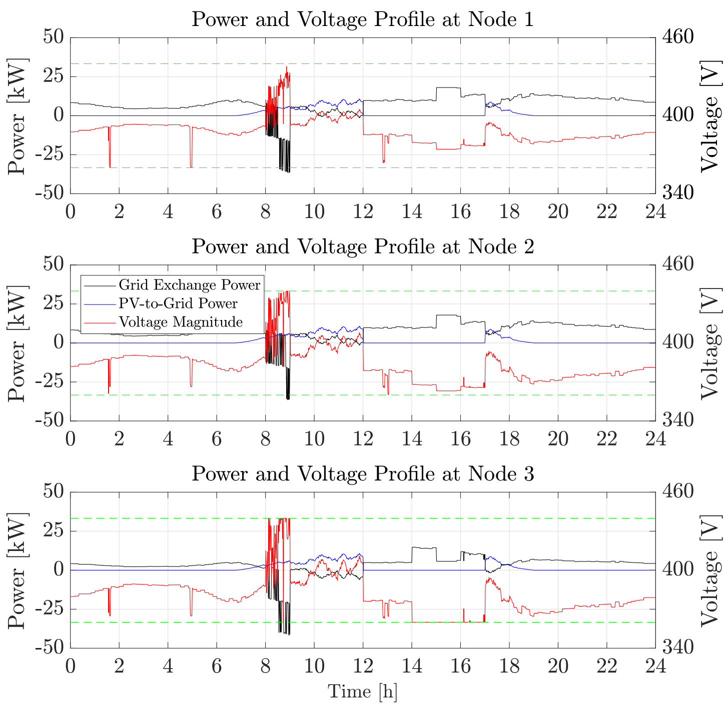

Figure 5.40: Voltage magnitude at all nodes for case study 4A (With-Grid Constraints)

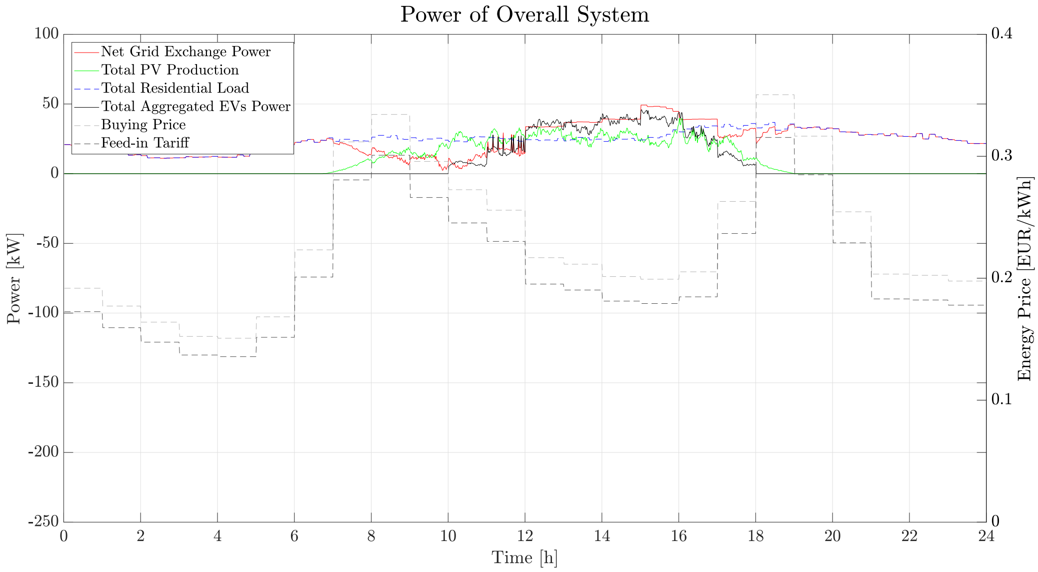

Figure 5.41: Power of overall system for case study 4B (With-Grid Constraints)

constraints case as presented in Table A.1.

Fig. 5.43 shows the EVs charging behavior at each node of the grid. Equally, as in case study 3C, the charging power of all aggregated EVs is evenly escalating by the time. The peak power which equals around 45 kW is reached during the valley period concerning the energy price. To avoid stress on the grid, the PMS determines to draw more power firstly at the third node, then the second node and last the first node.

The voltage profile at each node is depicted in Fig. 5.44. As previously mentioned above, the PMS draw more power from the grid in sequence regarding the node as represented by the black line on the graphs. The other interesting point that can be noticed is starting from 10.00 AM the PV generation at the third node is used to charge the EVs. This strategy is aimed to avoid an undervoltage if drawing power from the grid. In addition, the third node has the worst voltage deviation during the day because the longer distance of the load from the generation source, the higher voltage drop is.

5.4.3. Results of Case Study 4C (Autumn, 7 EVs per node)

This section presents the results of case study 4C, which employs 7 EVs per node during autumn. It is found that the MINLP model cannot solve the optimization problem and results in an infeasible solution. However, for the no-grid constraints studied case, it still comes to a global optimum solution by using a MILP model; hence the results are presented in Fig. 5.45, A.53, A.54, and A.55. By using the same trial & error method as discussed previously in case study 2B, it is found that by connecting 6 EVs per node, the MINLP can still acquire an optimal solution as shown in Fig. 5.47. Once employing 7 EVs per node, the optimization model starts leading to an infeasible solution, therefore connecting more than 7 EVs per node will always lead to an infeasible result.

5.4.4. Results of Case Study 4D (Autumn, 10 EVs per node)

Similarly, as the case study 4C, the MINLP model cannot find the optimal solution. Therefore only the no-grid constraints studied case result is presented in this section. The result is illustrated in Fig. 5.46, A.56, A.57, and A.58. It is shown that the higher a number of EVs connected per node is, the higher power fed to the grid for the V2G operation in the morning when the EVs just arrive at the charging points. The graphs in Fig. 5.46 also shows that it has the same manner as the previous case study 4C.

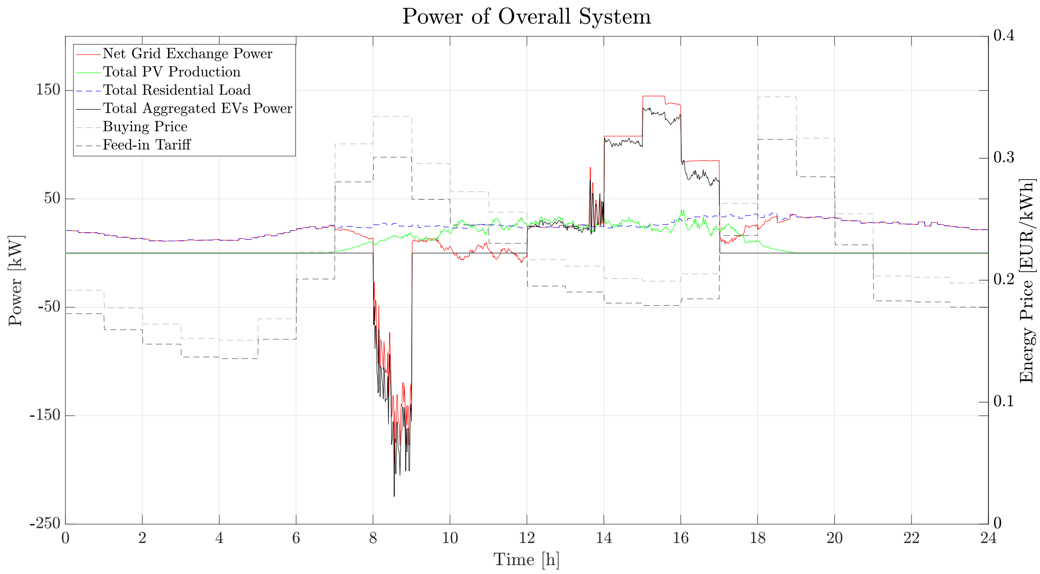

Figure 5.42: Power of overall system for case study 4B (No-Grid Constraints)

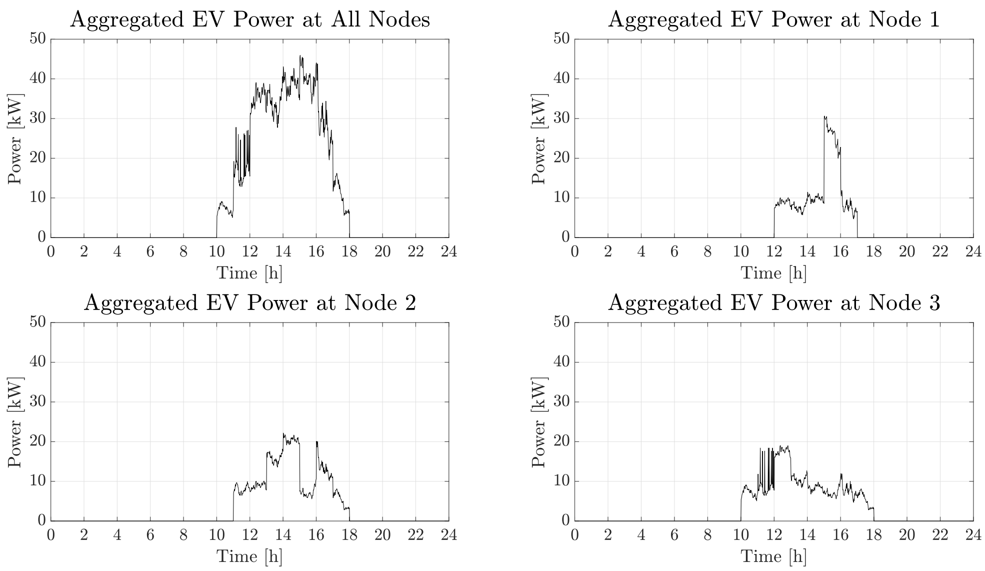

Figure 5.43: Aggregated EV power at all nodes for case study 4B (With-Grid Constraints)

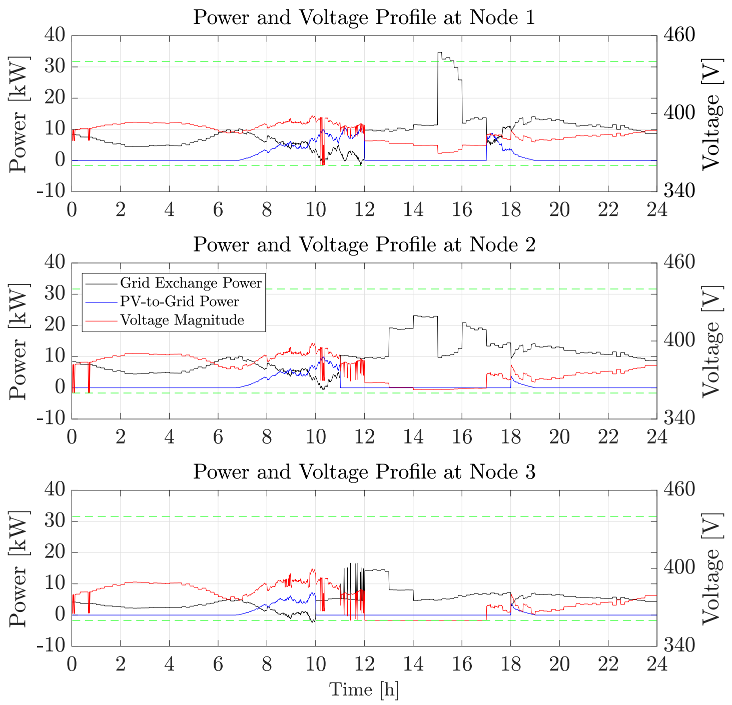

Figure 5.44: Voltage magnitude at all nodes for case study 4B (With-Grid Constraints)

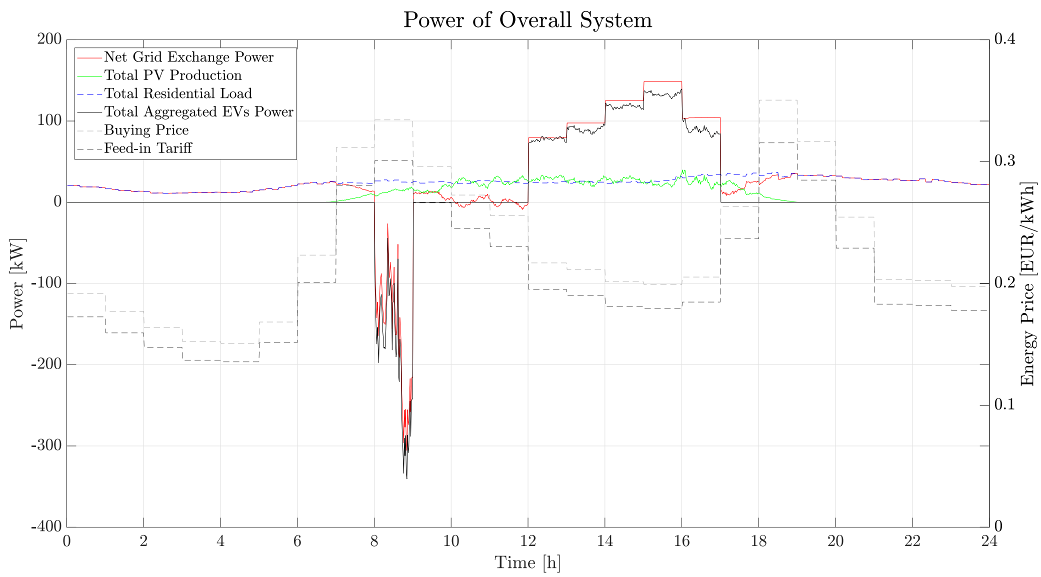

Figure 5.45: Power of overall system for case study 4C (No-Grid Constraints)

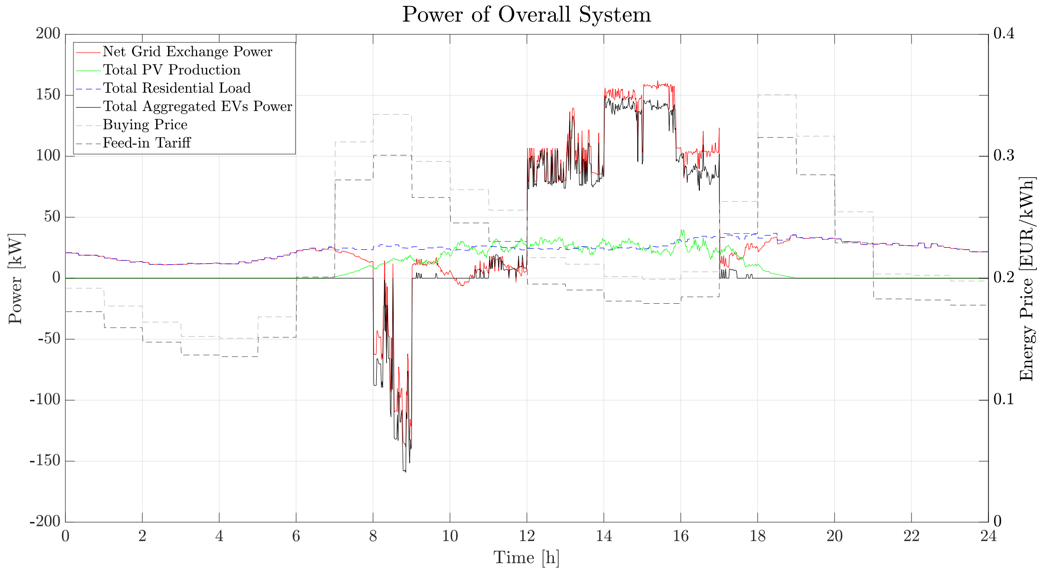

Figure 5.46: Power of overall system for case study 4D (No-Grid Constraints)

5.5. OVERVIEW OF RESULTS AND DISCUSSION

The main evaluation of the simulation results from all case studies are presented in this section. In the previous sections, it has been shown that the proposed power management system could optimally charge the EVs from PV system with minimum operational cost while considering the distribution network constraints. Therefore, to compare the performance of the proposed PMS of all case studies, several evaluated parameters are discussed in the following sections.

5.5.1. TOTAL OPERATIONAL COST

Fig. 5.47 illustrates the total operational cost comparison between the with-grid and no-grid constraints studied case. During summer, it is apparently seen that its total operational cost is the lowest among the other season. The proposed PMS could achieve a negative value which means the EVs fleet operator or called as the aggregator earn profits from the one-day operation. It can be concluded that a higher PV generation would result in a more profitable EVs charging operation. To calculate the increment in the percentage of the total operational cost between the with-grid and the no-grid constraints case, Eq. 5.1 is written as follows.

$$I_{TC} = \frac{TC_{with-grid} - TC_{no-grid}}{TC_{no-grid}} \times 100 \tag{5.1}$$

where I_{TC} is the increase of the total operational cost, in [%]. $TC_{with-grid}$ and $TC_{no-grid}$ are the total operational cost of the with-grid and the no-grid constraints studied case, respectively. Besides, the total operational cost of the with-grid constraints case, represented by the solid line, is evidently increased by 1.43% - 113.20% when compared to the no-grid constraints case, represented by the dashed line. This phenomenon happens because, in the with-grid constraints case, it has less flexibility to draw/feed power from/to the grid; hence the PMS decides to draw/feed power from/to the grid power as few as possible. This lack of flexibility means that when drawing power from or feeding power to the grid at a specific node, it will lead to a negative impact (under- or overvoltage) not only at that node, but the neighboring node will also get affected as supported by the above-mentioned results as shown in the voltage profile at each node, for instance in Fig. 5.44. Moreover, by only feeding small amounts of power to the grid, it leads to a low revenues via V2G operation and selling PV energy back to the grid. Therefore, it contributes to a higher total operational cost when compared to the no-grid constraints case.

Additionally, by implementing the proposed power management system for EVs charging considering the grid constraints, it may reduce the total operational cost drastically by 18.16% - 214.08% when compared to the uncontrolled charging as illustrated in Fig. 5.47. Taking the grid constraints into consideration is also technically beneficial especially from the Distribution System Operator perspective because the proposed

PMS could avoid the grid violations. These results mentioned above has proved that applying the proposed PMS could lead to technical and economic benefit.

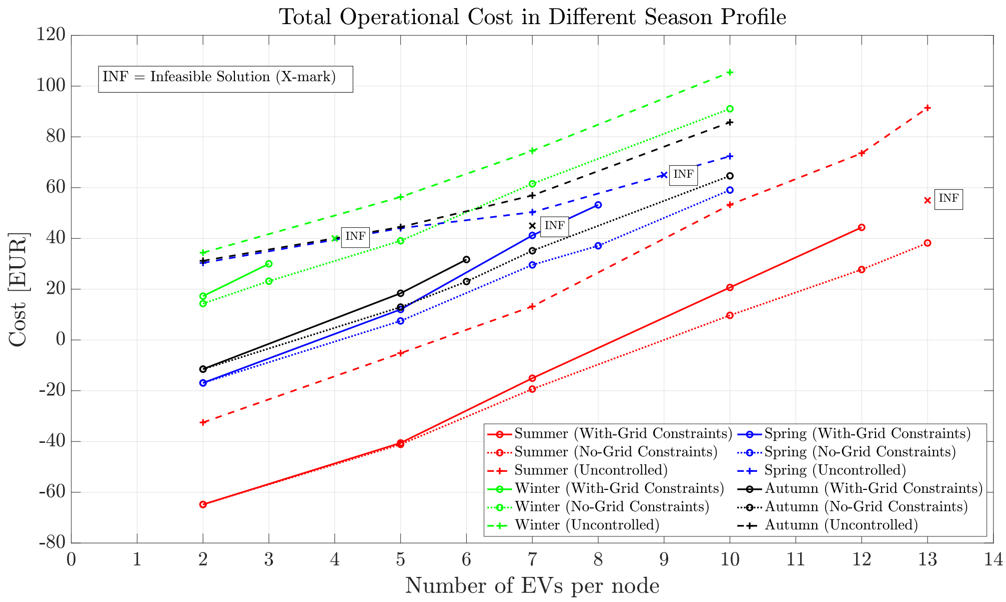

Figure 5.47: Total operational cost in different season profile

5.5.2. Maximum Amounts of EVs

The maximum amount of EVs which can be integrated into the distribution grid based on different PV profile is depicted in Fig. 5.48. It is found that up to 36 EVs can be integrated during summer. Fig. 5.48 describes that the higher the PV penetration is, the higher the number of integrated EVs are, and vice versa. The least integrated EVs take place during winter since it has very low irradiation so that the EVs need to draw power mostly from the grid. As previously discussed, the EVs cannot draw much power from the grid because drawing power at a certain node will affect the neighboring node to have a large voltage drop due to the line impedance. This circumstance is already shown in Fig. 5.20 where almost during the day, the voltage at the end of the feeder is always at the allowable lower limit. In short, it is shown that the increase of the EVs penetration into the EVs fleet could arise a serious problem to the distribution grid, in this case, the local DSO side.

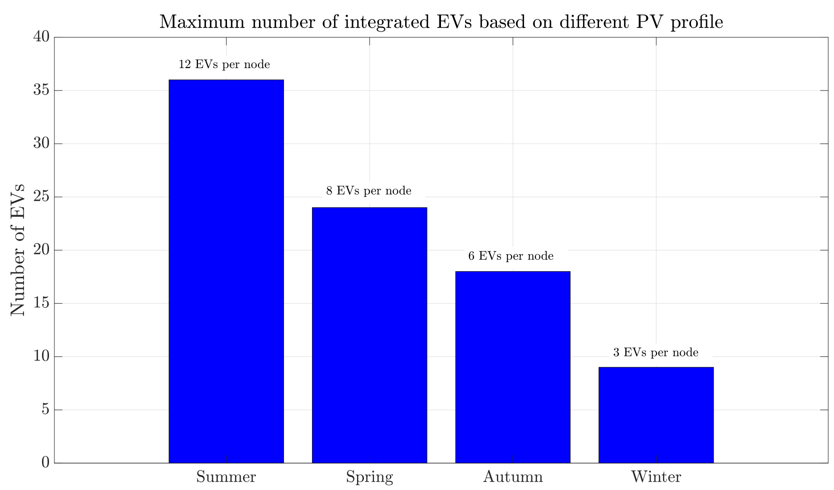

Figure 5.48: Maximum number of integrated EVs before resulting in an infeasible solution based on different PV profile

5.5.3. PV POWER ALLOCATION

To evaluate how the proposed power management system could trigger the synergy between PV generation and integrated EVs, then the PV power used for EVs charging needs to be calculated as depicted in Fig. 5.49. It is found that the highest PV power used to charge the EVs is achieved in the case study 3C which equals 75.19%. It is observed that for the with-grid constraints case, the PV power allocated for the EVs is always increasing with respect to the increase of integrated EVs in the distribution network. As a result, maximizing the PV power allocation to EVs may lead to minimizing the total operational cost.

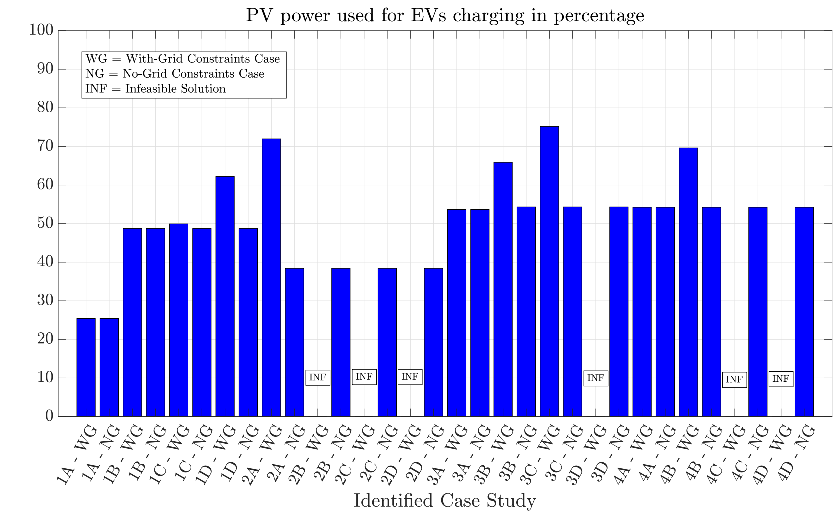

Figure 5.49: PV power used for EVs charging for all case studies

5.5.4. TRANSFORMER PEAK POWER

Fig. 5.50 shows the transformer peak power of each case study. It is seen that in the case study 1D (no-grid constraints), the peak power goes beyond the allowable limit of the transformer rated power. This phenomenon happens because in the no-grid constraints case, there is no limitation for the distribution transformer power as Eq. 3.9 was removed from the MINLP model.

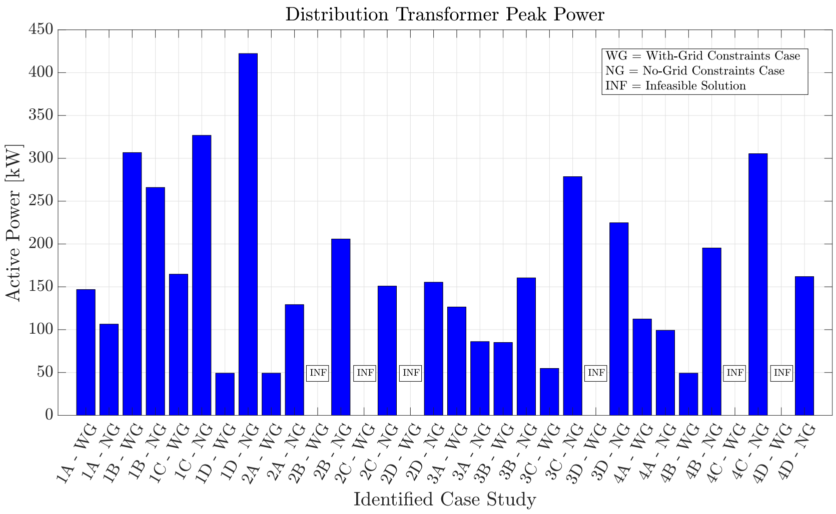

Figure 5.50: Transformer peak power for all case studies

5.5.5. DURATION OF VOLTAGE LIMIT VIOLATION

This section evaluates how the proposed PMS could avoid the voltage limit violation for all case studies as depicted in Fig. 5.51, 5.52, and 5.53. The duration of violation is calculated by computing how long the bus voltage at each node amounts to lower and higher than the allowable voltage deviation, in which 10% above and under the nominal voltage. It means that when the bus voltage is lower than 90% or higher than 110% of the nominal voltage, it is considered a grid violation. It is observed that for all the with-grid constraints studied case, the bus voltage at all nodes never goes beyond the allowable voltage deviation as the voltage constraints are taken into account written in Eq. 3.10. Moreover, the longest duration of the voltage violation at node 1, node 2, and node 3 happens in the case study 4D which employs 10 EVs per node during autumn. As a result, the average duration of voltage limit violation for the no-grid constraints studied case at node 1, node 2, and node 3 are 124, 132, and 145 minutes for the entire day, respectively.

5.5.6. MAXIMUM AND MINIMUM VOLTAGE

Figs. 5.54, 5.55, 5.56, 5.57, 5.58, and 5.59 shows the maximum and minimum voltage at the first, the second and the third node, respectively. During observing the results of all case studies, it is found that the maximum and minimum voltage for the with-grid constraints case is 440 V and 360 V, respectively. In the with-grid constraints case, the maximum and minimum voltage that can be reached is always 440 V and 360 V since Eq. 3.10 is included in the MINLP model. Besides, the highest value of the maximum voltage is reached in the case study 1D (no-grid constraints) which could reach up to around 550 V, 630 V, and 670 V at node 1, node 2, and node 3, respectively. These results as mentioned above show that by implementing the smart charging, it may lead to preventing the distribution grid violation; hence the DSO will not receive any negative impact due to the large penetration of EVs in the network.

5.5.7. V2G OPERATION

Table 5.1 shows in which case study the V2G operation takes place. For the no-grid constraints case, the V2G scheme always perform in all case studies. Besides, for the with-grid constraints case, 6 out of 10 feasible case studies operate the V2G process. This result has shown that the V2G scheme could help reducing the total operational cost.

Table 5.1: V2G occurrence for all case studies

Case Study	With-Grid Constraints	No-Grid Constraints
1A	✓	✓
1B	✓	✓
1C	✓	✓
1D	-	✓
2A	-	✓
2B	-	✓
2C	-	✓
2D	-	✓
3A	✓	✓
3B	✓	✓
3C	-	✓
3D	-	✓
4A	✓	✓
4B	-	✓
4C	-	✓
4D	-	✓

5.5.8. SIMULATION TIME

This section presents how long the MINLP executes the optimization problem to obtain the optimal solution. As previously mentioned, the MINLP was simulated by using General Algebraic Modelling System (GAMS) version 24.9.2 software with DICOPT solver. Fig. 5.60 shows the simulation time for all case studies. The most extended duration happens in the case study 1D (with-grid constraints), in which employing 10 EVs per node during summer. As seen in the bar diagram, the higher the EV penetration, the longer the simulation takes time to find the optimal solution. This long duration of execution is due to the use of the binary variables which force the MINLP to find the possible integer value either 0 or 1. Furthermore, the optimal solution found in the feasible case studies are obtained with a MINLP relative gap of 0.1%.

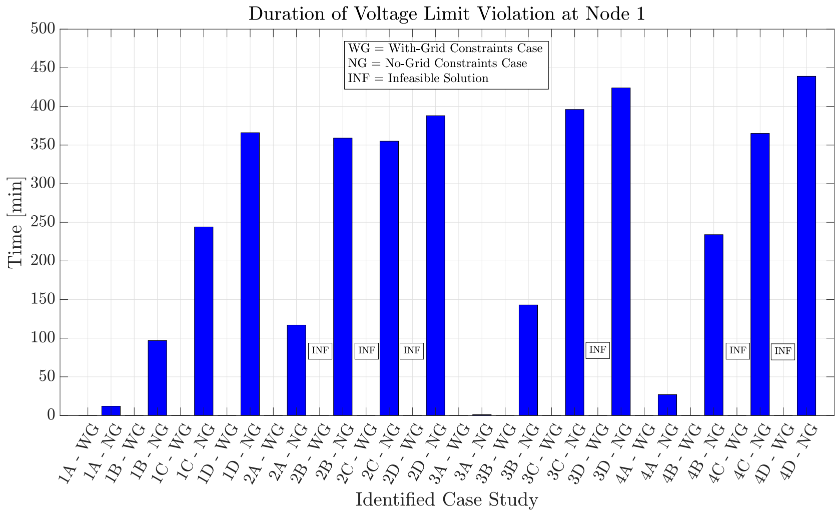

Figure 5.51: Duration of voltage limit violation at node 1 for all case studies

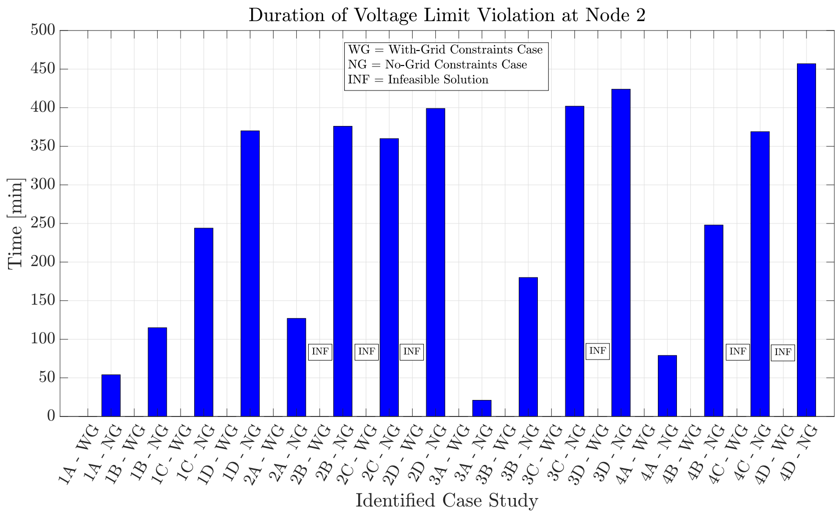

Figure 5.52: Duration of voltage limit violation at node 2 for all case studies

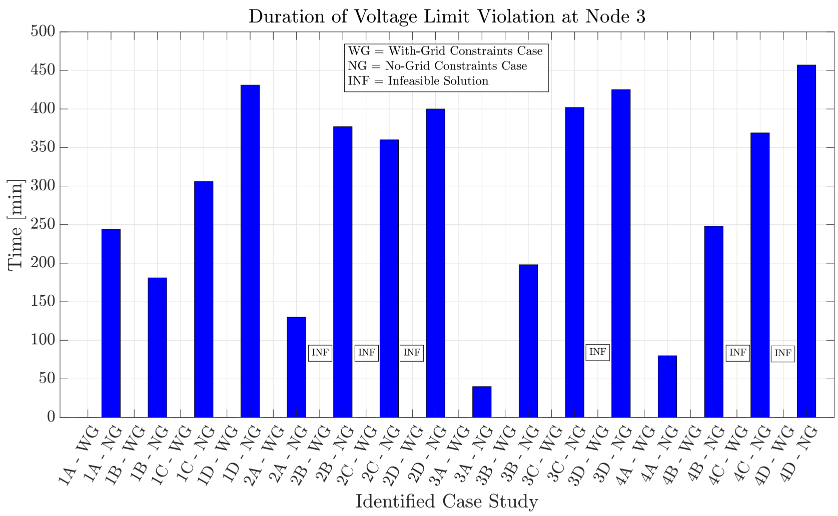

Figure 5.53: Duration of voltage limit violation at node 3 for all case studies

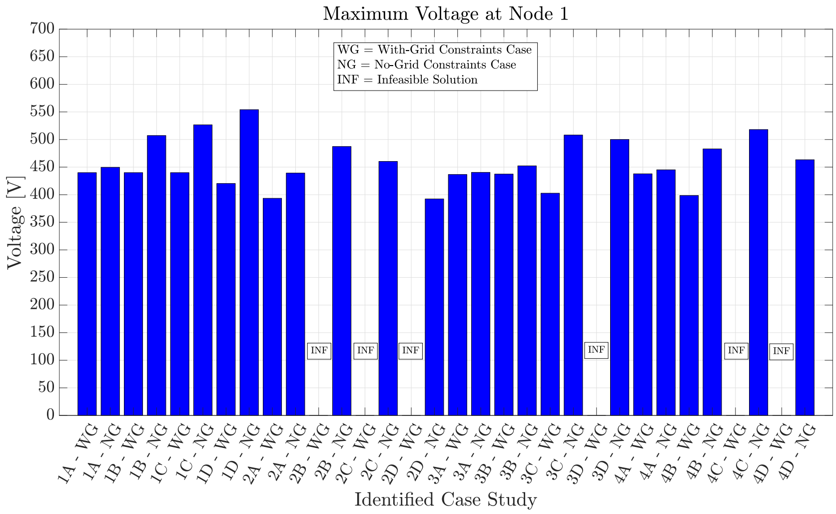

Figure 5.54: Maximum voltage at node 1 for all case studies

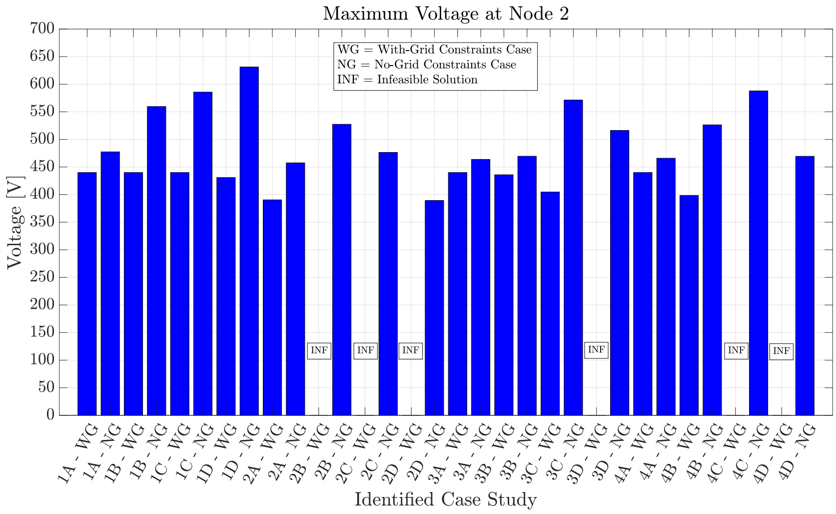

Figure 5.55: Maximum voltage at node 2 for all case studies

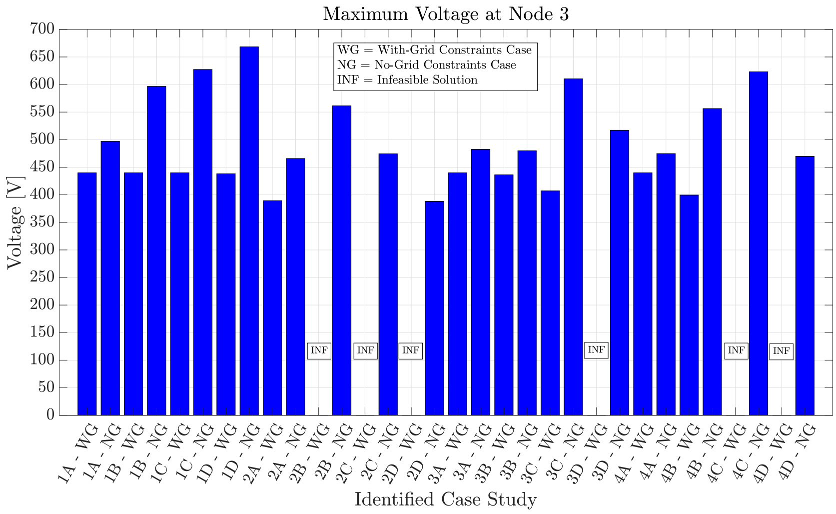

Figure 5.56: Maximum voltage at node 3 for all case studies

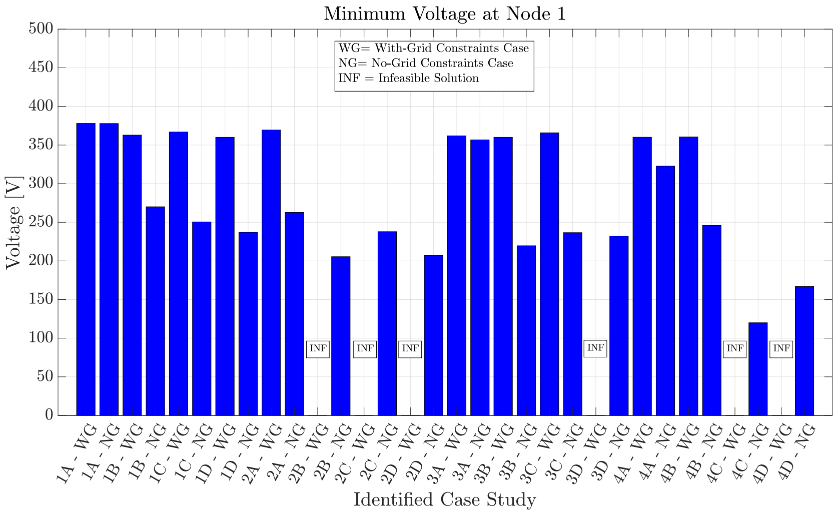

Figure 5.57: Minimum voltage at node 1 for all case studies

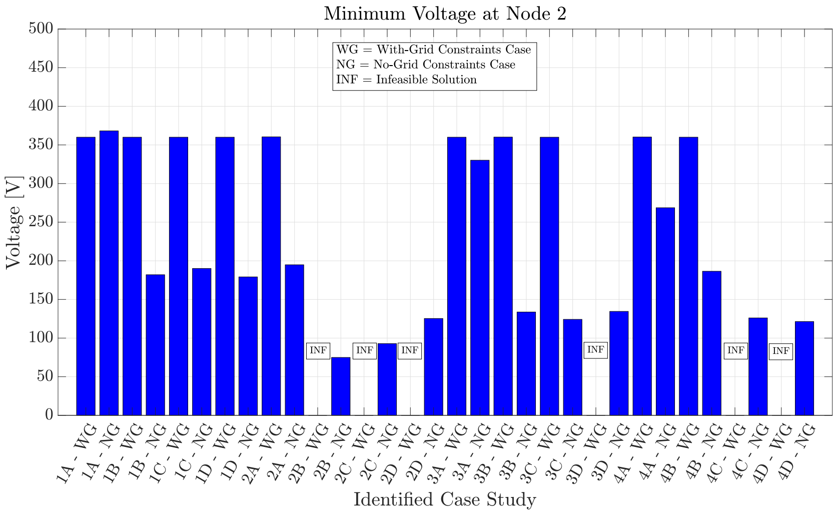

Figure 5.58: Minimum voltage at node 2 for all case studies

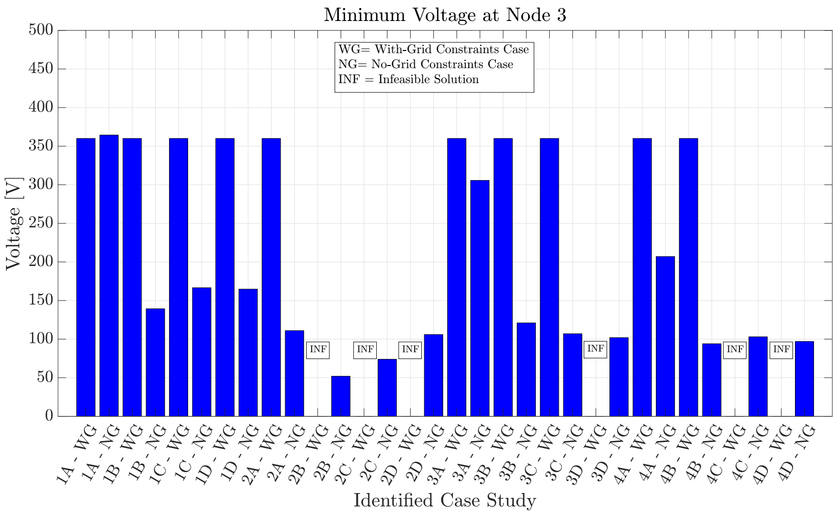

Figure 5.59: Minimum voltage at node 3 for all case studies

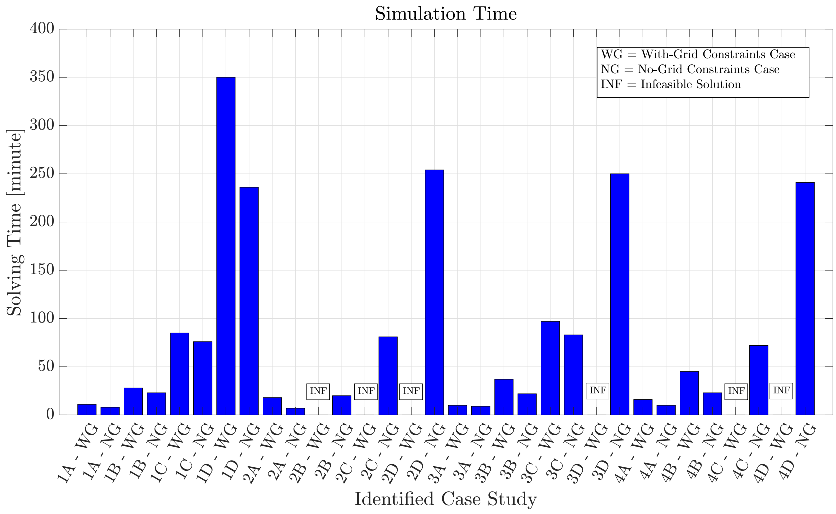

Figure 5.60: Total simulation time for all case studies

6

CONCLUSIONS AND FUTURE WORKS

This chapter presents the conclusions of all results obtained in this thesis. To conclude all of the results acquired in this study, the research questions as previously stated in Chapter 1 will again be presented and answered. Further, several recommendations for the future research in the scope of EVs smart charging are also outlined in this final chapter.

6.1. CONCLUSIONS

This section will discuss the main conclusions of the research study of optimal power management system of EVs charging by answering the research questions based on the previously explained results.

1. **How to formulate the optimal power management system of EVs charging from PV system in a low voltage distribution network considering the grid constraints?**
   ⇒ To formulate the proposed power management system, it is required first to define a set of constraints and the objective function so that it can be modeled into a real-life situation. The first step of modelling the proposed PMS was to construct the mathematical equations. Therefore, the following sub-research questions will be answered so that it clearly defines how the proposed power management system would optimally charge the EVs from PV system in a low voltage distribution network while considering the grid constraints.

   (a) **What are the EV constraints taken into considerations?**
   ⇒ The EV constraints implemented in the optimization model are based on several technical aspects as clearly stated in the equalities and inequalities in Eqs. 3.1 - 3.6. Firstly, the (dis)charging power is limited to the maximum rated power of the charger. Then, it is constrained that the EVs cannot charge and discharge via the V2G scheme simultaneously. Moreover, the proposed PMS always check whether the EVs are connected to the charger or not. Finally, a charging rate is restricted to avoid a large variation in the (dis)charging power at each timestep.

   (b) **What are the PV system constraints taken into considerations?**
   ⇒ A 32 kWp PV system is installed at each node of the implemented distribution network. The PV can feed its energy production into the EVs or back to the grid. As a result, the PV system at each node is constrained as written in Eq. 3.8.

   (c) **What are the grid constraints taken into considerations?**
   ⇒ The distribution grid with the voltage level of 230/400 V and its characteristics implied in this study is based on the CIGRE benchmark on low voltage network. It is constrained that to ensure the voltage magnitude at every node is always within the allowable voltage deviation based on the European standard EN50160 [51]. Furthermore, a set of constraints regarding the distribution grid is previously mentioned in Eqs. 3.9 - 3.16.

   (d) **What is the objective function of the proposed power management system?**
   ⇒ The objective function of the proposed power management system is to minimize the total operational cost of EVs charging integrated in a low voltage distribution grid. To find the objective function, it is required to select which optimization technique is suitable to solve the problem. It is

found that a mixed integer non-linear programming (MINLP) problem with Discrete and Continuous Optimizer (DICOPT) solver is selected and then executed in the General Algebraic Modelling System (GAMS) version 24.9.2 software.

2. **What is the impact of considering the grid constraints on the proposed power management system for the identified case studies?**
⇒ The impact of implementing the grid constraints on the proposed PMS has been analyzed thoroughly in section 5.5. It is concluded that considering the grid constraints could affect the total operational cost, the mitigation of grid violation, and the PV self-consumption. Therefore, the following sub-research questions will be answered and explained to what extent the grid constraints affect these technical and economic aspects.

   (a) **To what extent does the grid constraints affect the total operational cost for the identified case studies?**

      - **Summer PV profile** During summer, the total operational cost of the with-grid constraints case has been increased by 1.43% - 113.20% when compared to the no-grid constraints case.
      - **Winter PV profile** During a day in winter, the PMS has shown an increase in the total operational cost between 20.38% - 29.59% in comparison to the no-grid constraints case.
      - **Spring PV profile** During spring, the operational cost of EVs charging is added up by 39.31% - 60.48% when compared to the no-grid cosntraints case.
      - **Autumn PV profile** For a one-day operation of EVs charging during autumn, the total cost is gained by 0.43% - 42.12% compared to the no-grid constraints studied case.

   (b) **To what extent does the grid constraints avoid the grid violations for the identified case studies?**

      - **With-Grid Constraints** For all case studies which consider the grid constraints, the PMS has accomplished avoiding the grid violation. The defined grid violation is the transformer peak power limit and the allowable voltage deviation. It has been shown that for all case studies the transformer peak power never goes beyond 400 kW and the voltage magnitude at every node is always within the allowable deviation, i.e., between 360 V and 440 V.
      - **No-Grid Constraints** It is found in the case study 1D that it violates the transformer peak power limitation. The peak power of the distribution transformer could reach more than 400 kW. Moreover, the longest duration of the voltage violation at the first, second, and third node takes place in the case study 4D. In addition, the average period of voltage limit violation at node 1, node 2, and node 3 are 124, 132, and 145 minutes over one day of operation, respectively.

   (c) **To what extent does the grid constraints increase the PV power allocated for EVs charging for the identified case studies?**

      - **Summer PV profile** During the one-day operation of EVs charging during summer, the PMS achieved an increment in the PV power used for EVs charging between 2.50% - 27.69% when compared to the no-grid constraints case.
      - **Winter PV profile** During winter, the results show that by implementing the proposed power management system could escalate the PV power allocated for EVs charging by 87.33% in comparison to the no-grid constraints case.
      - **Spring PV profile** In one day of spring season, implementing the PMS for EVs charging results in increasing the PV power used for EVs charging by 21.25% - 38.40% compared to the no-grid constraints studied case.
      - **Autumn PV profile** During autumn, the PMS has achieved in increasing the PV power allocated for EVs charging by 0.21% - 28.36% when compared to the no-grid constraints case.

6.2. RECOMMENDATION FOR FUTURE WORKS

In this section, several recommendations for future study in the scope of EVs smart charging in a low voltage distribution network are described as follows.

- The objective function of minimizing the power losses in the distribution lines can also be done by using the same model as explained extensively in this study.
- In further work, to validate the proposed model, the existing typical Dutch distribution network, for instance, the data from the local DSOs can be implemented.
- The proposed optimal power management system can be further used in the related studies, such as IEEE test feeder.
- To achieve the target for both the DSO and the aggregator perspective, a multi-objective function is considerably feasible to be done in future work.
- A multiplexing technique where multiple EVs can be charged by using the same charger is potentially profitable to be installed in the EV charger. This technology would reduce the initial investment cost for the charging infrastructure.
- In future research, adjusting the resistance and the inductance of the line can be added up to the input parameters to perform more sensitivity analysis.

A

Appendices

A.1. Overview of All Simulation Results

Table A.1: Overview of results of all case studies

Case Study	Grid Constraints	Total PV-to-EV Energy [kWh]	Total PV Production [kWh]	PV Self-consumption [%]	Total Operational Cost [€]
1A	✓	166.30	654.45	25.41	-64.82
	-	166.30	654.45	25.41	-64.82
1B	✓	318.88	654.45	48.72	-40.56
	-	318.88	654.45	48.72	-41.15
1C	✓	326.84	654.45	49.94	-15.07
	-	318.88	654.45	48.72	-19.35
1D	✓	407.18	654.45	62.22	20.68
	-	318.88	654.45	48.72	9.70
2A	✓	20.44	28.4	71.96	17.25
	-	10.91	28.4	38.42	14.33
2B	✓	***INFEASIBLE SOLUTION***			
	-	10.91	28.4	38.42	39.06
2C	✓	***INFEASIBLE SOLUTION***			
	-	10.91	28.4	38.42	61.52
2D	✓	***INFEASIBLE SOLUTION***			
	-	10.91	28.4	38.42	91.07
3A	✓	151.44	282.24	53.66	-16.93
	-	151.44	282.24	53.66	-16.93
3B	✓	185.92	282.24	65.87	12.02
	-	153.34	282.24	54.33	7.49
3C	✓	212.22	282.24	75.19	41.18
	-	153.34	282.24	54.33	29.56
3D	✓	***INFEASIBLE SOLUTION***			
	-	153.34	282.24	54.33	59.05
4A	✓	129.29	238.39	54.23	-11.48
	-	129.29	238.39	54.23	-11.53
4B	✓	165.96	238.39	69.62	18.39
	-	129.29	238.39	54.23	12.94
4C	✓	***INFEASIBLE SOLUTION***			
	-	129.29	238.39	54.23	35.14
4D	✓	***INFEASIBLE SOLUTION***			
	-	129.29	238.39	54.23	64.64

A.2. SUMMER PV PROFILE

A.2.1. RESULTS OF CASE STUDY 1A (SUMMER, 2 EVS PER NODE)

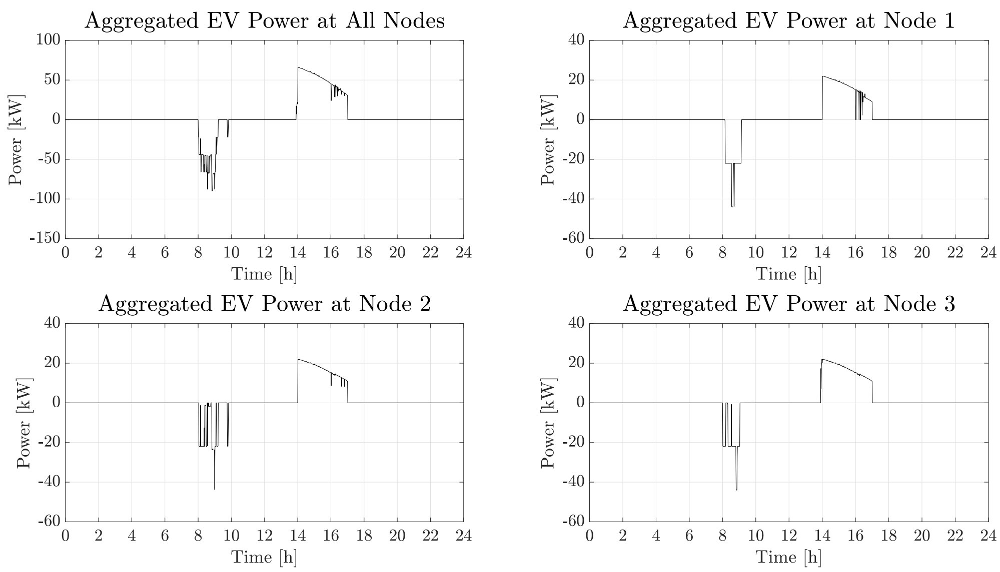

Figure A.1: Aggregated EV power at all nodes for case study 1A (No-Grid Constraints)

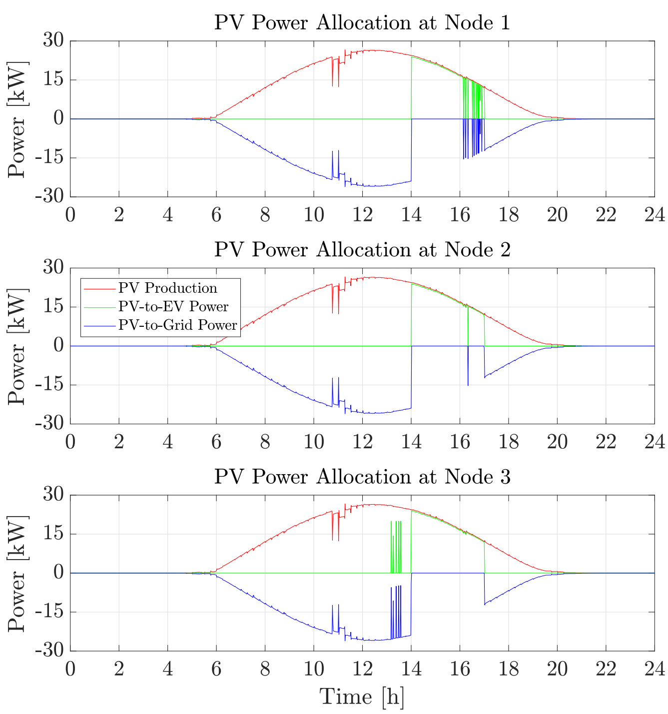

Figure A.2: PV power allocation at all nodes for case study 1A (With-Grid Constraints)

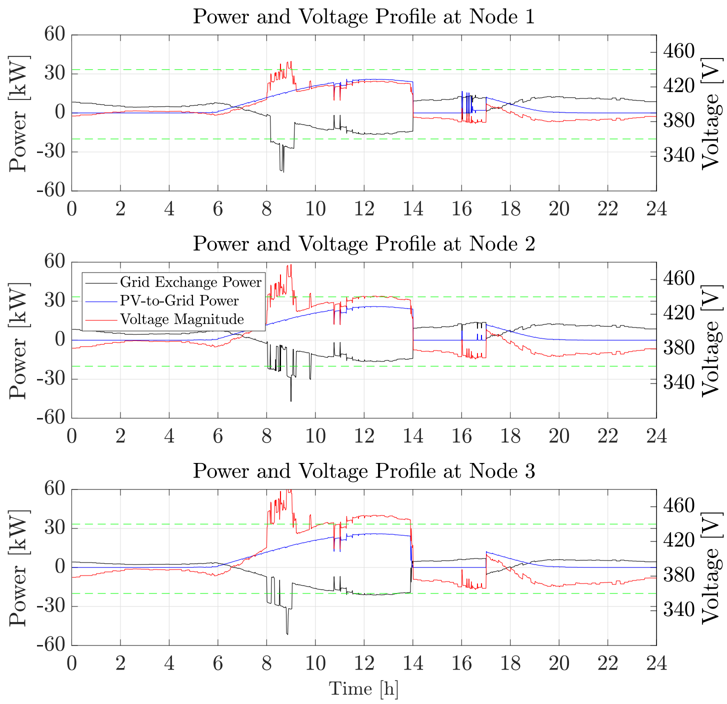

Figure A.4: Voltage magnitude at all nodes for case study 1A (No-Grid Constraints)

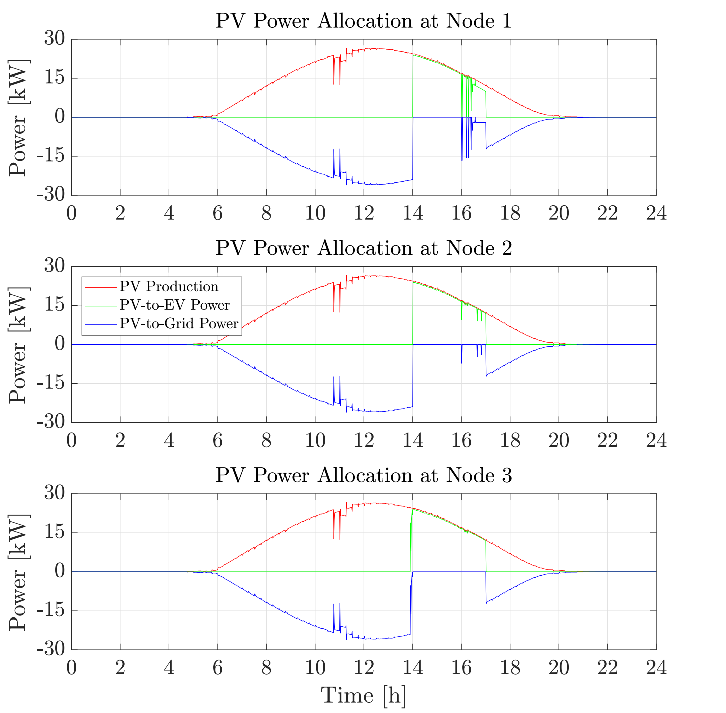

Figure A.3: PV power allocation at all nodes for case study 1A (No-Grid Constraints)

A.2.2. RESULTS OF CASE STUDY 1B (SUMMER, 5 EVS PER NODE)

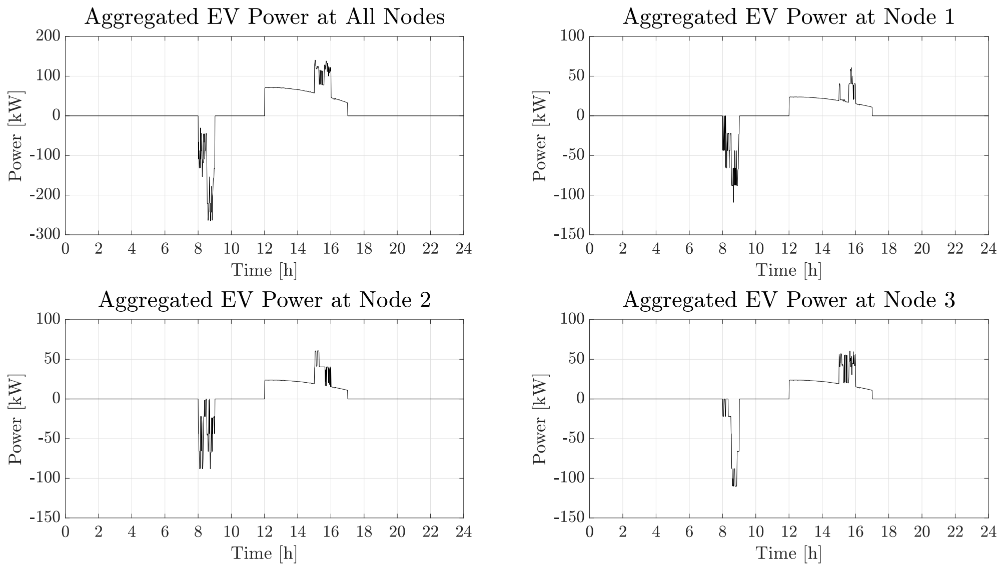

Figure A.5: Aggregated EV power at all nodes for case study 1B (No-Grid Constraints)

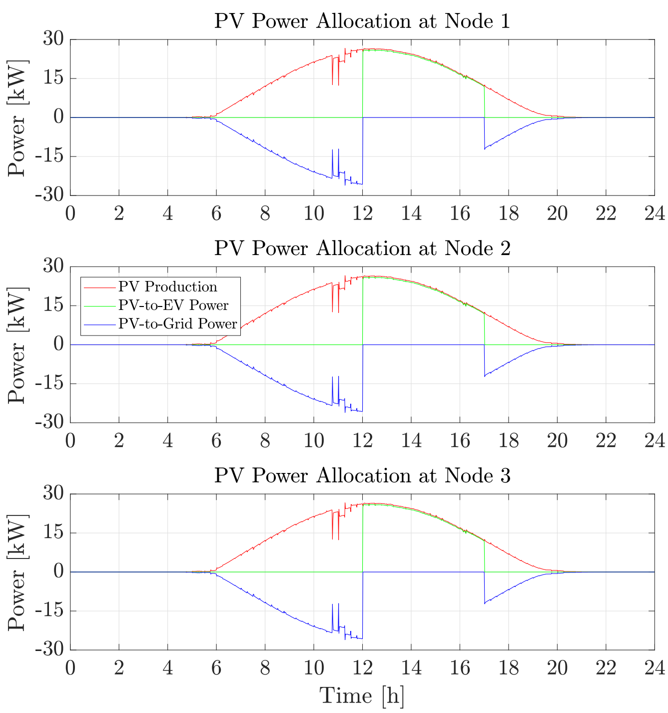

Figure A.6: PV power allocation at all nodes for case study 1B (With-Grid Constraints)

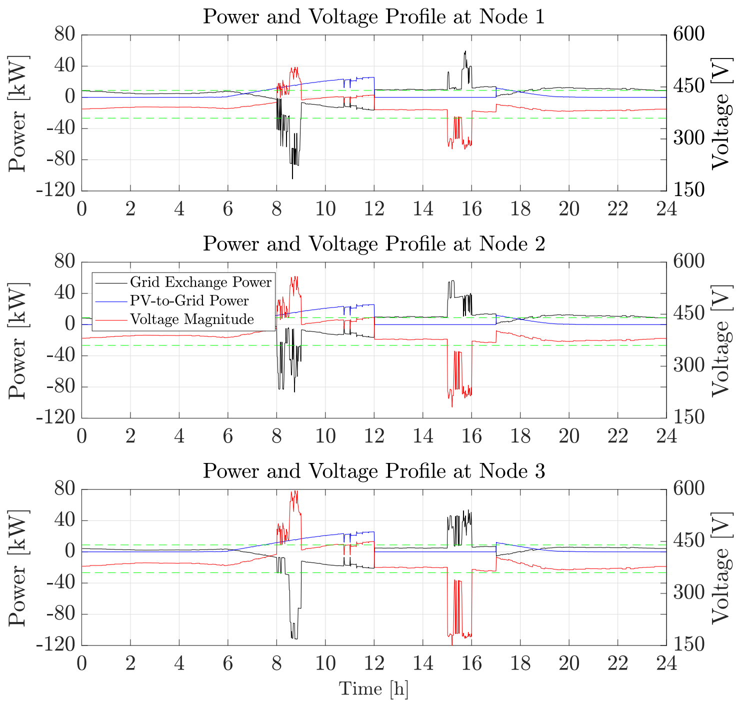

Figure A.8: Voltage magnitude at all nodes for case study 1B (No-Grid Constraints)

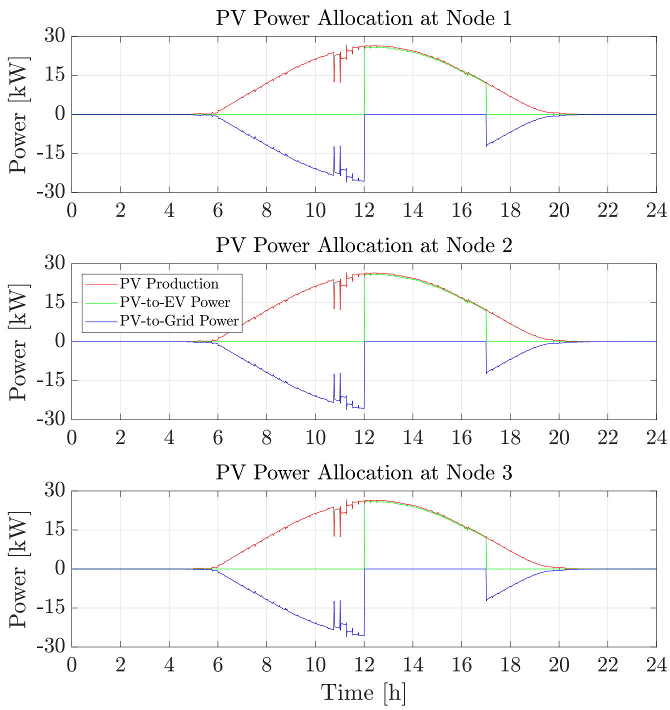

Figure A.7: PV power allocation at all nodes for case study 1B (No-Grid Constraints)

A.2.3. RESULTS OF CASE STUDY 1C (SUMMER, 7 EVS PER NODE)

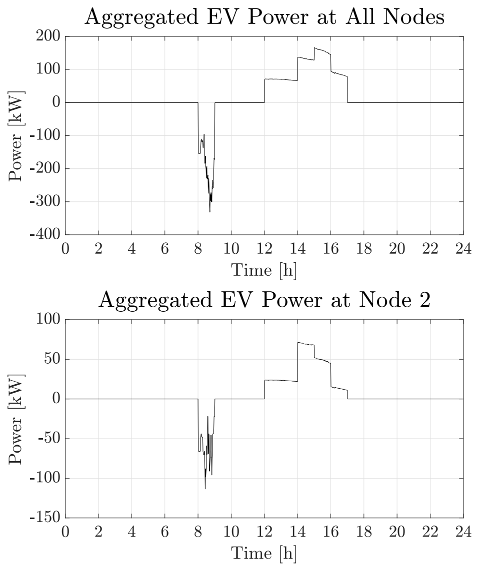

Figure A.9: Aggregated EV power at all nodes for case study 1C (No-Grid Constraints)

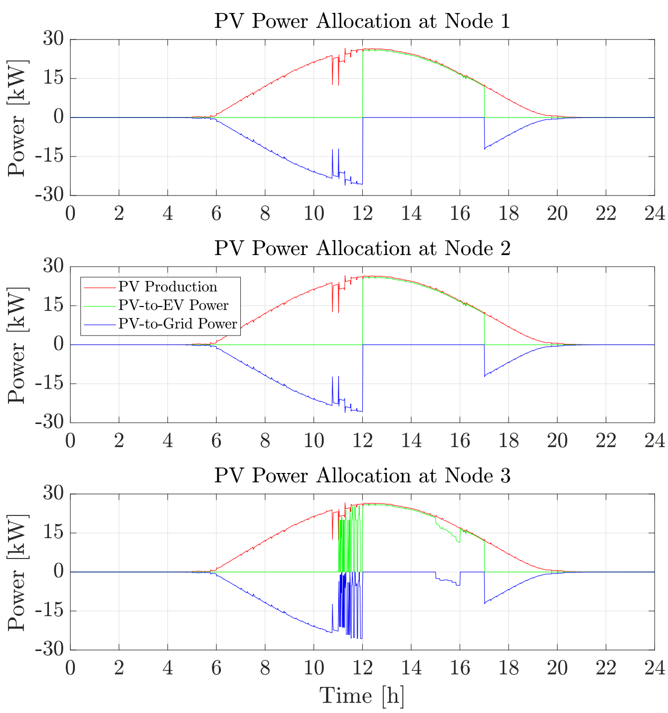

Figure A.10: PV power allocation at all nodes for case study 1C (With-Grid Constraints)

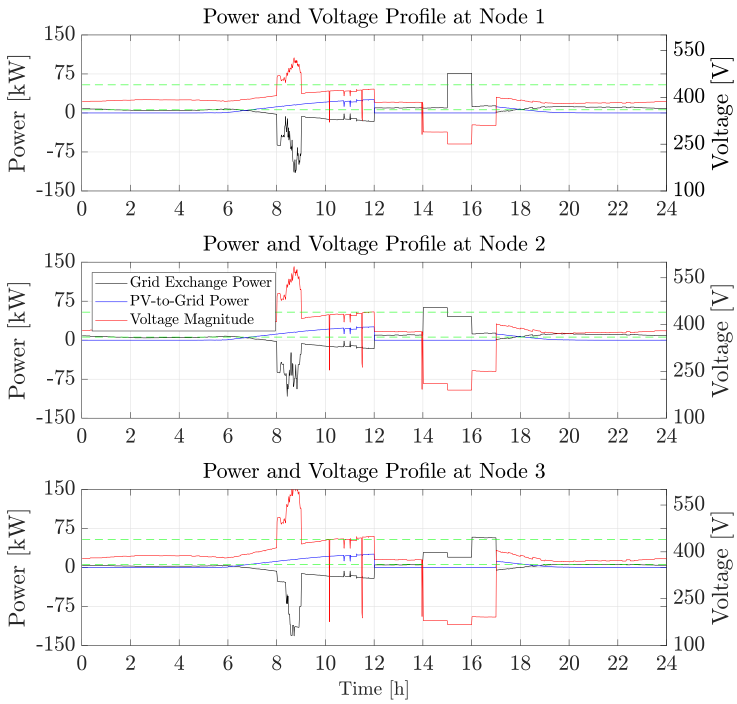

Figure A.12: Voltage magnitude at all nodes for case study 1C (No-Grid Constraints)

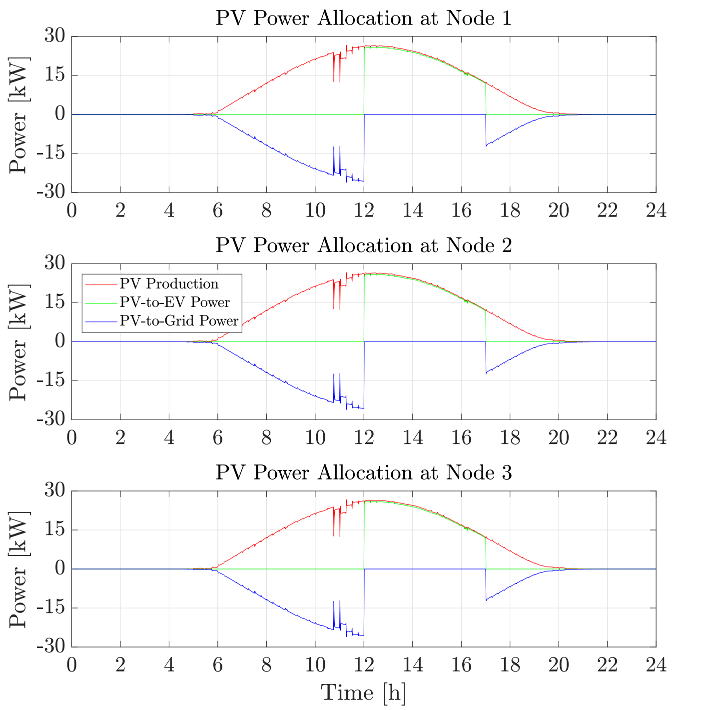

Figure A.11: PV power allocation at all nodes for case study 1C (No-Grid Constraints)

A.2.4. RESULTS OF CASE STUDY 1D (SUMMER, 10 EVS PER NODE)

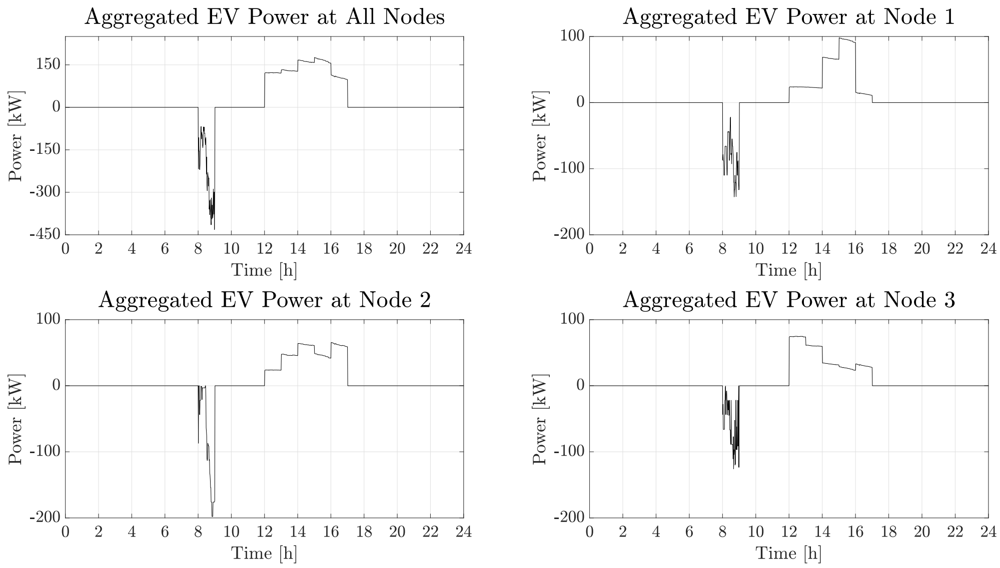

Figure A.13: Aggregated EV power at all nodes for case study 1D (No-Grid Constraints)

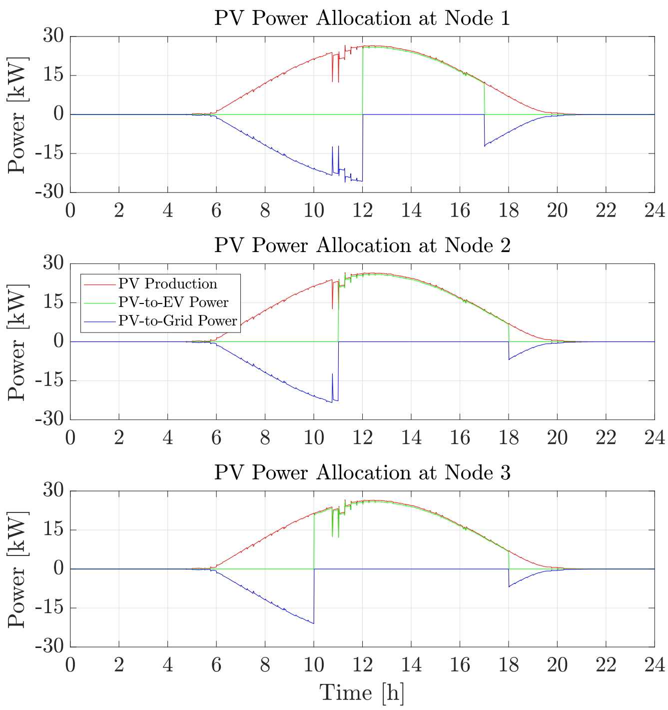

Figure A.14: PV power allocation at all nodes for case study 1D (With-Grid Constraints)

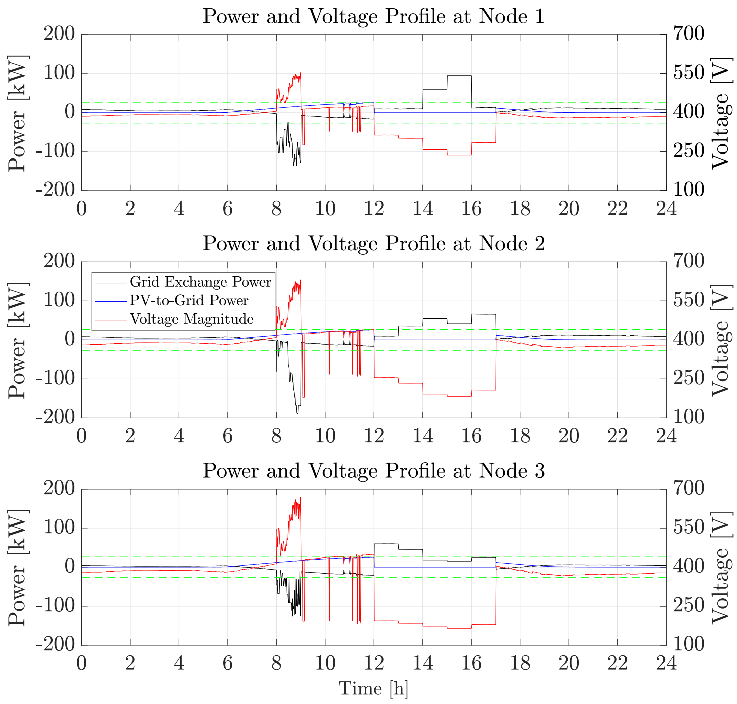

Figure A.16: Voltage magnitude at all nodes for case study 1D (No-Grid Constraints)

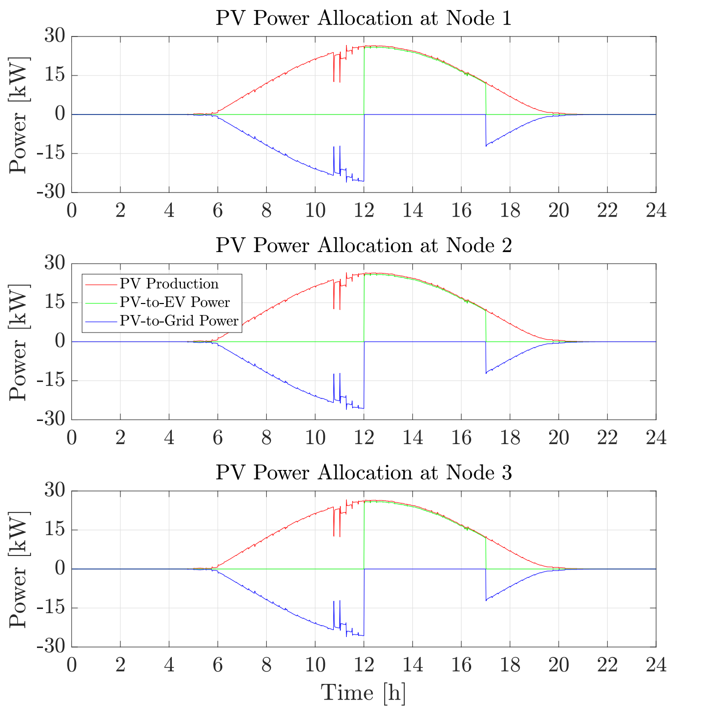

Figure A.15: PV power allocation at all nodes for case study 1D (No-Grid Constraints)

A.3. WINTER PV PROFILE

A.3.1. RESULTS OF CASE STUDY 2A (WINTER, 2 EVS PER NODE)

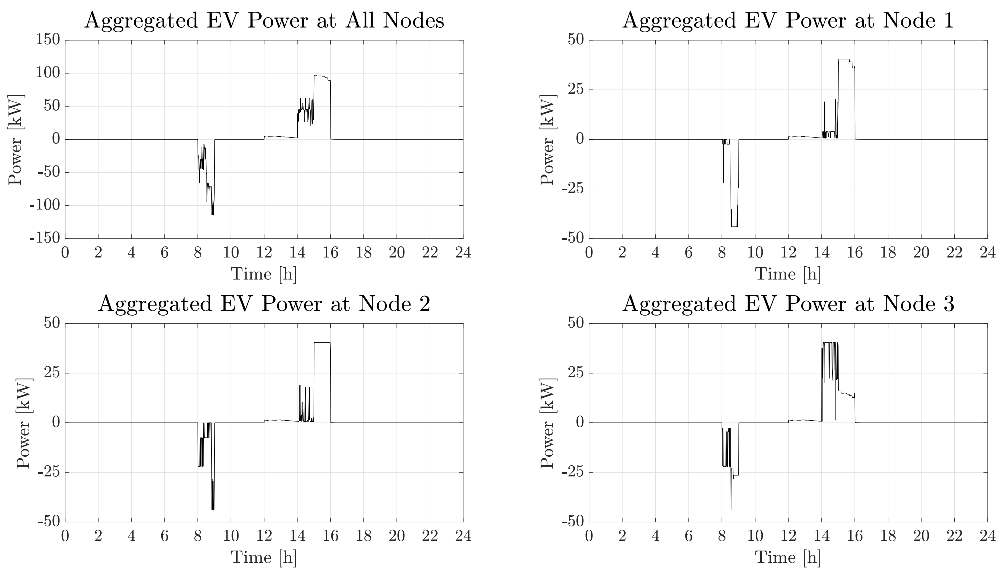

Figure A.17: Aggregated EV power at all nodes for case study 2A (No-Grid Constraints)

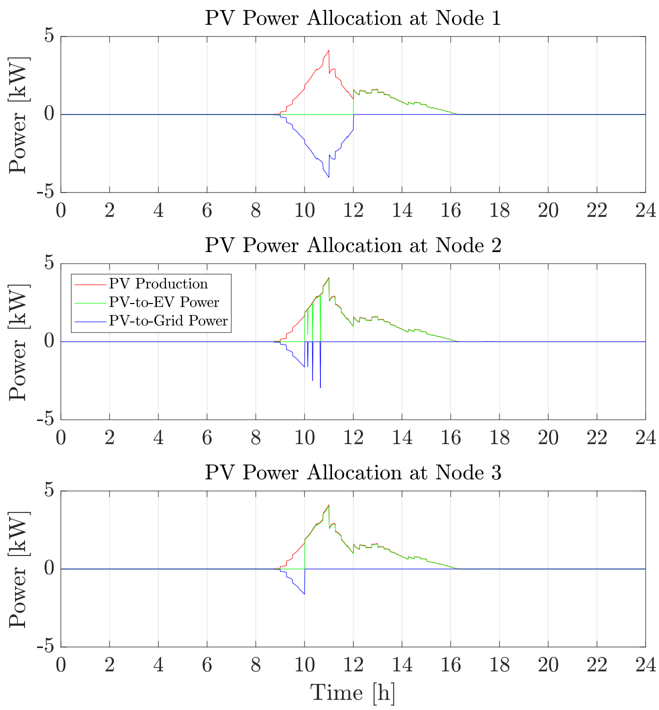

Figure A.18: PV power allocation at all nodes for case study 2A (With-Grid Constraints)

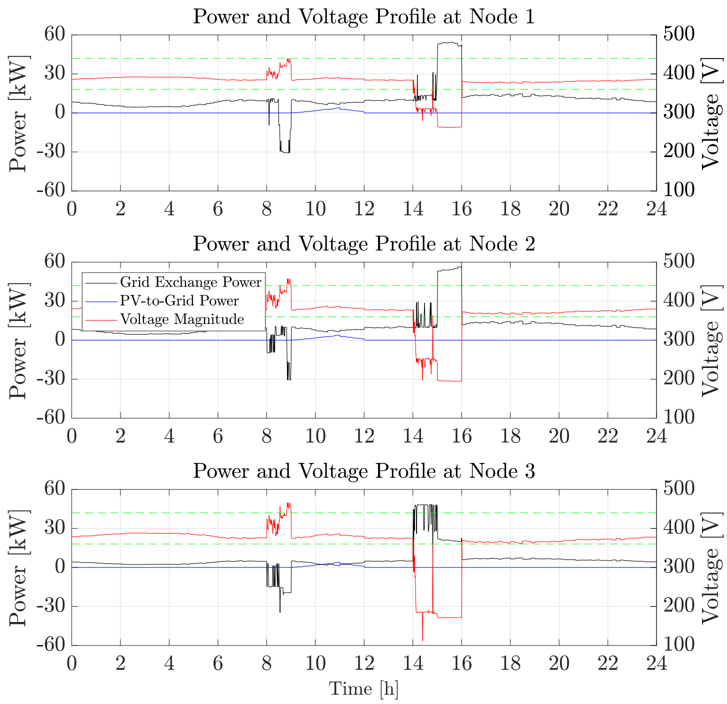

Figure A.20: Voltage magnitude at all nodes for case study 2A (No-Grid Constraints)

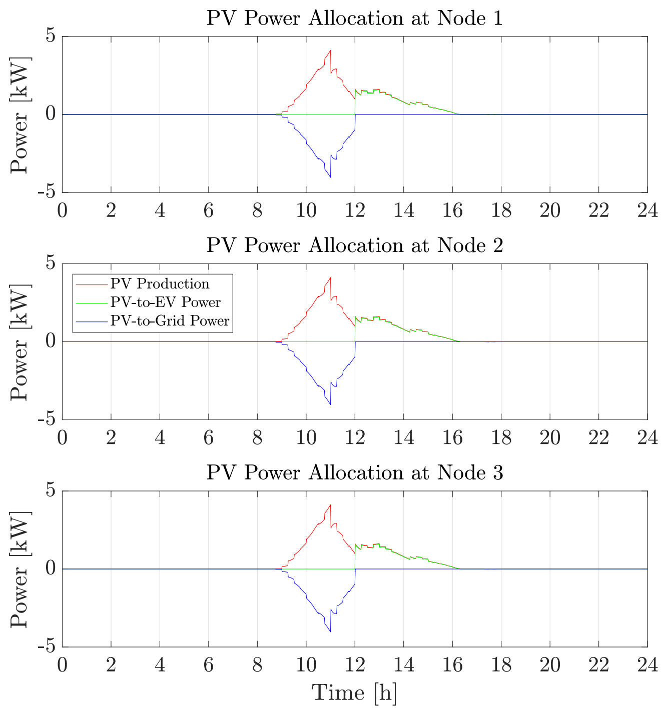

Figure A.19: PV power allocation at all nodes for case study 2A (No-Grid Constraints)

A.3.2. RESULTS OF CASE STUDY 2B (WINTER, 5 EVS PER NODE)

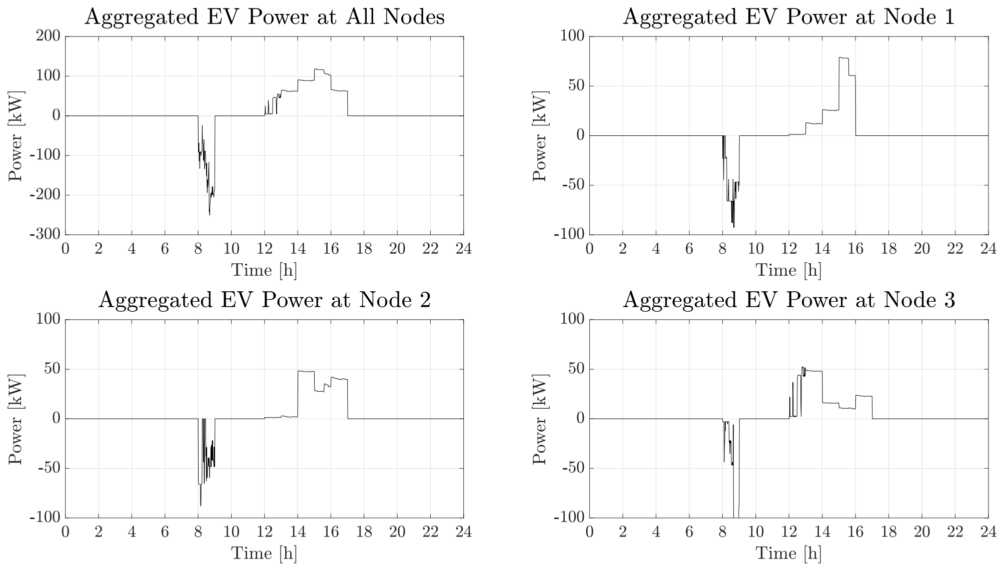

Figure A.21: Aggregated EV power at all nodes for case study 2B (No-Grid Constraints)

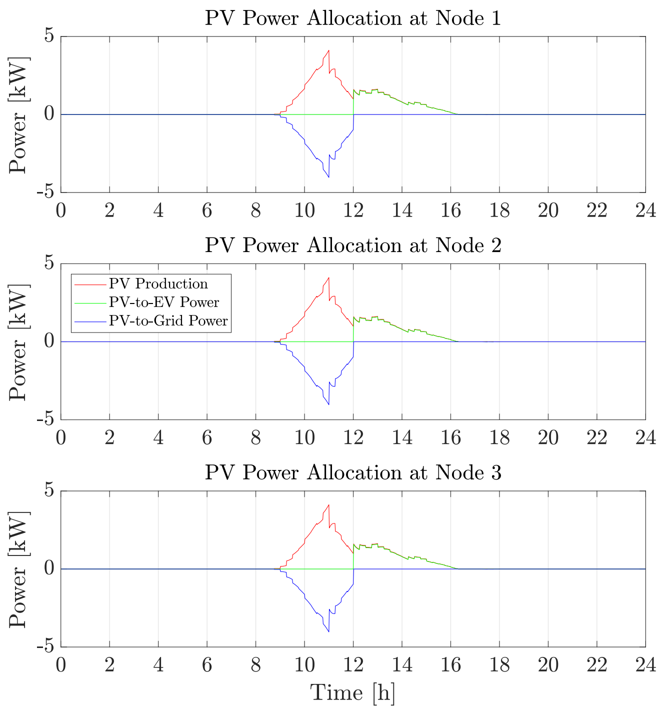

Figure A.22: PV power allocation at all nodes for case study 2B (No-Grid Constraints)

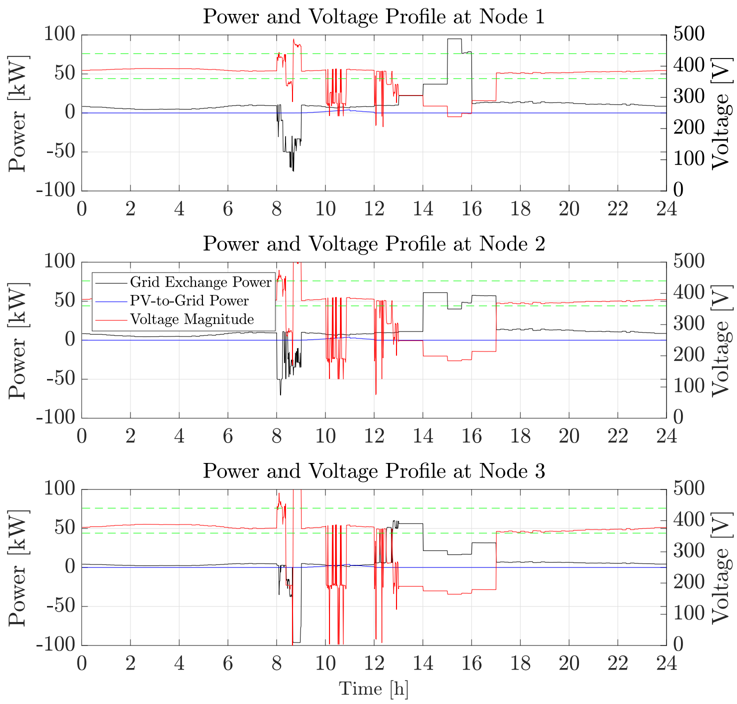

Figure A.23: Voltage magnitude at all nodes for case study 2B (No-Grid Constraints)

A.3.3. Results of Case Study 2C (Winter, 7 EVs per node)

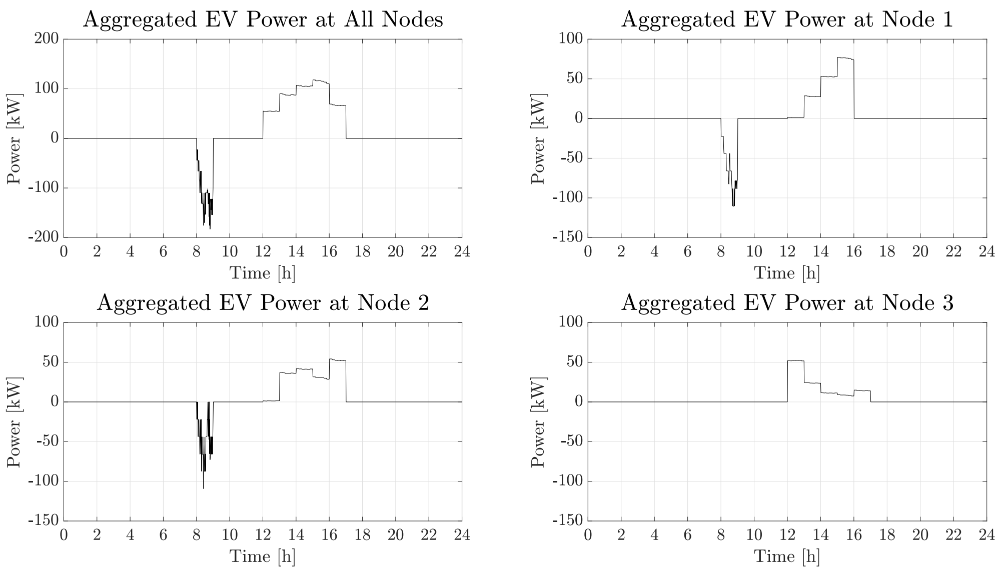

Figure A.24: Aggregated EV power at all nodes for case study 2C (No-Grid Constraints)

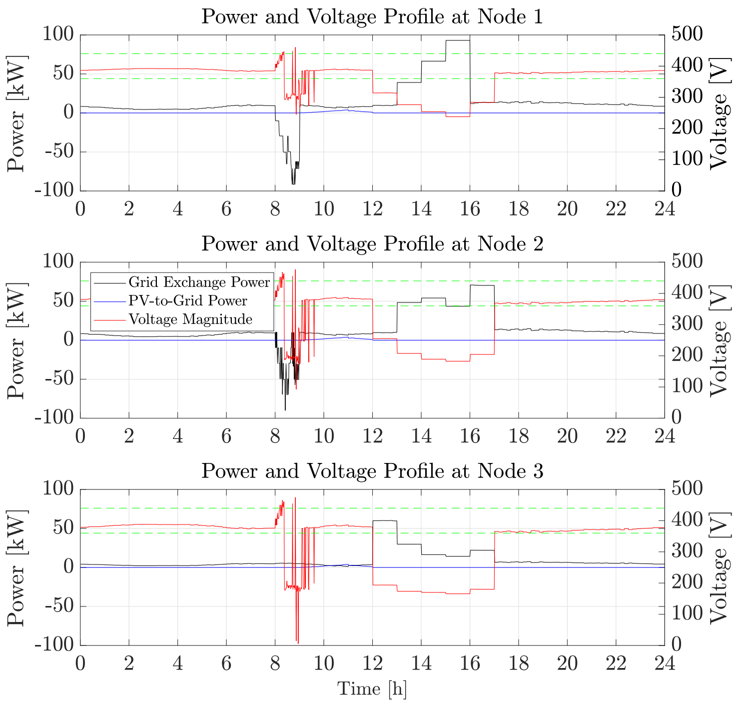

Figure A.26: Voltage magnitude at all nodes for case study 2C (No-Grid Constraints)

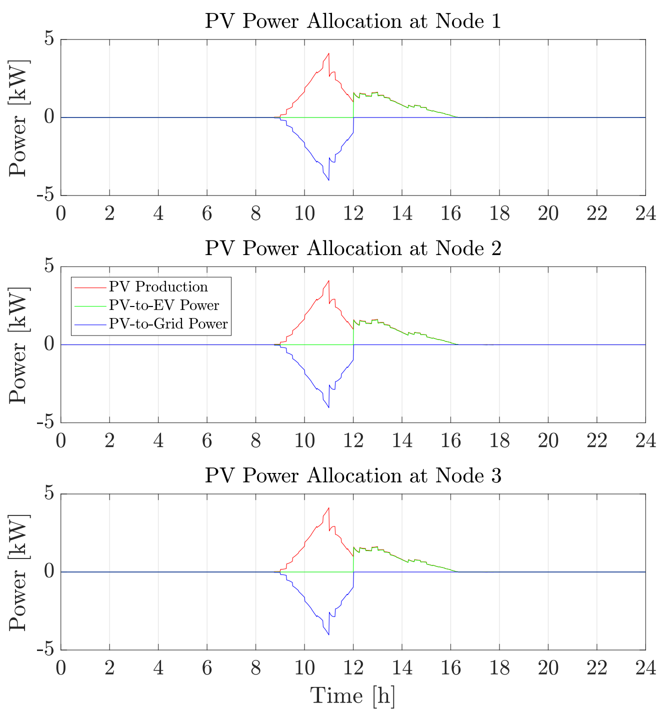

Figure A.25: PV power allocation at all nodes for case study 2C (No-Grid Constraints)

A.3.4. RESULTS OF CASE STUDY 2D (WINTER, 10 EVS PER NODE)

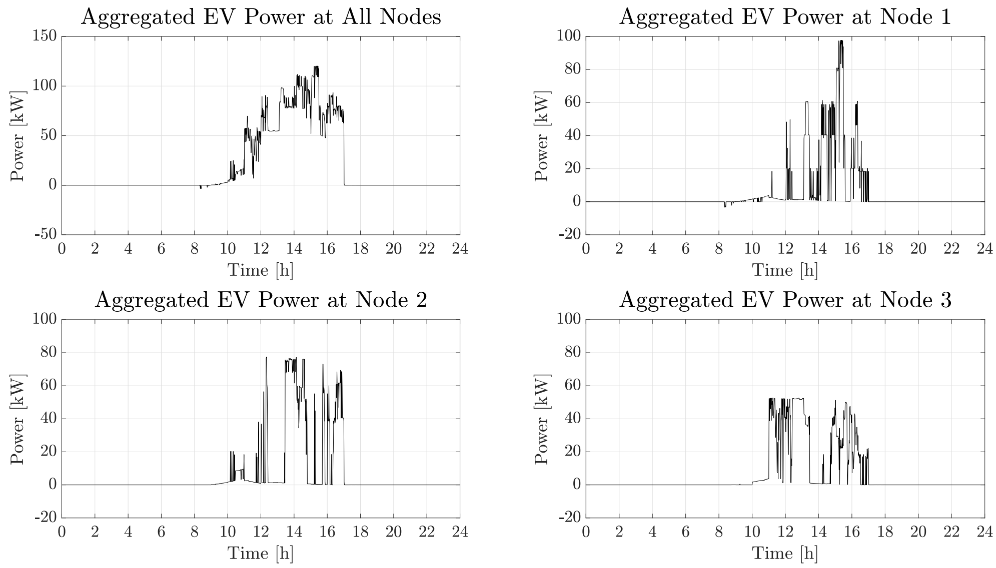

Figure A.27: Aggregated EV power at all nodes for case study 2D (No-Grid Constraints)

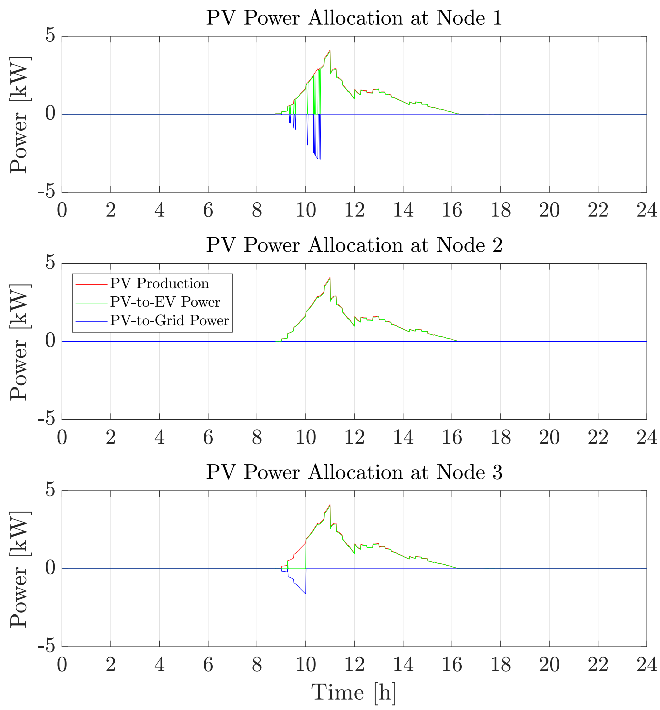

Figure A.28: PV power allocation at all nodes for case study 2D (No-Grid Constraints)

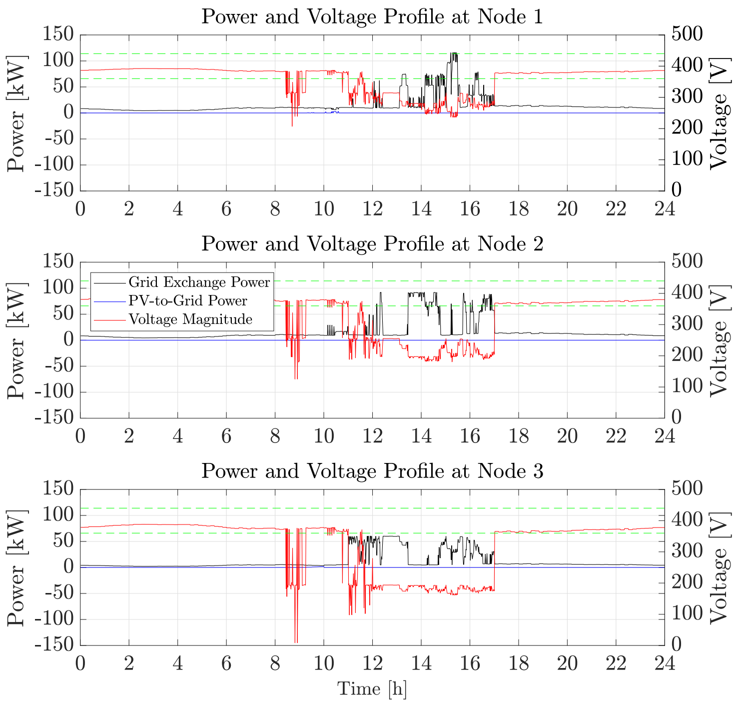

Figure A.29: Voltage magnitude at all nodes for case study 2D (No-Grid Constraints)

A.4. Spring PV Profile

A.4.1. Results of Case Study 3A (Spring, 2 EVs per node)

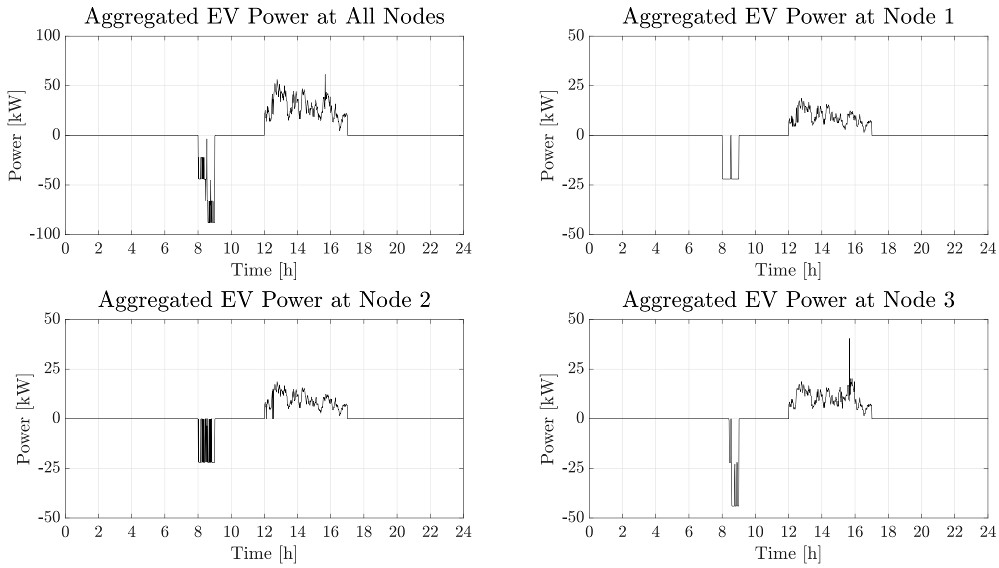

Figure A.30: Aggregated EV power at all nodes for case study 3A (No-Grid Constraints)

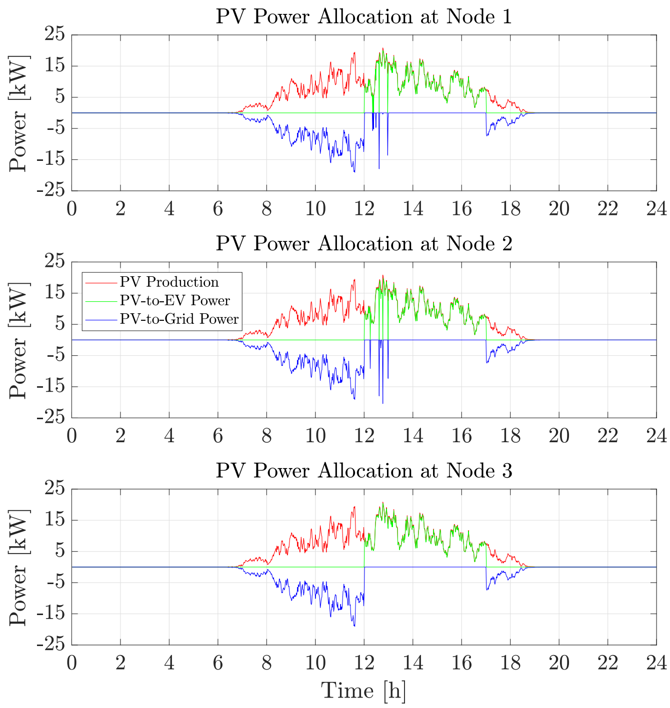

Figure A.31: PV power allocation at all nodes for case study 3A (With-Grid Constraints)

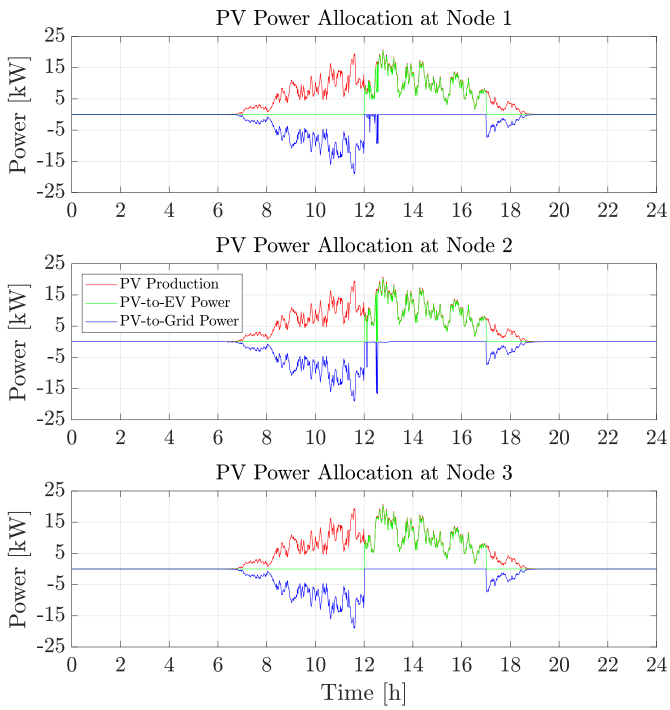

Figure A.32: PV power allocation at all nodes for case study 3A (No-Grid Constraints)

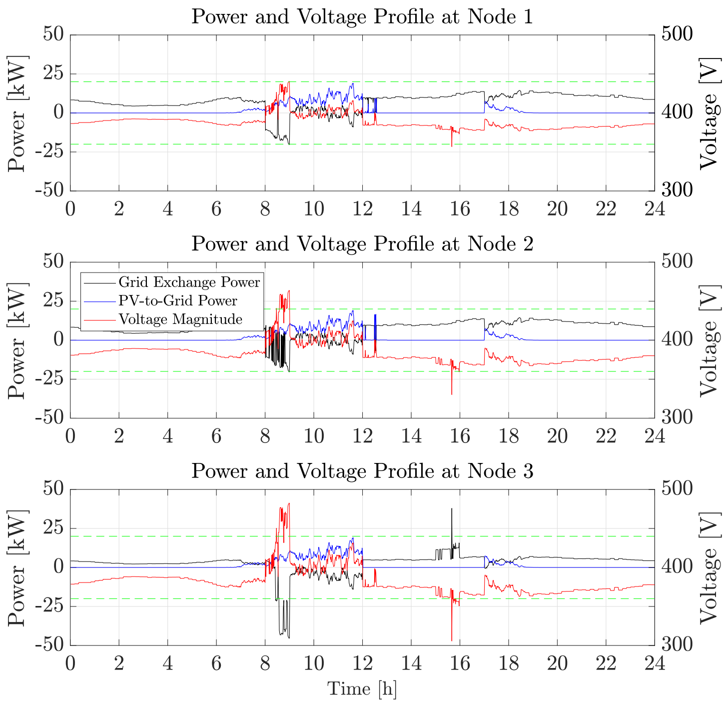

Figure A.33: Voltage magnitude at all nodes for case study 3A (No-Grid Constraints)

A.4.2. RESULTS OF CASE STUDY 3B (SPRING, 5 EVS PER NODE)

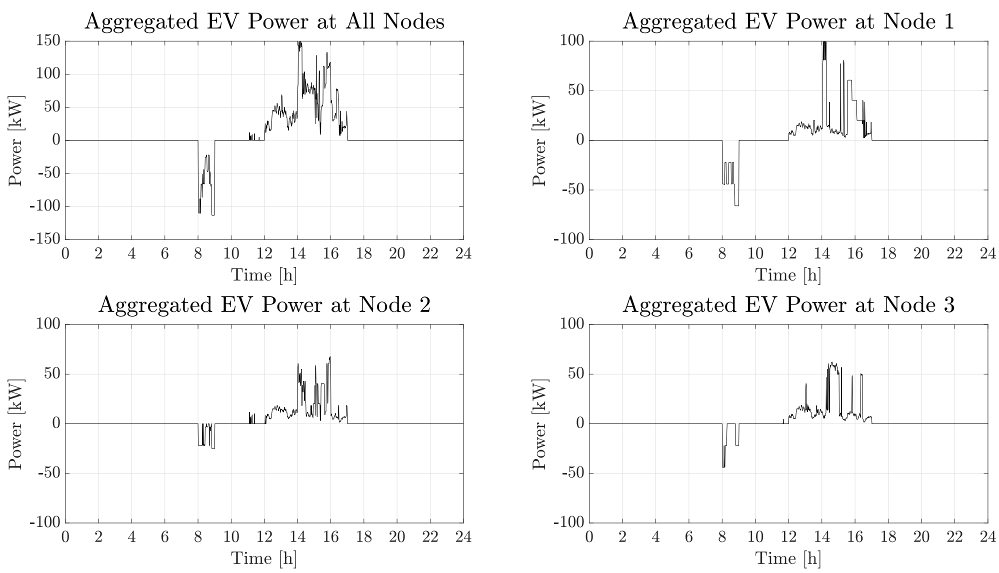

Figure A.34: Aggregated EV power at all nodes for case study 3B (No-Grid Constraints)

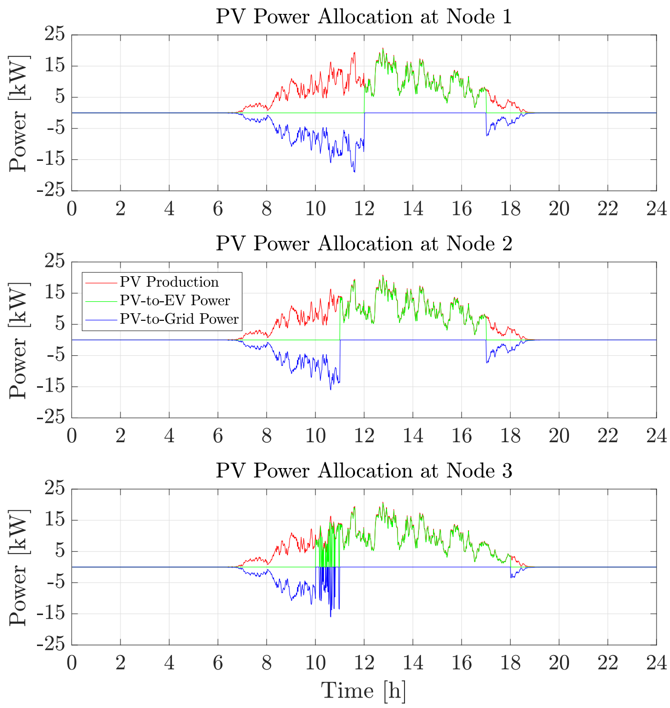

Figure A.35: PV power allocation at all nodes for case study 3B (With-Grid Constraints)

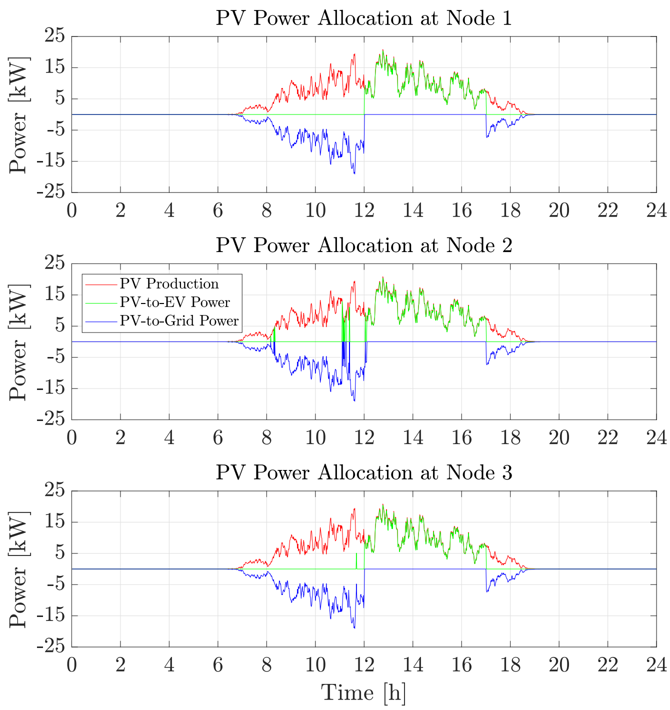

Figure A.36: PV power allocation at all nodes for case study 3B (No-Grid Constraints)

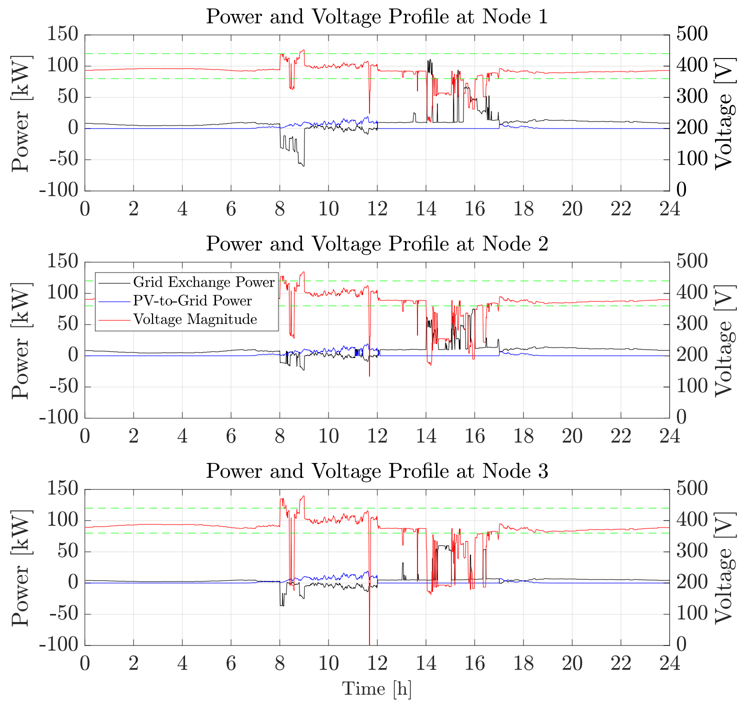

Figure A.37: Voltage magnitude at all nodes for case study 3B (No-Grid Constraints)

A.4.3. RESULTS OF CASE STUDY 3C (SPRING, 7 EVS PER NODE)

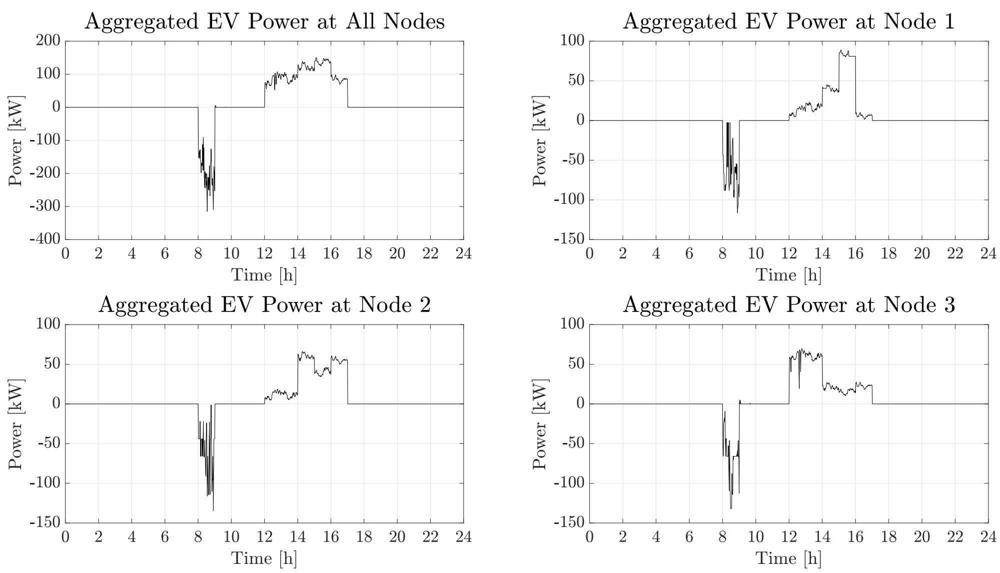

Figure A.38: Aggregated EV power at all nodes for case study 3C (No-Grid Constraints)

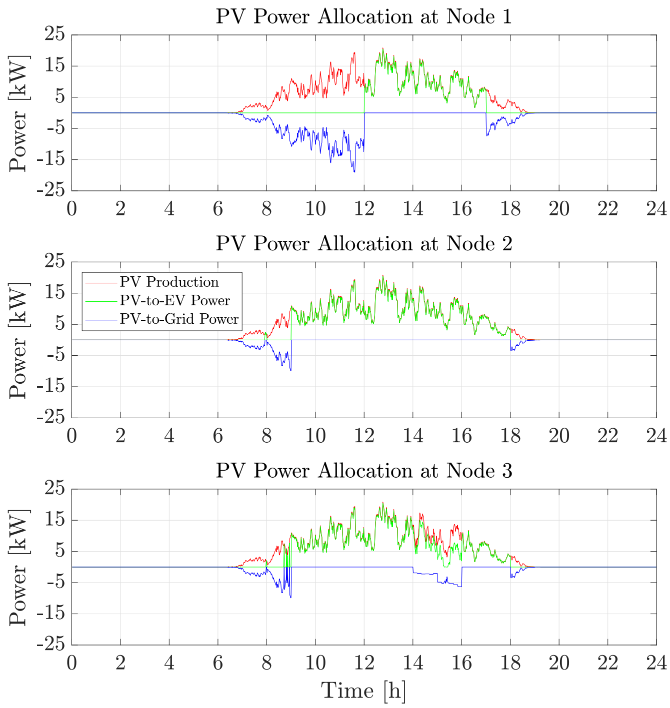

Figure A.39: PV power allocation at all nodes for case study 3C (With-Grid Constraints)

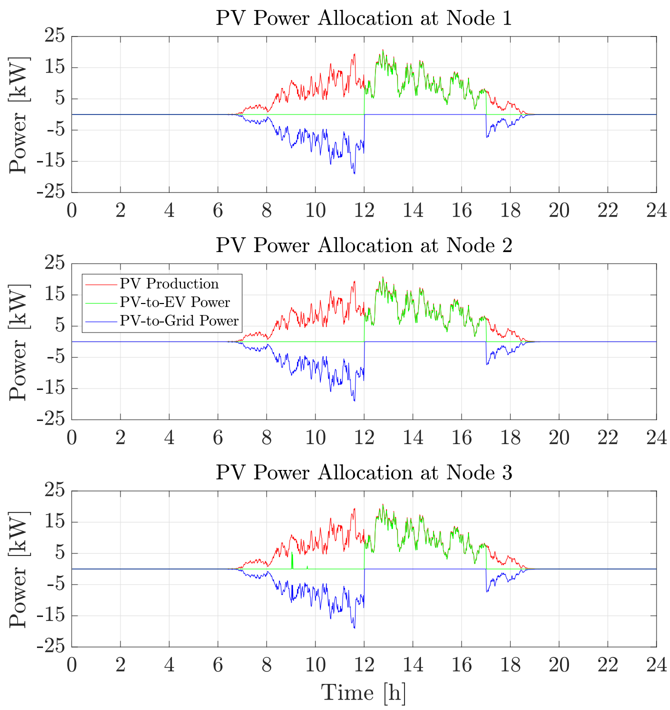

Figure A.40: PV power allocation at all nodes for case study 3C (No-Grid Constraints)

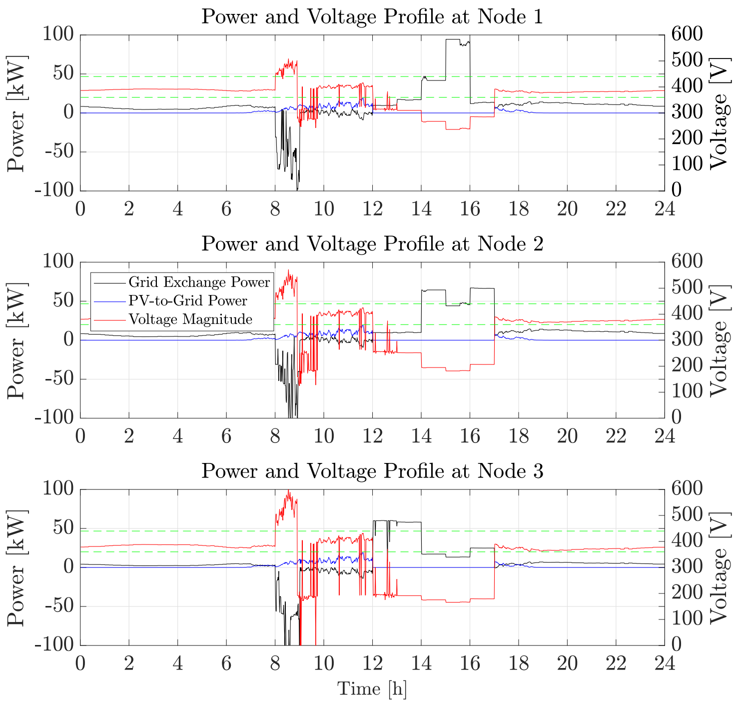

Figure A.41: Voltage magnitude at all nodes for case study 3C (No-Grid Constraints)

A.4.4. RESULTS OF CASE STUDY 3D (SPRING, 10 EVS PER NODE)

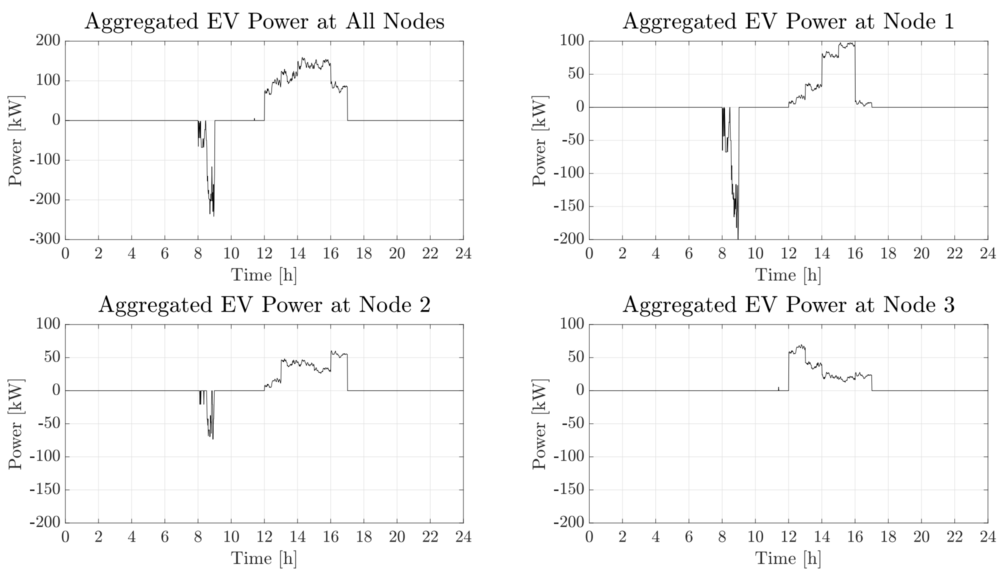

Figure A.42: Aggregated EV power at all nodes for case study 3D (No-Grid Constraints)

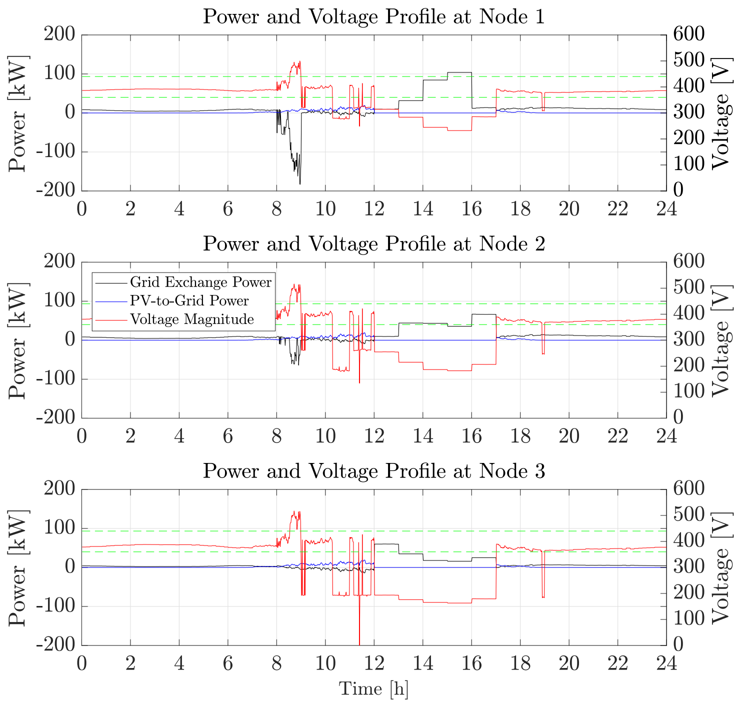

Figure A.44: Voltage magnitude at all nodes for case study 3D (No-Grid Constraints)

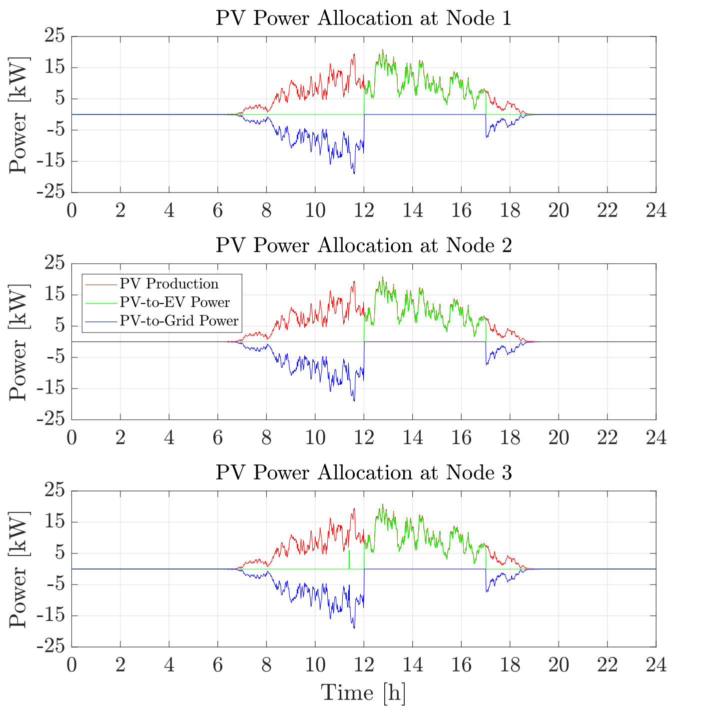

Figure A.43: PV power allocation at all nodes for case study 3D (No-Grid Constraints)

A.5. AUTUMN PV PROFILE

A.5.1. RESULTS OF CASE STUDY 4A (AUTUMN, 2 EVS PER NODE)

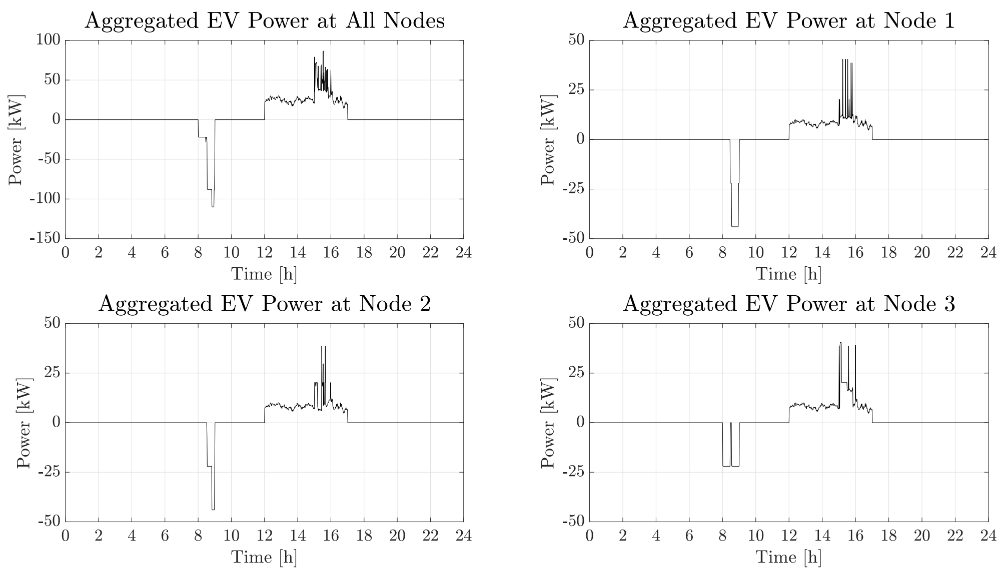

Figure A.45: Aggregated EV power at all nodes for case study 4A (No-Grid Constraints)

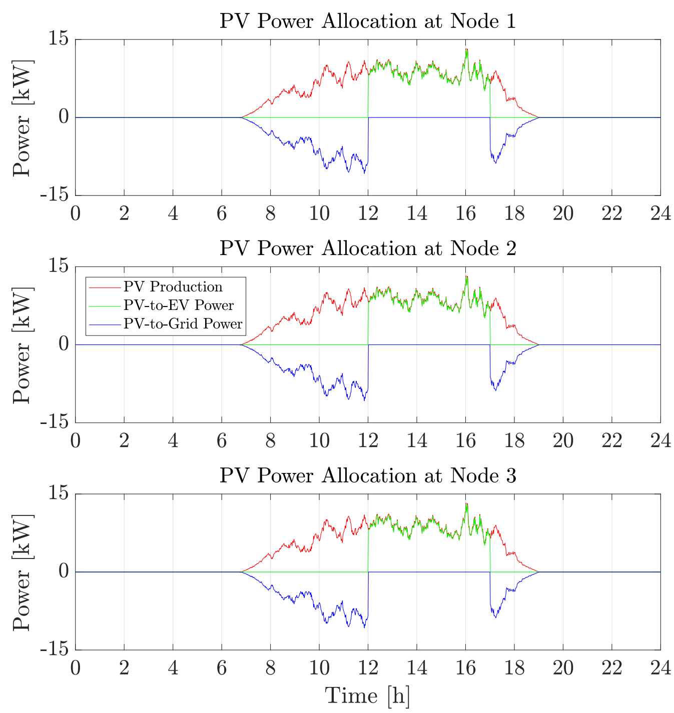

Figure A.46: PV power allocation at all nodes for case study 4A (With-Grid Constraints)

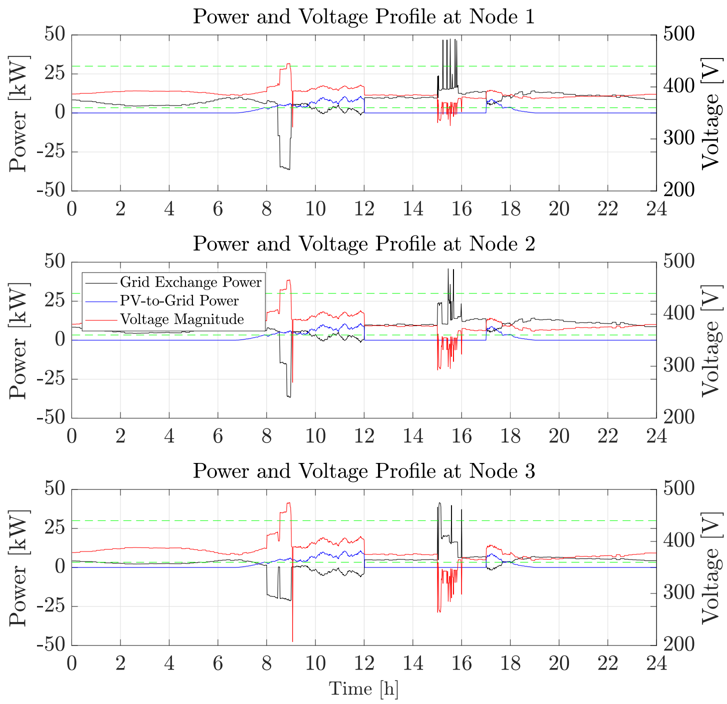

Figure A.48: Voltage magnitude at all nodes for case study 4A (No-Grid Constraints)

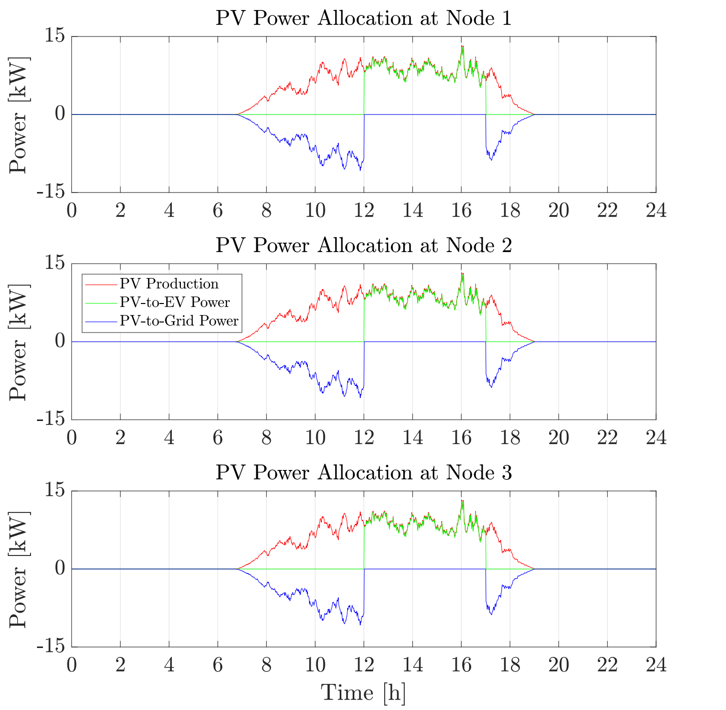

Figure A.47: PV power allocation at all nodes for case study 4A (No-Grid Constraints)

A.5.2. RESULTS OF CASE STUDY 4B (AUTUMN, 5 EVS PER NODE)

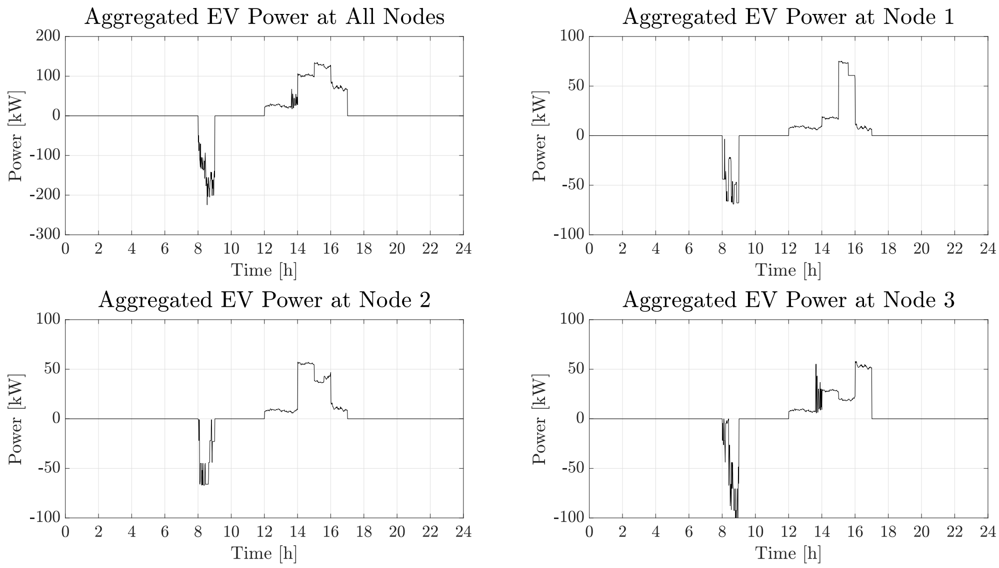

Figure A.49: Aggregated EV power at all nodes for case study 4B (No-Grid Constraints)

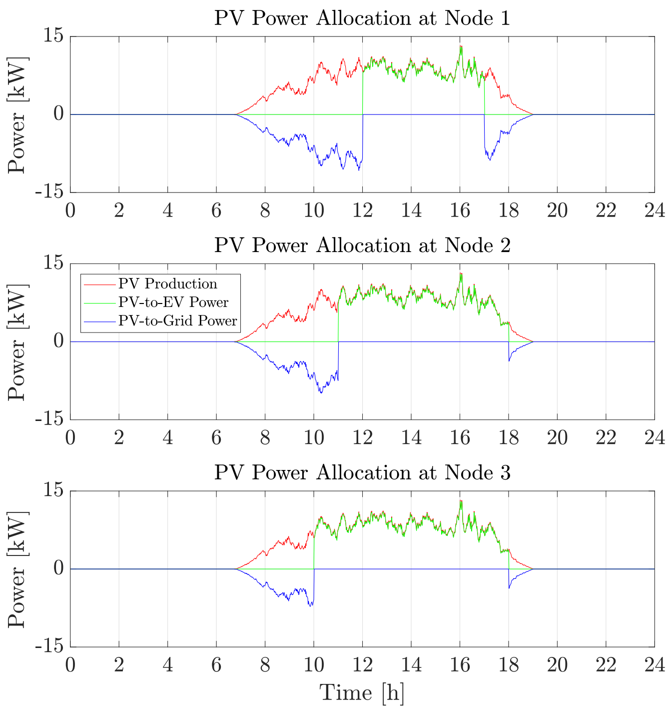

Figure A.50: PV power allocation at all nodes for case study 4B (With-Grid Constraints)

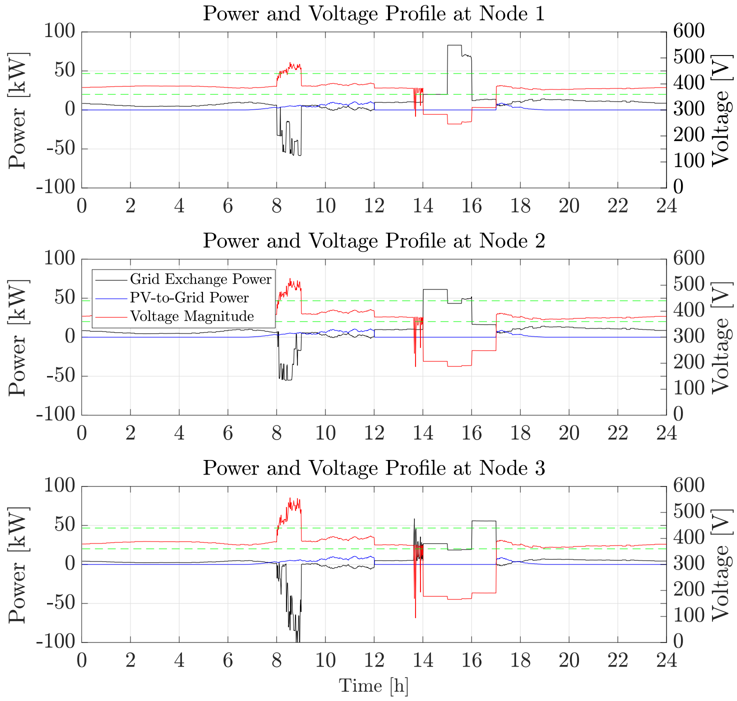

Figure A.52: Voltage magnitude at all nodes for case study 4B (No-Grid Constraints)

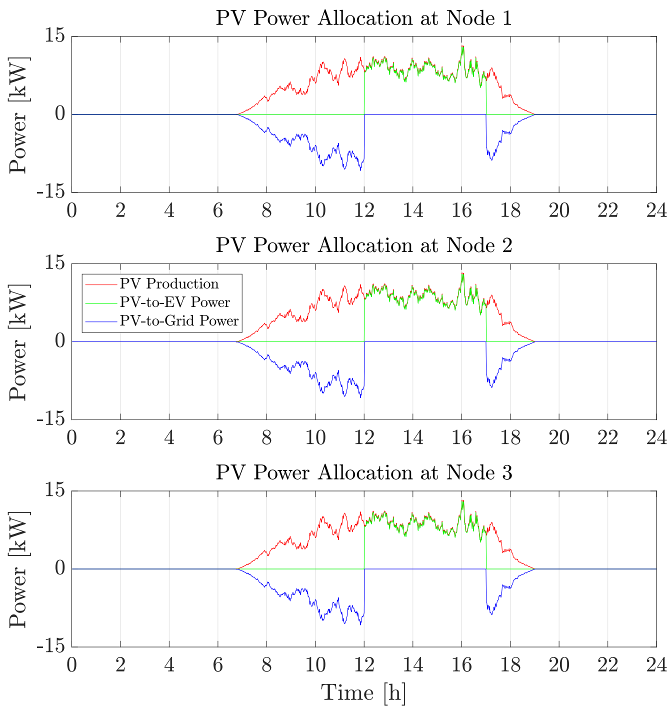

Figure A.51: PV power allocation at all nodes for case study 4B (No-Grid Constraints)

A.5.3. RESULTS OF CASE STUDY 4C (AUTUMN, 7 EVS PER NODE)

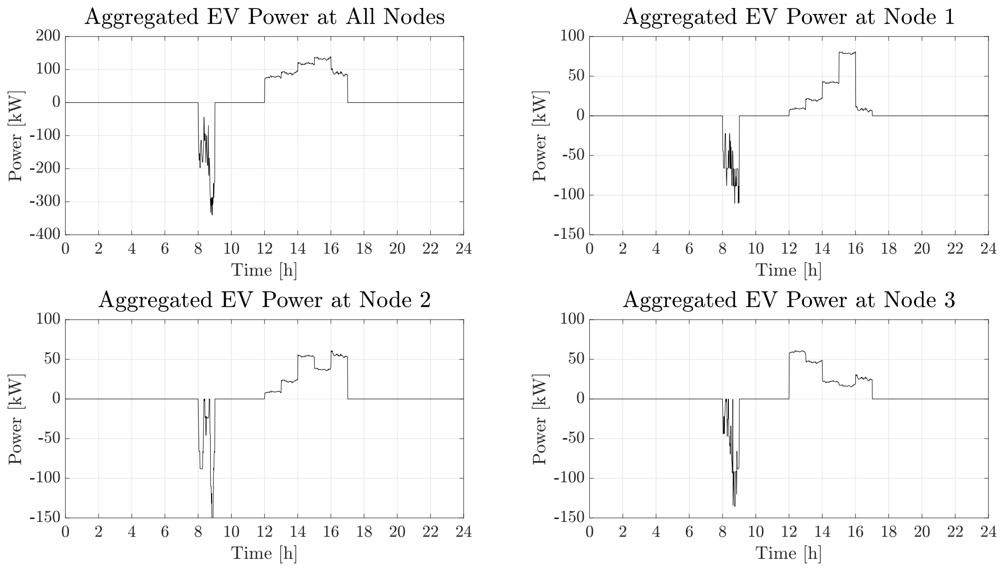

Figure A.53: Aggregated EV power at all nodes for case study 4C (No-Grid Constraints)

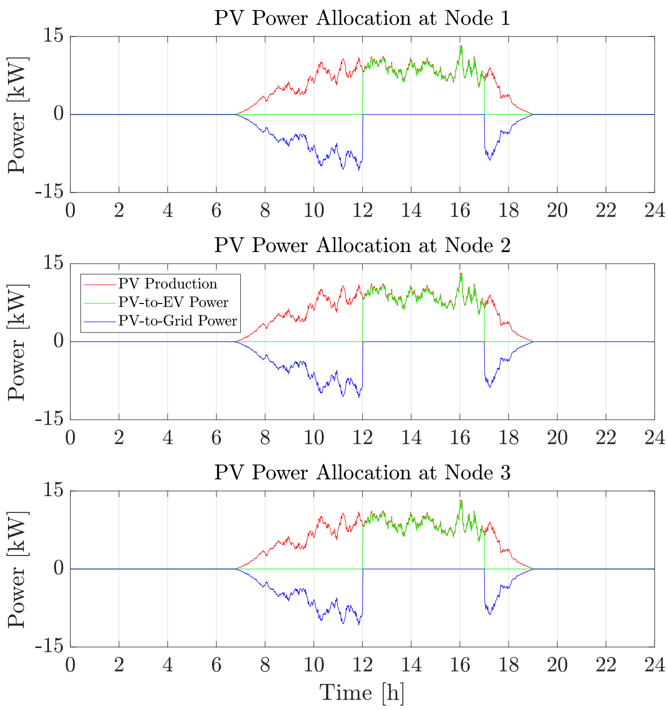

Figure A.54: PV power allocation at all nodes for case study 4C (No-Grid Constraints)

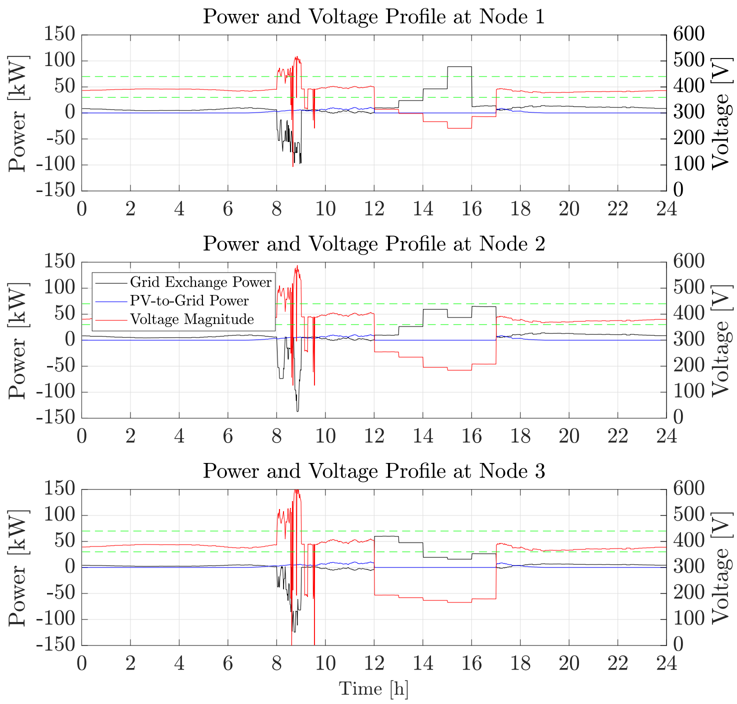

Figure A.55: Voltage magnitude at all nodes for case study 4C (No-Grid Constraints)

A.5.4. Results of Case Study 4D (Autumn, 10 EVs per node)

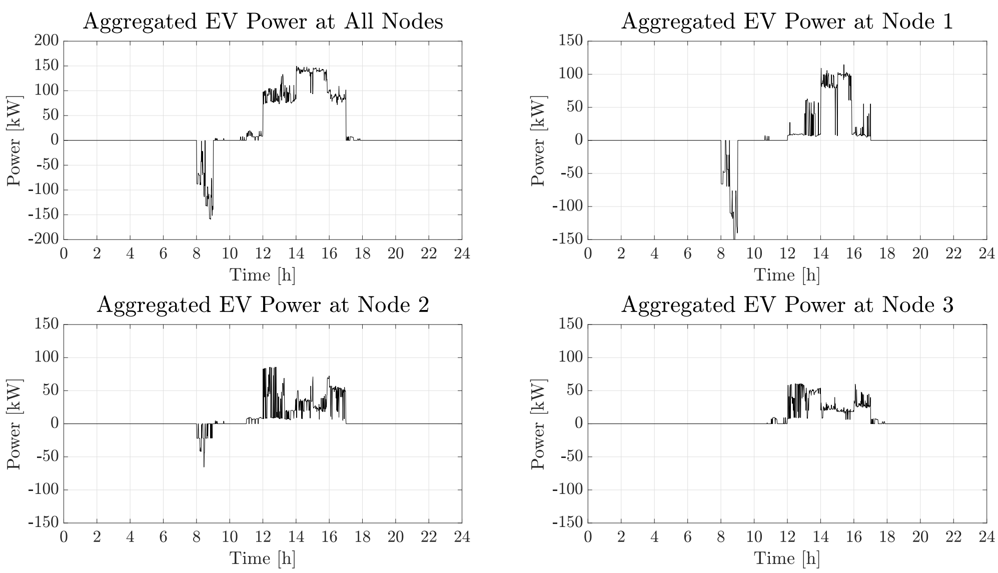

Figure A.56: Aggregated EV power at all nodes for case study 4D (No-Grid Constraints)

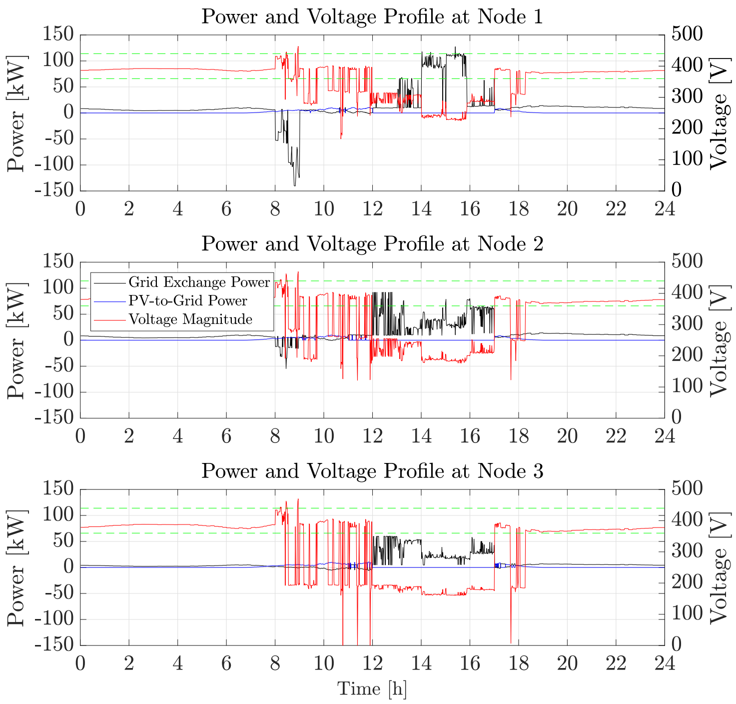

Figure A.58: Voltage magnitude at all nodes for case study 4D (No-Grid Constraints)

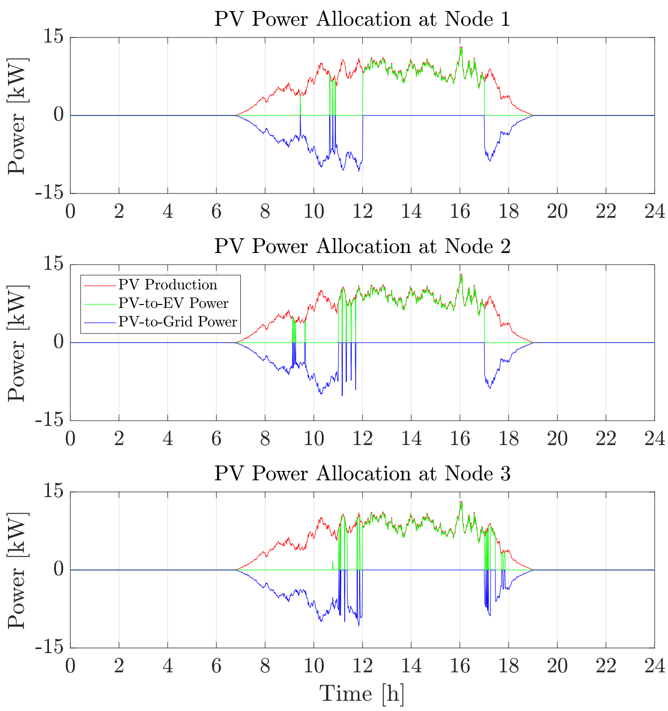

Figure A.57: PV power allocation at all nodes for case study 4D (No-Grid Constraints)

BIBLIOGRAPHY

[1] Rijksdienst voor Ondernemend Nederland, *Electric passenger cars and charging points in The Netherlands: Analysis of 2017,* (2018), Cited 29-01-2018 from: https://www.rvo.nl.

[2] Centraal Bureau van Statistiek, *Number of all-electric cars increasing rapidly,* (2018), Cited 31-05-2018 from: https://www.cbs.nl.

[3] SolarPower Europe, *Q4/2016 & Full Year: Developments in European Solar Markets & Beyond,* (2016).

[4] A. Jäger-Waldau, M. Szabó, N. Scarlat, and F. Monforti-Ferrario, *Renewable electricity in Europe,* Renewable and Sustainable Energy Reviews **15**, 3703 (2011).

[5] Centraal Bureau van Statistiek, *Share of renewable energy at 5.9% in 2016,* (2016).

[6] Energieonderzoek Centrum Nederland, *Nationale Energieverkenning 2017,* (2017).

[7] G. R. C. Mouli, M. Kefayati, R. Baldick, and P. Bauer, *Integrated pv charging of ev fleet based on energy prices, v2g and offer of reserves,* IEEE Transactions on Smart Grid , 1 (2017).

[8] UCLA Smart Grid Energy Research Center, *What is WINSmartEV: Vehicle to Grid (V2G),* (2015), Cited 01-12-2018 from: http://smartgrid.ucla.edu/.

[9] L. Liu, F. Kong, X. Liu, Y. Peng, and Q. Wang, *A review on electric vehicles interacting with renewable energy in smart grid,* Renewable and Sustainable Energy Reviews **51**, 648 (2015).

[10] K. Clement, E. Haesen, and J. Driesen, *Coordinated charging of multiple plug-in hybrid electric vehicles in residential distribution grids,* in *2009 IEEE/PES Power Systems Conference and Exposition* (2009) pp. 1–7.

[11] S. Papathanassiou, N. Hatziargyriou, and K. Strunz, *A benchmark low voltage microgrid network, CIGRE Symposium*, CIGRE Symposium "Power systems with dispersed generation: technologies, impacts on development, operation and performances" (2005).

[12] B. Asare-Bediako, W. Kling, and P. Ribeiro, *Future residential load profiles: Scenario-based analysis of high penetration of heavy loads and distributed generation,* Energy and Buildings **75**, 228 (2014).

[13] J. J. Spoelstra, *Charging behaviour of dutch ev drivers,* Master of Science Thesis: Utrecht University (2014).

[14] D. van der Meer, *Enabling sustainable transportation by charging evs with pv power at the workspace - an optimal charging strategy,* Master of Science Thesis: Delft University of Technology (2016).

[15] Rijwiel en Automobiel Industrie, *Verkoopcijfers 2016,* (2016), Cited 29-01-2018 from: https://www.raivereniging.nl.

[16] Energiekamer, *Tarievencode Elektriciteit,* (2019), Cited 22-05-2018 from: https://www.acm.nl.

[17] Rijksdienst voor Ondernemend Nederland, *Electromobility in the Netherlands Highlights 2015,* (2015), Cited 29-01-2018 from: https://www.rvo.nl.

[18] F. E. Ltd, *Scenarios for the Dutch electricity supply system: A report prepared for the Dutch Ministry of Economic Affairs* (Frontier Economics, 2015).

[19] J. Hu, H. Morais, T. Sousa, and M. Lind, *Electric vehicle fleet management in smart grids: A review of services, optimization and control aspects,* Renewable and Sustainable Energy Reviews **56**, 1207 (2016).

[20] K. Clement-Nyns, E. Haesen, and J. Driesen, *The impact of charging plug-in hybrid electric vehicles on a residential distribution grid,* IEEE Transactions on Power Systems **25**, 371 (2010).

[21] H. Morais, T. Sousa, Z. Vale, and P. Faria, *Evaluation of the electric vehicle impact in the power demand curve in a smart grid environment*, Energy Conversion and Management **82**, 268 (2014).

[22] D. P. Tuttle and R. Baldick, *The evolution of plug-in electric vehicle-grid interactions*, IEEE Transactions on Smart Grid **3**, 500 (2012).

[23] R. J. Bessa, M. A. Matos, F. J. Soares, and J. A. P. Lopes, *Optimized bidding of a ev aggregation agent in the electricity market*, IEEE Transactions on Smart Grid **3**, 443 (2012).

[24] M. Yilmaz and P. T. Krein, *Review of the impact of vehicle-to-grid technologies on distribution systems and utility interfaces*, IEEE Transactions on Power Electronics **28**, 5673 (2013).

[25] S. G. Wirasingha, N. Schofield, and A. Emadi, *Plug-in hybrid electric vehicle developments in the us: Trends, barriers, and economic feasibility*, in *2008 IEEE Vehicle Power and Propulsion Conference* (2008) pp. 1–8.

[26] C. Guille and G. Gross, *A conceptual framework for the vehicle-to-grid (V2G) implementation*, Energy Policy **37**, 4379 (2009).

[27] W. Kempton and J. Tomić, *Vehicle-to-grid power fundamentals: Calculating capacity and net revenue*, Journal of Power Sources **144**, 268 (2005).

[28] M. Ghofrani, A. Arabali, and M. Ghayekhloo, *Optimal charging/discharging of grid-enabled electric vehicles for predictability enhancement of pv generation*, Electric Power Systems Research **117**, 134 (2014), cited By :11.

[29] P. T. Baboli, S. Bahramara, M. P. Moghaddam, and M. R. Haghifam, *A mixed-integer linear model for optimal operation of hybrid ac-dc microgrid considering renewable energy resources and phevs*, in *2015 IEEE Eindhoven PowerTech* (2015) pp. 1–5.

[30] A. Y. Saber and G. K. Venayagamoorthy, *Resource scheduling under uncertainty in a smart grid with renewables and plug-in vehicles*, IEEE Systems Journal **6**, 103 (2012).

[31] T. Ma and O. A. Mohammed, *Optimal charging of plug-in electric vehicles for a car-park infrastructure*, IEEE Transactions on Industry Applications **50**, 2323 (2014).

[32] C. Chen and S. Duan, *Optimal integration of plug-in hybrid electric vehicles in microgrids*, IEEE Transactions on Industrial Informatics **10**, 1917 (2014).

[33] M. Musio, P. Lombardi, and A. Damiano, *Vehicles to grid (v2g) concept applied to a virtual power plant structure*, in *The XIX International Conference on Electrical Machines - ICEM 2010* (2010) pp. 1–6.

[34] D. van der Meer, G. R. C. Mouli, G. M.-E. Mouli, L. R. Elizondo, and P. Bauer, *Energy management system with pv power forecast to optimally charge evs at the workplace*, IEEE Transactions on Industrial Informatics **14**, 311 (2018).

[35] M. Zhang and J. Chen, *The energy management and optimized operation of electric vehicles based on microgrid*, IEEE Transactions on Power Delivery **29**, 1427 (2014).

[36] A. Y. Saber and G. K. Venayagamoorthy, *Plug-in vehicles and renewable energy sources for cost and emission reductions*, IEEE Transactions on Industrial Electronics **58**, 1229 (2011).

[37] S. Bracco, F. Delfino, F. Pampararo, M. Robba, and M. Rossi, *A dynamic optimization-based architecture for polygeneration microgrids with tri-generation, renewables, storage systems and electrical vehicles*, Energy Conversion and Management **96**, 511 (2015).

[38] P. Sánchez-Martín, S. Lumbreras, and A. Alberdi-Alén, *Stochastic programming applied to ev charging points for energy and reserve service markets*, IEEE Transactions on Power Systems **31**, 198 (2016).

[39] J. Hu, S. You, M. Lind, and J. Østergaard, *Coordinated charging of electric vehicles for congestion prevention in the distribution grid*, IEEE Transactions on Smart Grid **5**, 703 (2014).

[40] T. K. Kristoffersen, K. Capion, and P. Meibom, *Optimal charging of electric drive vehicles in a market environment,* Applied Energy **88**, 1940 (2011).

[41] S. Deilami, A. S. Masoum, P. S. Moses, and M. A.S. Masoum, *Paper Presentation—Real-Time Coordination of Plug-In Electric Vehicle Charging in Smart Grids to Minimize Power Losses and Improve Voltage Profile,* IEEE Transactions on Smart Grid **2**, 456 (2011).

[42] T. Tran-Quoc and L. Nguyen-Van, *Integration of electric vehicles into an industrial grid: Impact assessment and solutions,* in *2016 IEEE Power and Energy Society General Meeting (PESGM)* (2016) pp. 1–5.

[43] T. Sousa, H. Morais, J. Soares, and Z. Vale, *Day-ahead resource scheduling in smart grids considering vehicle-to-grid and network constraints,* Applied Energy **96**, 183 (2012), smart Grids.

[44] Z. Lukszo, *Engineering optimization and integrating renewables in electricity markets,* Lecture Notes: Delft University of Technology (2017).

[45] I. Vlasman, *Developing smart charging strategies at a commercial building for large-scale integration of photovoltaics and electric vehicles,* Master of Science Thesis: Delft University of Technology (2017).

[46] E. Apostolaki-Iosifidou, P. Codani, and W. Kempton, *Measurement of power loss during electric vehicle charging and discharging,* Energy **127**, 730 (2017).

[47] P. Richardson, D. Flynn, and A. Keane, *Local versus centralized charging strategies for electric vehicles in low voltage distribution systems,* IEEE Transactions on Smart Grid **3**, 1020 (2012).

[48] D. Kim, H. Kwon, M.-K. Kim, J.-K. Park, and H. Park, *Determining the flexible ramping capacity of electric vehicles to enhance locational flexibility,* Energies **10** (2017), 10.3390/en10122028.

[49] M. van der Kam and W. van Sark, *Smart charging of electric vehicles with photovoltaic power and vehicle-to-grid technology in a microgrid; a case study,* Applied Energy (2015), 10.1016/j.apenergy.2015.04.092.

[50] SMA, *SUNNY TRIPOWER 12000TL-US / 15000TL-US / 20000TL-US / 24000TL-US / 30000TL-US technical specification,* (2013), Cited 27-07-2018 from: https://www.sma.de/.

[51] Eurelectric, *Application guide to the european standard en 50160 on voltage characteristics of electricity supplied by public distribution systems,* Voltage Disturbances (1995).

[52] S. B. Peterson, J. Apt, and J. Whitacre, *Lithium-ion battery cell degradation resulting from realistic vehicle and vehicle-to-grid utilization,* Journal of Power Sources **195**, 2385 (2010).

[53] G. R. C. Mouli, M. Leendertse, V. Prasanth, P. Bauer, S. Silvester, S. van de Geer, and M. Zeman, *Economic and co2 emission benefits of a solar powered electric vehicle charging station for workplaces in the netherlands,* in *2016 IEEE Transportation Electrification Conference and Expo (ITEC)* (2016) pp. 1–7.

[54] EVbox, *EVBox introduces Elvi, a new home electric vehicle charger,* (2017), Cited 24-07-2018 from: https://www.evbox.com/.

[55] R. Torensma, *The future of public charging infrastructure in the netherlands,* Master of Science Thesis: Utrecht University (2017).

[56] allego, *Regular charging,* (2018), Cited 25-07-2018 from: https://www.allego.eu/.

[57] Rijksdienst voor Ondernemend Nederland, *Statistics Electric Vehicles in the Netherlands (up to and including June 2018),* (2018), Cited 24-07-2018 from: https://www.rvo.nl/.

[58] G. R. Chandra Mouli, P. Bauer, and M. Zeman, *System design for a solar powered electric vehicle charging station for workplaces,* Applied Energy (2016), 10.1016/j.apenergy.2016.01.110.

[59] Koninklijk Nederlands Meteorologisch Instituut, *Cabauw experimental site for atmospheric research,* (2016), Cited 22-06-2018 from: http://www.cesar-database.nl/.